ANNUAL PROGRESS REPORT NO. 1

KINETICS OF OXIDATION AND QUENCHING OF COMBUSTIBLES IN EXHAUST SYSTEMS OF GASOLINE ENGINES

D. J. Patterson
B. Carnahan
R. H. Kadlec
H. A. Lord
J. J. Martin
W. Mirsky
E. Sondreal

PERIOD: February 24, 1969 to February 23, 1970

1969 - 1970

This project is under the technical supervision of the:

Coordinating Research Council
APRAC-CAPE 8-68 Steering Committee

and is work performed by the:

Department of Mechanical Engineering
The University of Michigan
Ann Arbor, Michigan

Under Contract No. CAPE-8-68(1-68)-CRC
and Contract No. CPA-22-69-51-HEW

ACKNOWLEDGMENT

Contributions to this report were made by several faculty and graduate students from the Departments of Chemical and Mechanical Engineering, The University of Michigan. In particular, the write-up of Phase II Progress was made largely by Mr. Everett Sondreal under the guidance of Professor Robert Kadlec and Professor Bruce Carnahan of the Department of Chemical Engineering. The program exhaust was written by Professor Carnahan. The assistance of Mr. Marshall Graves who organized the data and prepared most of the figures related to Phase I progress is gratefully acknowledged.

Special thanks are in order to the members of the ARPAC CAPE-8-68 Project Steering Committee whose astute comments have been most helpful in preparing this report.

TABLE OF CONTENTS

	Page
LIST OF TABLES	iv
LIST OF FIGURES	v
OBJECTIVES	viii
INTRODUCTION	1
DETAILED PROGRESS PHASE I	2
A. Multicylinder "Conventional" Reactor	2
Engine-reactor system	2
Instrumentation	3
Baseline engine evaluation	4
B. Experimental Reactor Study	8
Objectives	8
General requirements of stirred tank system	9
General description of stirred tank system	9
Mixing in the reactor	9
References	12
DETAILED PROGRESS PHASE II	13
Modelling an Exhaust Reactor as a Stirred Tank	13
References	21
DETAILED PROGRESS PHASE III	25
A. Spectroscopic Analysis	25
B. Measurement of Instantaneous Engine Exhaust Velocity and Temperature	26
C. Hydrocarbon Class Analysis by Subtractive Column	27
APPENDIX. ENGINE TEST DATA SUMMARY FOR CURVES OF FIGURES 9-24	77
DISTRIBUTION LIST	83

LIST OF TABLES

Table		Page
I.	Chevrolet Engine Characteristics	2
II.	DuPont Type V Reactor Characteristics	3
III.	Gas Analysis Techniques	5
IV.	Engine Road Load Horsepower Calculations	6
V.	Spectrometer-NDIR Comparison for Variable Fuel/Air Ratio	25
VI.	Spectrometer-NDIR Comparison for Variable Load	26
VII.	Spectrometer-NDIR Comparison for Variable Spark Timing	26

LIST OF FIGURES

Figure		Page
1.	Chevrolet 350 in.^{3} engine set-up for emission test in Room 243 of The University of Michigan Automotive Laboratory.	29
2.	Type V DuPont exhaust manifold reactor.	29
3.	DuPont type V reactor at The University of Michigan.	30
4.	Cutaway view of type V reactor.	30
5.	Modified intake manifold.	31
6.	Flow schematic of University of Michigan hydrocarbon, CO, NO, O_2, and CO_2 exhaust gas analysis system.	32
7.	Flow schematic of University of Michigan subtractive column-flame ionization hydrocarbon analysis system.	33
8.	Calculated road load engine horsepower requirement as a function of car speed.	34
9.	CO_2, CO, O_2, and NO emission vs. air/fuel ratio.	35
10.	Hydrocarbon and aldehyde emission vs. air/fuel ratio.	36
11.	Mass emission vs. air/fuel ratio.	37
12.	Hydrocarbon class analysis vs. air/fuel ratio.	38
13.	CO_2, CO, O_2, and NO concentration emission vs. spark timing.	39
14.	Hydrocarbon emissions vs. spark advance.	40
15.	Mass emission vs. spark advance.	41
16.	Hydrocarbon class analysis vs. spark advance.	42
17.	CO_2, CO, O_2, and NO emission vs. engine speed.	43
18.	Hydrocarbon emission vs. engine speed.	44
19.	Mass emission vs. engine rpm.	45
20.	Hydrocarbon class analysis vs. engine speed.	46

LIST OF FIGURES (Continued)

Figure		Page
21.	CO_2, CO, O_2, and NO emission vs. torque.	47
22.	Hydrocarbon and aldehyde emission vs. load.	48
23.	Mass emission vs. load.	49
24.	Hydrocarbon class analysis vs. load.	50
25.	Two-tank experimental reactor system schematic.	51
26.	Experimental reactor cross section.	52
27.	Variation in hydrocarbon concentration downstream of exhaust valve.	53
28.	Comparison of reaction rate equations for oxidation of carbon monoxide.	58
29.	Variation in exhaust temperature.	59
30.	Variation in exhaust flow.	59
31.	Hydrocarbon concentration (methane).	60
32.	Carbon monoxide concentration.	60
33.	Flow out of reactor.	61
34.	Temperature and pressure in reactor.	62
35.	Emission concentrations in reactor.	63
36.	Reactor temperature and pressure based on an enthalpy-averaged temperature and a modulated input.	64
37.	Reactor gas composition based upon an enthalpy-averaged feed temperature and a modulated input.	65
38.	Reactor temperature and pressure based on an enthalpy-averaged feed temperature and time-averaged input for each cylinder.	66
39.	Reactor gas composition based upon an enthalpy-averaged feed temperature and time-averaged inputs for each cylinder.	67

LIST OF FIGURES (Concluded)

Figure		Page
40.	Emission concentrations during reactor warm-up.	68
41.	Exhaust manifold simulation.	69
42.	A combined mass and energy balance on CO.	74
43.	Spectrographic analysis of exhaust gas (typical).	75

OBJECTIVES

The objectives of this study are:

- To quantify the effects that the various chemical and physical processes have on emission characteristics of exhaust thermal reactors installed on selected typical engines operating at various conditions on a dynamometer test stand.

- To obtain concentration measurements of pertinent chemical species and classes at the entrance to, within, and at the exit from thermal reactors, and from this data to determine gross chemical reaction rates.

- To obtain information which will be helpful in predicting the design of gasoline engine exhaust reactors.

- To develop a computer model for thermal reactors.

INTRODUCTION

The approach taken in this study deviates somewhat from that described in the original proposal. Originally, the intent was to follow an elemental volume of exhaust gas from the time it left the exhaust valve to the time it entered the atmosphere. Chemical and physical measurements on this volume were to be resolved both spatially and temporally. However, the study is now being directed towards obtaining needed new reaction rate data for pertinent chemical classes and species using an experimental well-stirred two-tank reactor system. This information will be used in a computer simulation to predict reactor performance under a variety of conditions, including time varying inputs. Therefore, emphasis is being placed on determining gross rate constants for CO, O_2, total HC, and possibly hydrocarbon classes, taking into account the residence time distribution of these species within the reactor.

A computer model is being developed to simulate the overall chemical kinetics of the reaction processes in the engine mounted reactor, using the rate data obtained from the experimental two-tank reactor mentioned above. A first generation model has been developed which used rate data found in the literature. This model will be updated as soon as rate constants and residence time distributions are experimentally determined from measurements on the experimental reactor. The current computer model has already brought out the need for better rate data and for more accurate experimental determinations of input enthalpy. This latter factor has brought about an increased effort to experimentally determine instantaneous exhaust velocity and temperature measurements.

Current major efforts are now primarily in the following areas:

(a) Experimental determination of the performance of the engine mounted DuPont reactors.

(b) Preparation of the two-tank reactor system for preliminary operation.

(c) Further development of the computer model.

(d) Experimental determination of instantaneous exhaust gas velocity and temperature.

(e) Development of a system for the experimental determination of residence time distribution within the experimental reactor.

DETAILED PROGRESS PHASE I

A. Multicylinder "Conventional" Reactor

ENGINE-REACTOR SYSTEM

At the outset of this program, conversations were held with representatives of various automotive and petroleum companies regarding engines and "conventional" manifold reactors appropriate to The University of Michigan study. Those contacted included General Motors, Ford, Chrysler, DuPont, Ethyl, Mobil, Texaco, and Chevron. Visits were made to General Motors, Ford, DuPont, Mobil, and Texaco laboratories. As a result of these discussions, a decision was made to focus on the Chevrolet 350 $in.^3$ coupled with the DuPont type V thermal exhaust reactor.

A 350 $in.^3$ V-8 engine, donated by the General Motors Corporation, was received and set up for dynamometer testing. Table I lists the manufacturer's specifications for the engine. This engine was selected because it would remain in production for some years, because it is the largest volume production V-8 engine and because DuPont reactors were readily available for this engine. Figure 1 shows the engine installed for test in Room 243 of The University of Michigan Automotive Laboratory. The standard vehicle exhaust system was installed.

TABLE I

CHEVROLET ENGINE CHARACTERISTICS

Model year	1969
Displacement	350 $in.^3$
Compression ratio	9.0:1
No. of cylinders	8
Bore	4.0 in.
Stroke	3.48 in.
Con. rod length	5.7 in.
Firing order	1-8-4-3-6-5-7-2
Fuel specification	regular
Carburetion	Rochester 2-bbl
Emission control	AIR
Rated power	255 BHP at 4200 rpm
Rated torque	365 lb ft at 1600 rpm
Exhaust opening	66° BBC
Exhaust closing	32° ATC
Intake opening	16° BTC
Intake closing	70° ABC
Left exhaust manifold	13 lb/64.6 $in.^3$
Right exhaust mainfold	13.25 lb/73 $in.^3$
Exhaust port volume	3.66 $in.^3$/cyl

Type V reactors and appropriate modified engine parts were procured from the DuPont Corporation. The DuPont reactors were selected because they appeared to be the most effective exhaust manifold thermal reactors available at the time. Figure 2 shows a schematic of the standard type V reactor. The reactor consists of an outer shell in which is mounted a tubular core and a radiation shield to insulate the hot core from the cooler outer shell. Air is injected into each exhaust port. The exhaust gas-air mixture is swept into the reactor core during the exhaust stroke as the arrows suggest. When conditions are favorable vigorous chemical reactions occur which convert hydrocarbon and carbon monoxide compounds to carbon dioxide and water vapor. The hot reacting gases then flow around the radiation shield into the exhaust system. Figure 3 shows a cutaway reactor. References 1, 2, and 3 describe reactor characteristics and performance in more detail.

TABLE II

DuPONT TYPE V REACTOR CHARACTERISTICS

Year received	1969
Overall length	21.375 in.
Overall diameter (exc. port)	5.5 in.
Overall internal vol, flange-to-flange	259 $in.^3$/reactor
Inner core volume	60 $in.^3$/reactor
Weight	26 lb/reactor
Primary material	310 stainless
Maximum recommended core temperature	1750°F

An engine modification required for optimum reactor operation involves the intake manifold heating system. The conventional exhaust gas crossover passage entrances are blocked. Instead, hot water is routed to the crossover. This conserves exhaust energy while providing manifold heat. An intake manifold properly modified was supplied by DuPont. This manifold is shown in Figure 5.

One of the reactors received by The University of Michigan was modified to accept quartz windows at the center of each end of the reactor. This provides a straight optical path through the hot core. One window is large enough (1-3/4 in. dia) to allow a visual inspection of the combustion process. The location of the large quartz window is apparent from Figure 3. The other window is smaller (3/4 in. dia).

INSTRUMENTATION

In order to analyze the effectiveness of the engine-exhaust thermal

reactor system, various pieces of instrumentation were assembled. Engine power was measured by a Westinghouse 200 hp electric dynamometer. Fuel flow was measured by a General Motors displacement-type burette system. Fuel-air ratio was controlled by pressurization or evacuation of the carburetor float bowl. Air flow was measured by a General Motors rounded edge orifice air cart and a Meriam micro-manometer. Thermocouples were used to measure various critical engine temperatures. Exhaust temperatures were monitored by unshielded immersion thermocouples purchased from Industrial Instrument Supply Corporation. A large tank was mounted above the engine to minimize pulsation effects. A Kistler Model 601A quartz pressure transducer was installed in cylinder No. 1 to measure cylinder pressure. A second Kistler Model 701A quartz transducer was installed at the exhaust manifold outlet to monitor exhaust system transient pressure. Mercury manometers were used to measure the intake and exhaust system average pressures. Continuous gas sampling taps were installed at each exhaust port, at the exhaust wye, and at the tailpipe. An overview of the engine and instrumentation is shown in Figure 1.

Gas Analysis

Gas analyses were made with a variety of instrumentation. Table III lists this equipment. The O_2 analyzer as well as nondispersive IR analyzers for CO, CO_2, NO, and HC have been incorporated into a large semi-portable cart—which can be seen in Figure 1. A schematic of this cart is shown in Figure 6. The subtractive column analyzer and flame ionization detector have been combined in a smaller portable cart. Figure 7 shows a schematic of this system. Air Central, Incorporated Model No. 08-800-71 diaphragm gas pumps are used to draw the samples.

BASELINE ENGINE EVALUATION

After obtaining the engine and setting up the instrumentation, an evaluation was made of the unmodified production 350 $in.^3$ Chevrolet engine. Both performance and emission data were measured. Road load engine horsepower was calculated. The results are shown in Figure 8 based on assumptions listed in Table IV. The baseline engine was evaluated at several speed and load points. A majority of data was recorded around a speed of 1200 rpm and load of 30 hp. (130 ft-lb torque) which is about 50% of full load at 30 mph. This corresponds to about 12 in. of manifold vacuum. Thus it is somewhat typical of accelerations on the Federal Test Procedure (9). Air/fuel ratio, spark timing, speed, and load were varied about this 1200 rpm set point. The emission results are plotted in Figures 9-24 and tabulated in the Appendix. No correction for dilution or non-chemically correct operation is applied. Performance data for these tests is tabulated in the Appendix also.

TABLE III

GAS ANALYSIS TECHNIQUES

Specie	Technique	Manufacturer	Range
Carbon monoxide	NDIR[1,2]	Beckman Inst. Model 315A	0-10%
Carbon dioxide	NDIR[1,2]	Beckman Inst. Model 315A	0-15%
Nitric oxide	NDIR[1,3]	Beckman Inst. Model 315A	0-4000 ppm
Hydrocarbon	NDIR[1]	Beckman Inst. Model 315A	0-1000 ppm
Hydrocarbon	FID[4]	Beckman Inst. Model 109A	0-3000 ppm
O_2	Amperometric	Beckman Inst. Model 715	0-5% or 0-25%
Aldehydes	DNPH[5]	Wet chemical and Bausch & Lomb Spectronic 20 spectrophotometer	
Hydrocarbon classes	Subtractive column plus FID[6]		
Individual hydrocarbons	Gas chromatograph	Perkin-Elmer 800	
Hydrogen	Thermal conductivity	Instrument under construction	

1. NDIR - Nondispersive infrared.
2. Orsat used as check of calibration gases.
3. Modified Saltzman used as check of calibration gases.
4. FID - Flame ionization detector.
5. DNPH - Dinitrophenylhydrozone wet chemical method--colorimetric procedure (References 5, 6, 7).
6. Subtractive column technique according to Sigsby, (Reference 8). Additional discussion in this report under Detailed Progress Phase III.

TABLE IV

ENGINE ROAD LOAD HORSEPOWER CALCULATIONS

(1969 Chevelle with 350 $in.^3$ Engine)

Vehicle Information*

Weight including 600 lb test load, W	3945 lb
Frontal area, A_f	21.6 ft^2
N/V ratio with 2.73 axle and powerglide	36.4:1
Coef. of rolling resistance, C_w	.017
Coef. of air resistance, C_d	.0013

Driveline efficiency

mph	10	15	20	25	30	35	40	45	50
Efficiencies	.81	.817	.82	.819	.821	.824	.825	.823	.825

Calculations

$$\text{Road load hp} = \frac{V}{375}\left[C_w \times W + C_d \times A_f \times V^2\right]$$

$$= \frac{V}{375}\left[.017 \times 3945 + .0013 \times 21.6\ V^2\right]$$

where V is vehicle speed in mph

Engine hp Requirement = Road load hp/driveline efficiency

Engine rpm = mph x N/V

= mph x 36.4

Results are plotted in Figure 8.

---

*Courtesy Chevrolet Division, General Motors Corporation.

A. Air/Fuel Ratio

Figure 9 shows the emission concentrations of CO, CO_2, O_2, and NO as a function of air/fuel ratio. Engine conditions were 1200 rpm, 30 BHP and MBT spark. Indolene clear fuel was used. Hydrocarbon emissions as hexane are shown in Figure 10. Both NDIR and FID readings are shown. Aldehydes, measured by the DNPH method, are also plotted in Figure 10. These data compare favorably to those in the published literature.

Figure 11 shows the CO, NO, and FID hydrocarbon emissions on a mass basis. The parameter used is brake specific emission rate (BSER), pounds of emission per bhp-hr. The pounds of emission per pound of fuel termed fuel fraction emission rate (FFER) is also plotted. Figure 12 shows the class analysis results from the subtractive column analyzer. Note that the percent paraffins decreased slightly and the olefins increased slightly as the mixture was leaned. Aromatics remained about constant. No comparable data exist in the literature. One must keep in mind that the subtractive column results include acetylene with the olefins and approximately half the benzene with the paraffins.[8] Additional verification of the subtractive column analyzer by gas chromatography will increase our confidence in these results. The Appendix includes a data summary for this test series.

B. Spark Timing

Figure 13 shows the emission concentrations of CO_2, NO, O_2, and CO as a function of spark timing. Engine conditions were 1200 rpm, 30 BHP, and approximately 15.4:1 A/F ratio. Indolene 30 fuel was used to avoid knocking. Note that NO increased linearly with spark advance. Figure 14 shows the FID and NDIR hydrocarbon emissions. Aldehyde measurements were not recorded for this test. These data compare favorably with data published in the literature. Figure 15 shows the BSER and FFER for the CO, NO, and HC emissions. Figure 16 shows the class analysis results from the subtractive column analyzer. Note that aromatics were nearly constant whereas paraffins increased and olefins decreased as the spark was advanced. No comparable data exists in the literature. The Appendix includes a data summary for this test series.

C. Engine Speed

Figure 17 shows the effect of engine speed on CO_2, NO, CO, and O_2 concentration emissions. Engine operating conditions were 30 hp, MBT spark and about 14.8:1 air/fuel ratio. Indolene 30 test fuel was used. Under these optimized constant load conditions NO decreased linearly with speed. Figure 18 shows the hydrocarbon emissions. Both measurements decrease with speed increase. These concentration readings compare favorably with literature values. Figure 19 shows the BSER and FFER rates. The apparent decrease in CO mass emission rate results from the lower CO concentration at higher

speeds. Figure 20 shows the hydrocarbon class analysis versus engine speed. Paraffins decrease and olefins and aromatics increase slightly at higher speeds. No comparable literature values exist. The Appendix includes a data summary for this test series.

D. Load

Figure 21 shows the effect of load on CO_2, CO, O_2, and NO emission. NO increases with load at a decreasing rate. At light loads CO and O_2 increase and CO_2 decreases slightly. Engine conditions were 1200 rpm, MBT spark and about 15.8:1 air/fuel ratio. Indolene 30 fuel was used. Figure 22 shows hydrocarbon and aldehyde emissions. Incomplete combustion at loads lighter than 30 ft-lb did not increase aldehyde emissions significantly. These data compare favorably to thosein the published literature. Figure 23 shows BSER and FFER emission parameters for this test. Finally Figure 24 shows a class analysis. At light loads the class analysis approaches that of the Indolene fuel itself. No comparable data exists in the literature regarding class analysis. The Appendix includes a data summary for this test series.

B. Experimental Reactor Study

OBJECTIVES

The experimental reactor was included in the program to permit a critical examination of those parameters affecting changes in the chemical composition of an elemental volume of exhaust gas as it passes through an exhaust reactor. Discussions among those involved in the study reflected the opinion that global reaction rate constants for the disappearance of certain compounds and/or classes of compounds in a perfectly mixed reactor were the most critical unknowns in reactor modeling. Thus the primary emphasis of the experimental reactor program has been placed on designing a system to permit the determination of these rate constants. An attempt will be made to account separately for the imperfect mixing effects expected in production vehicle reactors.

Factors of possible importance in addition to reaction rates in perfectly mixed systems, such as the composition profiles, flow rates, and mixing rates in the exhaust pulses, have also been studied to some extent with a separate system, a linear reactor. This work, which corresponds closely to that anticipated at the outset of the project, will be discussed in a following section.

GENERAL REQUIREMENTS OF STIRRED TANK SYSTEM

The stirred tank experimental reactor is to provide kinetic data for a perfectly mixed system. Basically this requires that air and exhaust gas of measured composition flow steadily at measured rates through a highly stirred reactor having a known and uniform pressure, temperature, and composition. Means must be provided to independently vary the inlet composition, relative exhaust and air flow rates, overall flow rate, and reactor temperature. The design features incorporated to achieve these objectives are described in the following section.

GENERAL DESCRIPTION OF STIRRED TANK SYSTEM

The stirred tank system, which will also be called the two-tank system, is sketched in Figure 25. This system will be attached directly to the exhaust port of a propane fueled single cylinder CFR variable compression ratio engine. Hot exhaust will pass from the exhaust port through a perforated exhaust inlet tube and into a 1350 $in.^3$ surge and mixing tank and then through a nozzle into the 50 $in.^3$ reactor. The high velocity jets generated by the nozzle will be used to keep the reactor well stirred. Air will be injected through a heated line into the reactor inlet nozzle. A throttle and by-pass loop will control flowrate in order to permit the reactor residence time to be varied without changing engine conditions. The two tanks and connecting piping will be constructed of Hastelloy-X or similar high temperature alloys and should be capable of continuous operation at up to 2000°F.

Gas samples will be withdrawn at the reactor inlet and outlet through water cooled sampling probes. Gas temperatures will be measured with shielded thermocouples in the surge tank, at the reactor entrance, at three locations inside the reactor, and at the by-pass flowmeter. The degree of uniformity of temperature inside the reactor will be checked by comparing the three thermocouple readings. As a spot check the thermocouples can be moved around inside the reactor, and in addition the composition can be determined at various locations by inserting water-cooled sampling probes through the thermocouple taps. Surge tank and reactor pressures will be measured with manometers. Propane and air flow rates to the engine as well as injection air flow rate will be measured with critical flow orifices and injection air temperature with a shielded thermocouple. Flow rate through the by-pass loop will be measured with a Venturi meter after the gas has been cooled by passing through a heat exchanger.

MIXING IN THE REACTOR

The most critical task of the reactor design is the maintenance of a high mixing rate. The mixing occurs in two steps; (1) the exhaust is mixed with air just upstream of the reactor inlet, and (2) the exhaust-air mixture

is mixed with the products of reaction in the reaction chamber. In the present design both steps depend upon the mixing effects of turbulent jets. Figure 26 is a cross-section view of the reactor showing the jet orifices.

A. Mixing of Exhaust With Air

The mixing of the exhaust with air is accomplished by using the high air supply pressure to force air through twelve 1/16 in. dia holes equally spaced around the circumference of the reactor inlet tube. At the maximum designed air flow rate of 30 lbm/hr this should result in an air velocity of from about 500 ft/sec to sonic velocity through the holes depending on the air temperature. The resulting mixture is then discharged through the reactor inlet nozzle into the reactor.

B. Mixing of Reactants With Products

The reactor is designed to operate at a flow rate of up to 60 lbm/hr. For the present nozzle design this should require a pressure drop of about 4 psi across the twelve 3/32 in. dia inlet holes and result in a velocity through the holes of about 1100 ft/sec at an inlet temperature of 1000°F. The centerline velocity of a jet of this size discharging into an infinite medium would retain about 40% of its initial value after the 1.5 in. it travels in the reactor before striking a wall (see, eg., Abramovich (10)), and thus should possess enough kinetic energy to cause a fairly high level of recirculation and turbulence in the reactor. The micro-mixing parameter of Evangelista, Shinnar, and Katz (11), which represents the ratio of residence time to micro-mixing time, is 8.5 for this system. For a given reactor volume this parameter can only be increased by decreasing the number and/or size of the inlet holes, which consequently requires a higher pressure drop across the inlet nozzle. In order to check for imperfect mixing effects it will be necessary to use at least two different reactor nozzles resulting in different values of this parameter. The design permits nozzles to be easily interchanged, and the requirement of higher back pressures can be met by increasing the engine intake system pressure.

SYSTEM CONTROLS

Exhaust flow rate and composition can be controlled to a large extent by individually controlling the upstream pressures of the air and fuel supplied to the engine, while temperature can be controlled by varying the engine compression ratio and spark timing. Since this does not provide much control over hydrocarbon emissions, provisions have been made to allow the introduction of species into the surge tank if this is deemed necessary. In order to permit variation of reactor residence time while maintaining constant inlet composition by holding engine conditions constant, a by-pass

loop and throttle valve have been incorporated into the design. Injection air flow rate is independently controlled by adjusting the pressure upstream of the critical flow orifice, while temperature is controlled by adjusting the power to the air heaters with a variable transformer.

FABRICATION

Fabrication of the reactor system is underway at the Walker Manufacturing Corporation.

LINEAR REACTOR STUDY

The experimental program initially envisioned called for following an element of exhaust gas through a linear reactor by sampling the concentration as a function of time at several positions. Temperature, pressure, and velocity measurements would also be taken, and to permit the use of optical techniques the reactor was to be constructed of quartz. The design of this reactor was completed and some parts, including sections of quartz tubing, were purchased.

Rather than begin work with the complicated and relatively expensive quartz reactor, a linear reactor consisting of a simple straight mild steel pipe was attached to the exhaust port of the same single cylinder engine now being used with the two-tank system. Both steady and timed samples were obtained for the engine conditions listed below,

Spark Advance	30°(mbt)
RPM	1020 ± 10
I.M. Vacuum	8.5 - 8.8 in. Hg
Compression Ratio	8.5:1
Air/Fuel Ratio	.1% CO

using the method described by Daniel and Wentworth (12). Results for total FID hydrocarbon concentration as a function of crank angle at five locations along the reactor located approximately 4.5, 7, 10.5, 13.5, and 17.5 in. from the exhaust valve, respectively, are presented in Figures 27a-e. An attempt was also made to obtain the velocity as a function of position and time by following the peak concentration in the exhaust slug from these figures, and the results were compared to those obtained by a numerical solution based on the method of characteristics. Some degree of success was achieved, but more work would be required to obtain completely satisfactory agreement between the two methods.

References

(1). Cantwell, E.N., et al., "A Progress Report on the Development of Exhaust Manifold Reactors," SAE Preprint No. 690139, January 1969.

(2). Cantwell, E.N., et al., "Recent Development in Exhaust Manifold Reactor Systems," Inst. of Mech. Eng. Preprint ADP13(B)/70, May 1970.

(3) Cantwell, E.N., and J.J. Mikita, "Exhaust Minifold Thermal Reactors—A Solution to the Automotive Emission Problem," 68th Annual Nat. Pet. Ref. Assoc., April 1970.

(4) Saltzman, B.E., Analytical Chemistry, v. 32, p. 135, 1960.

(5) Oberdorfer, P.E., "Determination of Aldehydes in Automobile Exhaust Gas, "SAE Preprint 670123, January, 1967.

(6) U.S. Bureau of Mines, "Procedures of Determining Exhaust Carbonyls as 2, 4-Dinitrophenylhydrazones," APRAC Proj. CAPE-11-68 Final Report, 1968.

(7) Papa, L.J., "Colorimetric Determination of Carbonyl Compounds in Automotive Exhaust as 2, 4-Dinitrophenylhydrozones," Env. Sci. and Tech. V. 3, No. 4, April 1969, p. 397.

(8) Klosterman, D.L., and J.E. Sigsby, "Application of Subtractive Techniques to the Analysis of Automotive Exhaust," Environmental Science and Technology, 1, No. 4, April 1967, p. 309.

(9) U.S. Dept. of Health, Education, and Welfare, "Control of Air Pollution from New Motor Vehicles and New Motor Vehicle Engines," Federal Register 1968, 33 (June 4).

(10) Abramovich, The Theory of Turbulent Jets, M.I.T. Press (1963).

(11) Evangelista, J.J., R. Shinnar, and S. Katz, The Effect of Imperfect Mixing on Stirred Combustion Reactors, 12th Symposium (Int'l) on Combustion, pp. 901-912 (1969).

(12) Daniel, W.A., and J.T. Wentworth, Exhaust Gas Hydrocarbons—Genesis and Exodus, Society of Automotive Engineers, TP-6, p. 192. (Paper no.486B, SAE National Automobile Week, March 1962.)

Modelling an Exhaust Reactor as a Stirred Tank

A first-generation model has been developed to simulate the operation of a 300 $in.^3$ reactor attached to four cylinders of a 350 $in.^3$ displacement eight-cylinder engine. It is based on instantaneous mixing of air and exhaust at their respective instantaneous flow rates at the inlet to the reactor. The reactor itself is assumed to be well stirred, meaning that temperature and composition are uniform throughout, down to the level of "micromixing."

Recognizing that exhaust enters in pulsations identified with the firing of individual cylinders and that the flow rate of air may be staged, the program was written to accept up to 12 input streams each of which can be timed to enter the reactor over any portion of a 720° engine cycle. The values for rate of flow, temperature, and composition for a given input are generated by function subprograms, so that any desired pattern of variation can be introduced without rewriting the calling program. Each input may contain up to 20 chemical species, which may subsequently appear as either reactants or products in any of 10 reactions.

The computer model computes temperatures, pressures, compositions, enthalpies, heat loss, reaction rates, outflow, and accumulation. A Runge-Kutta method of fourth order is used to compute the total moles in the reactor, the total enthalpy of the reactor, and the moles of each chemical species at any given time from rates of reaction, rates of flow, and rate of heat loss. The reactor temperature is updated for each new value of enthalpy using a half-interval root-finding technique. Pressure is computed from the total mole content of the reactor and temperature by using the perfect gas law.

Heat loss from the reactor is computed as the product of an overall heat transfer coefficient times the difference between the temperature within the reactor and the ambient temperature. The overall coefficient has been treated as a constant and its value has been estimated, neglecting radiation, to be 0.775 Btu/°F hr, based on a reactor shell having 2 ft^2 of surface area surrounded by a 3-1/2 in. thickness of ceramic insulation.

Flow rate out of the reactor is computed as the product of 0.0025 times the instantaneous gage pressure within the reactor in psig. The constant 0.0025 was obtained by trial operation of the program to obtain an average operating pressure of approximately 1 psig.

Chemical reactions are communicated to the computer by arrays which give the coefficients of the chemical species in the chemical equation. Rate data for the reactions are introduced using correlations based on an Arrhenius-type power law of the form

$$r = k\, e^{-E/RT}\, P_S^A\, P_{O_2}^B.$$

All of the simulations run thus far are based on selected reaction kinetics available in the literature.

At the start, the only chemical reactions considered were the oxidations of carbon monoxide and hydrocarbon as methane. Published rates for oxidation of CO are shown in Figure 28. These differ by several orders of magnitude (probably because of variations in experimental conditions). The rate equation for CO chosen for use in the simulation was that obtained by Yuster (44) in studies on exhaust systems.

The rate of oxidation for methane was adapted from results given by Koslov (27). Koslov's rate equation contains the partial pressure of methane raised to the -0.5 power ($P_{CH_4}^{-0.5}$); because of difficulties posed by having a rate which became infinite as concentration approached zero, this was summarily changed to $P_{CH_4}^{1.0}$ along with a compensating change in the pre-exponential coefficient to adjust the rate to match Koslov's at 600 ppm methane. The rate equations finally used were as follows:

Carbon Monoxide - Yuster

$$r_{CO} = -1.91 \times 10^2\, e^{-35{,}600/RT}\, P_{CO}\, P_{O_2}$$

Methane - Koslov

$$r_{CH_4} = -2.08 \times 10^9\, e^{-60{,}000/RT}\, P_{CH_4}\, P_{O_2}^{1.5}$$

Units are: r-lb moles/sec in.^{3}; T - ^{0}K; p-psia; R-1.987 cal/g mole °K.

In the first simulation, input from each cylinder was assumed to enter at a flow, temperature, and composition which varied periodically during the course of the exhaust stroke measured in degrees of engine crank angle. The range and pattern of variation shown in Figures 29 through 32, was based on a consensus by project personnel. The variation in hydrocarbon concentration with crank angle agrees with the data given by Daniel (16). All values shown are consistent with operation of the engine at 1200 rpm with fuel consumption of 20 lb/hr and an air/fuel ratio of 15, which is essentially the stoichiometric ratio where the fuel is assumed to be normal octane. The mass-average concentrations of combustibles entering with the exhaust were 0.8% CO and 552 ppm hydrocarbon. Additional air at 100°F was assumed to be introduced into the reactor at a constant rate, which over a cycle amounted to 40% of the entering

exhaust to give a "dilution ratio" of 1.4. Exhaust temperature varied from 1200 to 2000°F.

The results of the simulation at instantaneously varying input conditions were characterized by wide swings in the outlet flow, temperature, and methane concentration and smaller variations in pressure, CO, and O_2, as shown in Figures 33 through 35. Performance approached repeated cyclic operation after three engine cycles of 720°, corresponding to 0.3 sec, starting with the reactor filled with nitrogen and assuming no thermal capacity in the reactor wall and insulation. Conversion of CO to CO_2 was computed to be approximately 60% and the conversion of CH_4 to CO_2 and H_2O approximately 95%. These values are in generally good agreement with experimental results given by Schwing (36) for similar operating conditions.

A second simulation was run at the same inlet conditions of temperature, flow, and composition as shown in Figures 29 through 32, but with averaging of these inlet conditions with time over the duration of each exhaust stroke. Separate exhaust pulses from individual cylinders were still introduced. This simplification caused the reactor temperature to drop from 1180°F to 960°F and reduced conversion of CO to 5% and that of CH_4 to 35%. The cause for the discrepancy was subsequently shown to be that time-averaging produced a major reduction in the enthalpy input for the inlet stream. That this would be expected to occur can be seen from the fact that the highest flow coincides with the highest temperature. Averaging temperature and flow separately negated the effect of this coincidence.

A third simulation was performed with inputs that were time-averaged over both the exhaust stroke of individual cylinders and over the firing of the four cylinders in each 720° engine cycle. Thus the input for this run was reduced to a steady flow at a uniform temperature and composition. Results were essentially the same as for the second simulation.

In a fourth set of simulations, temperature variation during the course of the exhaust stroke was averaged to give the same enthalpy input for the entering exhaust as at the instantaneous temperatures shown in Figure 29. This was accomplished by a program which determines the enthalpy of the input over one cycle of 720° from instantaneous flow, composition, and temperature, and then matches this enthalpy with a value computed from a constant temperature. The "enthalpy-averaged temperature" thus defined was computed for the instantaneous flow and composition. It should be noted that it has been shown that a summation of time-averaged flow and flow-averaged composition produces the same average temperature. Since the computation was not explicit in the enthalpy-averaged temperature, the solution was obtained by using a half-interval root finding technique. Use of this enthalpy-averaged temperature in the simulation program produced conversions for CO and CH_4 that were virtually the same as for the first simulation based on instantaneous temperatures. This was true whether enthalpy-averaged temperature was used in combination with instantaneous flow and composition or with time-averaged flow and flow-averaged composition. This result is shown in Figures 36 through 39

which are the resulting time variations of temperature, pressure, and CO, CH_4, and O_2 concentrations. These results compare favorably with those presented in Figures 34 and 35 for the instantaneous input. It was concluded that the cyclic properties of the input were not of themselves important in determining conversion, but that time-averaging unwittingly changed the energy content of the entering exhaust and was for that reason responsible for an unacceptably large error. This conclusion reinforces an observation made earlier, to the effect that the measurement of temperature at the inlet to the engine-mounted DuPont reactor should reflect the true energy content of the entering exhaust if the model is to be successfully based on independently determined reaction kinetics.

All of the previously mentioned simulations were based on computations performed using a step size of 1/50 of a 720° cycle. Decreasing the step size to 1/100 of a cycle produced only a negligible change in the indicated performance of the reactor, however increasing the step size to 1/10 and 1/5 cycle resulted in unacceptable errors.

Because of high cost associated with running at small step sizes, the simulation program could not be run to cover the relatively long period of time required to simulate reactor warm-up. To estimate the rate of warm-up, a hand calculation was performed on a reactor having 4 in. dia, 2 ft^2 shell area, 1/16 in. stainless steel walls, and 3-1/2 in. thickness of ceramic fiber insulation. The unsteady state heat balance was approximated by assuming that the gas in the reactor was immediately at its steady state temperature, that the temperature across the steel shell was uniform, and that the temperature profile across the insulation remained linear. Surface heat transfer coefficients were estimated to be 3.2 Btu/hr ft^2 °F inside and .92 Btu/hr ft^2 °F outside at steady state. On this basis, the shell wall temperature increased by 95% of its total change in 36 min. This time estimate is likely high, since the approximation of using a linear temperature profile across the insulation caused more heat to be lost during the warm-up than would actually occur. To bracket the warm-up period on the low side, we assumed perfect insulation at the outside surface of the steel shell, which yielded 95% warm-up in 21 min. Krambeck (28) computed reactor warm-up to occur in approximately 10 min for a 110 $in.^3$ reactor having an inner wall 1/32-in. thick, which indicates order of magnitude agreement.

The most important result of the approximate warm-up calculations was that the initial rate of temperature rise in the steel wall was bracketed between 1.5°F/sec and 2.6°F/sec for the two sets of assumptions given just previously. At intermediate times during warm-up, the rate of change in wall temperature would be somewhat less than these values. Thus, for one engine cycle lasting for 0.1 sec, the maximum change in wall temperature falls between 0.15 and 0.26°F. As noted previously, the temperature, flow, and composition leaving the reactor approach a repeated cycle after three engine cycles or 0.3 sec. During this time the wall temperature would change by less than 0.45 to 0.78°F. Since the temperature drop across the inside gas film resistance is always much larger than this, varying from approximately 1000°F at start-up

to 130°F at steady state, the change in wall temperature has a negligible effect on the energy balance computed over three engine cycles. Thus the effect of wall temperature during warm-up can be investigated by running separate simulations of three cycles each at different fixed wall temperatures between ambient and steady state. Reactor performance during warm-up computed on this basis is shown in Figure 40. Outlet temperature increase from approximately 1140°F just after start-up to 1260°F at steady state. Conversions change from 55% to 80% for CO and from 90% to 99% for CH_4.

While our main interest is in modelling the exhaust reactor itself, the exhaust ports leading into the reactor and the exhaust pipe leaving the reactor may also provide residence times sufficient for significant amounts of reaction. To evaluate the importance of the inlet port, a stirred-tank simulation was run on a volume of 7.5 $in.^3$ receiving exhaust from a single cylinder. Inlet conditions, which averaged 0.8% CO, 552 ppm CH_4, and 1572°F, were assumed to vary periodically in the same manner as for exhaust gas entering the 300 $in.^3$ reactor (Figures 29 through 32). Air was introduced at 100°F to achieve a dilution ratio of 1.4 as before; however, the flow rate for the air was staged to give 10% of the average rate over the 75° interval of crank angle corresponding to maximum exhaust flow and a higher rate over the remaining 645° of a 720° engine cycle. This assumption for air rates was intended to parallel the behavior of existing methods, which tend to admit air in inverse proportion to exhaust flow because of back pressure (21).

Temperatures, pressures, and concentrations in the exhaust port were observed to exhibit periodic oscillations of wide ampliture as a function of crank angle, as would be expected for a small volume receiving a cycling input. These results are shown in Figures 43a-e. Changes in hydrocarbon and carbon monoxide during the period after exhaust flow ceased for a cycle were represented by an exponential-type decline as combustion and dilution by the continuing flow of air dropped concentrations to near zero at the end of each 720° cycle. The most significant finding was that conversion of CH_4 was 70% and the conversion of CO 20% within the small volume of the port. It should be remembered that these conversions are based on the same selected literature values of kinetic constants used previously (44,27) and are therefore subject to an unknown error for the conditions of this problem. However, the tentative conclusion is that the exhaust port may be quite important in predicting overall conversions between the exhaust valve and the tailpipe of an exhaust system. Its importance may however be less than that shown due to imperfect mixing of air and exhaust within the small volume of the port.

In a final series of simulation on the 300 $in.^3$ stirred tank reactor, 4% hydrogen was added as an additional fuel species and the amount of carbon monoxide was increased to 8%. Hydrocarbon as methane was maintained at 552 ppm as before.

The proportion of H_2 in relation to CO was established on the basis of an equilibrium constant of 3.8 for the water gas shift reaction, as proposed

by D'Alleva (13). In the absence of information on the kinetics of homogeneous oxidation of hydrogen, it was assumed that the hydrogen was consumed immediately upon entering the reactor.

A chief reason for running a simulation at higher levels of combustibles was to check the Runge-Kutta solution for the combined mass and energy balance. This was accomplished by comparing the steady state predicted by the reactor model and that obtained from an independent calculation of the mass and energy balance lines. It was possible, using the kinetics for the combustion of CO, to compute the mass balance (temperature as a function of conversion) for various initial concentrations of CO. The resulting temperatures were determined explicitly for a specific initial concentration and exit conversion. The energy balance line was determined by first calculating the initial temperature of the exhaust mixed with injected air plus the energy contribution for the complete combustion of hydrogen. This was determined using the program which calculated the enthalpy-averaged temperature of the exhaust. It was then a simple matter to obtain the slope of the energy balance line and thereby predict the steady state.

Because of the characteristic "S" shape of the material balance curve, a series of energy balance lines for progressively higher inlet exhaust temperatures should reach a point of ignition evidenced by an abrupt increase in conversions and temperature. Results are presented in Figure 26 for inlet temperatures of 900°F, 1000°F, 1036°F, and 1072°F. The inlet concentrations of CO and H_2 were 8% and 4%, respectively. The program correctly predicts the ignition conditions for these temperatures. However, it incorrectly predicts a nonignition point for an inlet temperature of 1000°F and predicts the incorrect nonignition point for the 900°F inlet temperature. The conversions are much too high for the predicted temperature.

After correcting the above problem, modelling based on a stirred tank will be discontinued until after kinetic studies with the experimental reactor are completed.

SCHEMATIC DIAGRAM FOR PROGRAM EXHAUST

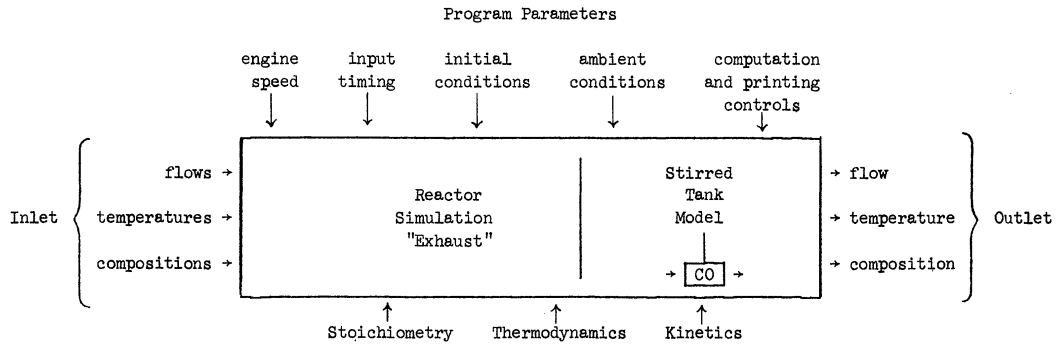

LIST OF DATA INPUTS

Specific heat constants	(A,B,C,D)
Heats of formation	(DHF)
Molecular weights	(MWT)
Gas constants	(RG & RK)
Number of inputs	(N)
Number of chemical species	(M)
Number of reactions	(Q)
Pre-exponential rate coefficients	(AA)
Activation energies	(E)
Stoichiometric coefficients	(NU)
Reaction rate exponents (orders)	(NE)
Engine rpm	(LAMBDA)
Input crank angles	(ALOW)
Crank angle spans for inputs	(ASPAN)
Minimum temperatures of inputs	(TLOW)
Temperature spans of inputs	(TSPAN)
Minimum flow rates of inputs	(FLOW)
Flow spans of inputs	(FSPAN)
Minimum concentrations in inputs	(XLOW)
Concentration spans of inputs	(XSPAN)
Reactor volume	(V)
Ambient pressure	(PA)
Ambient temperature	(TA)
Heat transfer coefficient (overall)	(HBAR)
Flow coefficient	(CFLOW)
Initial reactor temperature	(TOZERO)
Initial reactor pressure	(POZERO)
Initial reactor compositions	(XOZERO)
Tolerance for temperature calculations	(TEPS)
Duration of simulation in engine cycles	(MAXCYC)
Number of computational steps per cycle	(NSPCYC)
Print frequency	(FREQ)
Maximum number of half-interval iterations	(ITMAX)
Print controls	(PRINT)

MAXIMUM NUMBER OF PRINTED OUTPUTS

Numbers of inputs, species, and reactions
Heats of formation and specific heats
Stoichiometric equations and chemical rate equations
Input parameters

- engine rpm
- input timing
- temperature
- flow
- composition

Initial and ambient conditions
Computational and printing parameters
Reactor temperature, pressure, and mole balance versus crank angle
Reactor composition versus crank angle
Inlet flow, temperature, and enthalpy versus crank angle
Inlet composition versus crank angle
Energy balance versus crank angle
Reaction rates versus crank angle
Rates of species "appearance" versus crank angle
Intermediate computations used for debugging

FLOW DIAGRAM OF PROGRAM OPERATION

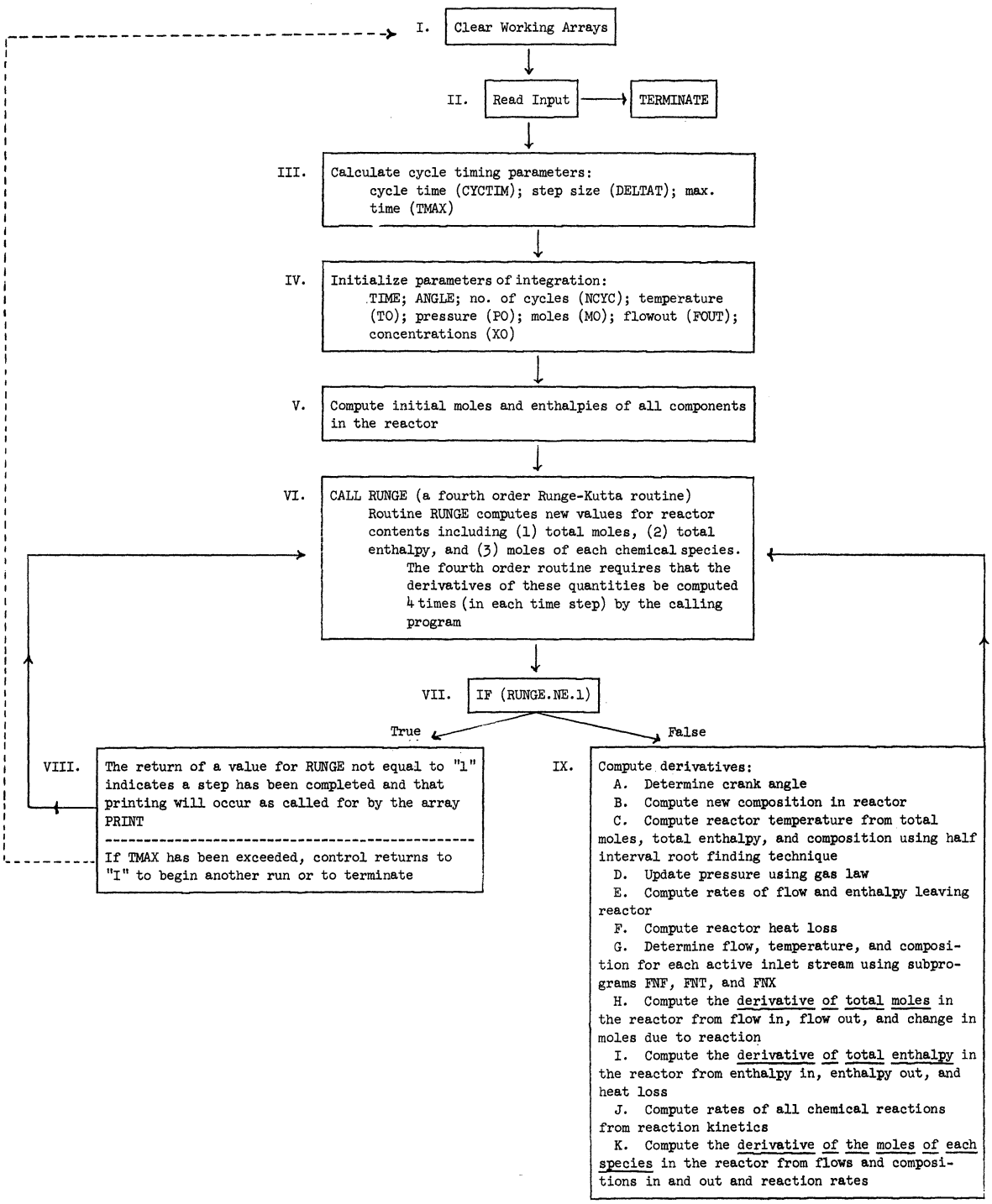

NOTES:

1. Subprograms FNF, FNT, and FNX supply values of flow, temperature, and composition as functions of crank angle.
2. All enthalpies are generated by a subroutine HMOLAR based on temperatures, specific heats, and heats of formation supplied by the calling program.
3. All time advance is accomplished within subprogram RUNGE.

REFERENCES

(1) Agnew, W. G. (General Motors), "Automotive Air Pollution Research." Proceedings of the Royal Society of London, 307, 153-181 (1968).

(2) Agnew, W. G. (General Motors), "Future Emission-Controlled Spark-Ignition Engines and Their Fuels." Research Publication GMR-880, General Motors Corporation, Warren Michigan. (Presented at the 34th Midyear Meeting of the Division Refinery, American Petroleum Institute, Chicago, Ill., May 12, 1969.)

(3) American Conference of Government Industrial Hygienists. "Threshold Limit Values for 1966." Cincinnati, 1966.

(4) Barnhill, T., "Summary Report on the Chemical Analysis of Automotive Exhaust Gas." Department of Chemical and Metallurgical Engineering, The University of Michigan. January 28, 1970.

(5) Baum, E., "Automobile Afterburner Studies: Noncatalytic Afterburning Without Ignition." U.C.L.A. Report 59-14, March 1959.

(6) Brownson, D. A., and R. F. Stebar (General Motors), "Factors Influencing the Effectiveness of Air Injection in Reducing Exhaust Emissions." Society of Automotive Engineers, TP-12. p. 103. (Originally published in SAE Transactions, 74, 1966.)

(7) Cantwell, E. N., I. T. Rosenlund, W. J. Barth, F. L. Kinnear, and S. W. Ross (DuPont), "A Progress Report on the Development of Exhaust Manifold Reactors." Paper No. 690139, SAE International Automotive Engineering Congress, Detroit, Michigan. January 13-17, 1969.

(8) Cantwell, E. N., and A. J. Pahnke (DuPont), "Design Factors Affecting the Performance of Exhaust Manifold Reactors." SAE Transactions, 74, 1966.

(9) Caplan, J. D. (General Motors), "Vehicle Emissions, II." Society of Automotive Engineers, TP-12, p. 20. (Originally published in SAE Transactions, 74, 1966.)

(10) Chandler, J. M., A. M. Smith, and J. H. Struck (Ford), "Development of the Concept of Non-flame Exhaust Gas Reactors." Paper No. 486M, SAE National Automobile Week, March 1962.

(11) Colucci, J. M., and C. R. Begeman, Journal Air Pollution Control Association, 15, 113 (1965).

(12) Curl, R. L., "Dispersed Phase Mixing: I. Theory and Effects in Simple Reactors." AIChE J., 9, No. 2, 175 (March 1963).

(13) D'Alleva, B. A., "Procedure and Charts for Estimating Exhaust Gas Quantities and Compositions." General Motors Research Laboratories Report GMR-372, May 15, 1960.

(14) Daigh, H. D., and W. F. Deeter, "Control of Nitrogen Oxides in Automotive Exhaust." Presented at the Mid-year Meeting of the American Petroleum Institute, San Francisco, May 1962.

(15) Daniel, W. A., and J. T. Wentworth (General Motors), "Exhaust Gas Hydrocarbons—Genesis and Exodus." Society of Automotive Engineers, TP-6, 192. (Paper No. 486 B, SAE National Automobile Week, March 1962.)

(16) Daniel, W. A. (General Motors), "Engine Variable Effects on Exhaust Hydrocarbon Composition (A Single-Cylinder Engine Study with Propane as the Fuel)." Paper No. 670124, SAE Automotive Engineering Congress, Detroit, Michigan, January 9-13, 1967.

(17) Danckwerts, P. V., "The Effect of Incomplete Mixing on Homogenous Reactions." Chemical Reaction Engineering, 12th Meeting Europ. Fed. Chem. Eng., Amsterdam, 1957.

17A) Eccleston, B. H., and R. W. Hurn, "Comparative Emissions from Some Leaded and Prototype Lead-Free Automobile Fuels." U.S. Department of the Interior, Bureau of Mines, Report of Investigations 7390. May 1970.

(18) Evangelista, J. J., R. Shinnar, and S. Katz, "The Effect of Incomplete Mixing in Stirred Combustion Reactors." Twelfth Symposium (International) on Combustion. Poitiers, France, July 1968.

(19) Eyzat, P., and J. C. Guibet, "A New Look at Nitrogen Oxides Formation in Internal Combustion Engines." SAE Paper No. 680124, Fuels and Lubricants 1968 Papers, p. 93.

(20) Fristrom, R. M., and A. A. Westenberg, Flame Structure. McGraw-Hill, New York, 1965, p. 349.

(21) Glass, W., D. S. Kim, and B. J. Kraus (ESSO), "Synchrothermal Reactor System for Control of Automotive Exhaust Emissions." SAE Paper No. 700147, Automotive Engineering Congress, Detroit, Michigan, January 12-16, 1970.

(22) Glasson, W. A., and C. S. Tuesday, "Hydrocarbon Reactivities in the Atmospheric Photo-oxidation of Nitric Oxide." Presented to the American Chemical Society Meeting, Atlantic City, September, 1965.

(23) Haagen-Smit, A. J. (California Institute of Technology), "Chemistry and Physiology of Los Angeles Smog." Industrial and Engineering Chemistry, 44, No. 6 (June 1952).

(24) Hirschler, D. A., L. F. Gilbert, F. W. Lamb, and L. M. Niebylski, Industrial and Engineering Chemistry, 49, 1131 (1957).

(25) Hottel, H. C., G. C. Williams, N. M. Nerheim, and G. R. Schneider, "Kinetic Studies in Stirred Reactors: Combustion of Carbon Monoxide and Propane." Tenth Symposium (International) on Combustion, 1965, p. 111.

(26) Jackson, M. W., W. M. Wiese, and J. T. Wentworth (General Motors), "Vehicle Emissions." Society of Automotive Engineers, TP-6, p. 175. (Paper No. 486A presented at the SAE National Automobile Week, March 1962.)

(27) Koslov, G. I., "On High Temperature Oxidation of Methane." Seventh Symposium (International) on Combustion, 1958, p. 142.

(28) Krambeck, E., "Math Model for Thermal Reactor Designs." Quarterly Reports, June 1968—June 1969. Ford Mobil Project XVII.

(28A) Levenspiel, O., and K. Bischoff, "Patterns of Flow in Chemical Process Vessels." Advances in Chemical Engineering, 4, 95-108. Academic Press, New York, 1963.

(29) Longwell, J. P., and M. A. Weiss (Esso), "High Temperature Reaction Rates in Hydrocarbon Combustion." Industrial and Engineering Chemistry; 47, No. 8, 1634 (August 1955).

(30) Lewis, B., and G. von Elbe (U.S. Bureau of Mines), Combustion, Flames and Explosions of Gases. Academic Press, New York, 1951, 739-748.

(31) Newhall, H. K., and E. S. Starkman, "Direct Spectroscopic Determination of Nitric Oxide in Reciprocating Engine Cylinders." SAE Transactions, 76, 743, 1967.

(32) Ninomiya, J. S., and A. Golovoy, "Effects of Air-Fuel Ratio on Composition of Hydrocarbon Exhaust from Iso-octane, Di-isobutylene, Toluene, and Tolune-n-Heptane Mixture." Paper No. 690504, SAE Mid-Year Meeting, Chicago, 1969.

(33) Patterson, D. J., "Kinetics of Oxidation and Quenching of Combustibles in Exhaust Systems of Gasoline Engines." Progress Report No. 11, CRC Project, Department of Mechanical Engineering, The University of Michigan, January 1970.

(34) Perry, R. H., C. H. Chilton, and S. D. Kirkpatrick, "Perry's Chemical Engineers Handbook," Vol. 4, McGraw-Hill, New York, 1963, p. 9, section 9.

(35) Ried, R. S., J. G. Mingle, and W. H. Paul, "Oxides of Nitrogen from Air Added in Exhaust Ports." Society of Automotive Engineers, TP-12, 230. (Paper 660115 presented at SAE Automotive Engineering Congress, Detroit, January 1966.)

(36) Schwing, R. C. (General Motors), "An Analytical Framework for the Study of Exhaust Manifold Reactor Oxidation." SAE Preprint 700109, January 1970.

(37) Sigworth, H. W. Jr., P. S. Myers, O. A. Uyehara, "The Disappearance of Ethylene, Propylene, n-Butane, and 1-Butene in Spark-Ignition Engine Exhaust." SAE Preprint 700472, May 1970.

(38) Sorenson, S. C., P. S. Myers, and O. A. Uyehara, "The Reactions of Ethane in Spark-Ignition Engine Exhaust Gas." SAE Preprint 700471, May 1970.

(39) Steinhagen, W. K., G. W. Niepoth, and S. H. Mick (General Motors), "Design and Development of the General Motors Air Injection Reactor System," Society of Automotive Engineers, TP-12, 146. (Paper 660106, SAE Automotive Engineering Congress, Detroit, January 1966.)

(40) Sturgis, B. M., J. W. Bozek, W. F. Biller, and S. B. Smith, "The Application of Continuous Infrared Instruments to the Analysis of Exhaust Gas." Society of Automotive Engineers, TP-6, 81. (Paper No. 11B, SAE National Meeting, January 1958.)

(41) U.S. Department of Health, Education, and Welfare, "Control of Air Pollution from New Motor Vehicle Engines; Standards for Exhaust Emissions, Fuel Evaporative Emissions, and Smoke Emissions, Applicable to 1970 and Later Vehicles and Engines." Federal Register Part II, 33, No. 108, June 4, 1968.

(42) U. S. Public Health Service, Div. of Air Pollution. "The Sources of Air Pollution and Their Control." PHS No. 1548, 1966.

(43) Wentworth, J. T., and W. A. Daniel (General Motors), "Flame Photographs of Light Load Combustion Point the Way to Reduction of Hydrocarbons in Exhaust Gas." Society of Automotive Engineers, TP-6, p. 121. (Paper No. 425, SAE Annual Meetings Jan 1955.)

(44) Yuster, S. T., P. Stoudhammer, J. Miller, S. Sourirajan, R. Henderson, and T. Masters, "Afterburner Studies as Applied to Automobile Exhaust Systems." U.C.L.A. Report 58-55, June 1958.

(45) Zwietering, T. N., "The Degree of Mixing in Continuous Flow Systems." Chemical Engineering Science, Vol. 11, No. 1, p. 1, 1959.

DETAILED PROGRESS PHASE III

A. Spectroscopic Analysis of Engine Exhaust Gas

To examine the feasibility of using a spectrometer as an analytical instrument for this study, a quantitative spectroscopic analysis of engine exhaust was made and the results were compared with those obtained with a non-dispersive infrared analyzer.

The instrument used was a Perkin-Elmer Model 112 spectrometer with a NaCl prism, a thermocouple detector, and a globar light source. Exhaust gas was drawn into a one-meter gas cell from the engine exhaust pipe through an ice bath and filter. The pressure in the sample cell was brought to 1 atm and an analysis made for CO, CO_2, NO, and total hydrocarbons using the 4.65-, 2.7-, 5.3-, and 3.4-micron bands, respectively. A sample record is shown in Figure 43. Calibration curves for both the spectrometer and the NDIR were obtained from span gases with known composition which were purchased from Olson Laboratories. Data were obtained at several fuel/air ratios, loads and spark positions, and are summarized in Tables V, VI, and VII. Average discrepancies are seen to be 36% for CO, 6% for CO_2, 29% for NO, and 64% for total hydrocarbons. Corrections for H_2O interference were made in obtaining the results for CO_2.

TABLE V

SPECTROMETER-NDIR COMPARISON FOR VARIABLE FUEL/AIR RATIO

RUN NO.	FUEL/ AIR RATIO	CO(%)		CO_2(%)		NO(ppm)		HC(ppm)	
		SPECT.	NDIR	SPECT.	NDIR	SPECT.	NDIR	SPECT.	NDIR
81	11.28	8.75	10.70	10.2	8.21	450	680	575	375
80	12.96	3.14	5.61	12.1	11.21	1300	2547	425	325
76	14.97	0.90	0.65	14.0	12.22	1700	2594	253	225
79	16.19	0.39	0.23	14.1	14.13	2300	2834	160	207
78	17.82	0.24	0.10	14.4	12.48	1675	1989	350	171
77	19.85	0.35	0.10	11.5	10.96	960	1186	265	180

TABLE VI

SPECTROMETER-NDIR COMPARISON FOR VARIABLE LOAD

RUN NO.	DYNAMOM-ETER SCALE	CO(%)		CO_2(%)		NO(ppm)		HC(ppm)	
		SPECT.	NDIR	SPECT.	NDIR	SPECT.	NDIR	SPECT.	NDIR
102	3.0	0.40	0.23	12.70	11.70	606	960	702	835
101	9.5	0.40	0.16	12.85	12.74	1130	897	577	306
100	16.7	0.43	0.16	13.05	12.87	1250	1761	555	225
99	25.4	1.06	0.37	13.30	12.48	2480	2106	358	216
103	33.0	0.68	0.86	11.90	12.74	1245	2066	787	415
104	42.0	2.06	1.28	11.10	12.48	1400	1837	710	365

TABLE VII

SPECTROMETER-NDIR COMPARISON FOR VARIABLE SPARK TIMING

RUN NO.	SPARK TIMING (deg.)	CO(%)	
		SPECT.	NDIR
117	17	0.7	0.65
116	25	0.8	0.51
113	33	1.58	1.63
114	41	1.43	1.49
115	50	0.8	0.37

B. Measurement of Instantaneous Engine Exhaust Velocity and Temperature

The discussion concerned with Phase II of this project has brought out the fact that the reactor model is quite sensitive to the enthalpy input to the reactor. An accurate experimental determination of the enthalpy input requires good measurements of both instantaneous engine exhaust velocity and temperature. Since no known conventional techniques are available for getting these measurements, developmental work is underway on a new technique which appears promising for both measurements.

The method uses laser-schlieren photography with a rotating-mirror camera. The laser-schlieren system is used to detect turbulent eddies as they move with the exhaust stream. The average eddy spatial velocity is assumed to be equal to the exhaust stream velocity. By projecting the resulting schlieren image through a narrow slit and moving the slit image at a fixed rate across a sheet of Polaroid film, by means of the rotating mirror, a photograph is

obtained which gives continuous records of both eddy position and time, over a short-time interval. The slope of the resulting image at any point gives instantaneous velocity.

Measurement of instantaneous gas temperature will be attempted using the same technique for measuring the speed of a spark-induced shock wave in the gas stream. Since shock velocity is proportional to $T^{1/2}$, the gas stream temperature can be estimated from the measured shock velocity.

This work has been started using equipment made available from previous studies at The University of Michigan Automotive Laboratory. This equipment has been modified and installed on a CFR engine where preliminary results have been obtained. These results are promising and work is continuing.

C. Hydrocarbon Class Analysis by Subtractive Column

A subtractive column analyzer was built to measure the three principal hydrocarbon classes. The technique used is identical to that of Sigsby and Klosterman, Environmental Science and Technology, 1, No. 4, April 1967, p. 311.

Olefins and acetylenes are removed by a mercury sulfate-sulfuric acid scrubber. Aromatics are removed by a palladium sulfate-sulfuric acid scrubber. A flame ionization analyzer is used as the hydrocarbon detector.

Figure 7 shows a flow schematic of The University of Michigan system. The unit has three parallel paths. The exhaust sample is directed either through path S_1 (total hydrocarbons, S_2 (total minus olefins and acetylenes), or S_3 (total minus olefins, acetylenes, and aromatics). Provisions were made for zeroing the FID and for backflushing. Dry nitrogen is used for the backflush.

To check the performance of the analyzer three calibration gases were blended. These gases (as analyzed by the manufacturer) were:

paraffinic:	4620 ppmc propane in nitrogen
aromatic:	315 ppmc toluene plus 282 ppmc benzene in nitrogen—597 ppmc
olefinic:	100 ppmc acetylene, 150 ppmc propylene, 101 ppmc ethylene, and 205 ppmc 1—butene in nitrogen—total 556 ppmc

The FID measured results on new columns are reported as ppmc in the table below. The FID was calibrated on the propane mixture.

	Calibrating Gases		
	4620 ppmc Paraffinic	597 ppmc Aromatic	556 ppmc Olefinic
Column Used			
Backflush	0	0	0
Aromatic and Olefin Sub.	4620	192	0
Olefin Sub.	4620	570	0
None	4620	570	582
Calculated Results			
Paraffins and Benzene	4620	192	0
Olefins and Acelytene	0	0	582
Aromatics	0	378	0

These data show that the columns subtracted the constituents as expected. Apparently all the acetylene is reported with the olefins and part of the benzene (192 ppmc of 315 ppmc in mix or 60%) is reported with the paraffins. A detailed GC analysis is required to substantiate the subtractive column values.

Experience shows that the percent benzene which breaks through varies from column-to-column. Flowing dry nitrogen through the aromatic subtractor improves benzene retention. A 60% breakthrough is about average. Column life appears to be on the order of one hour actual analysis time. This varies with flow rate and gas composition. We usually change columns when they are about 50% discolored.

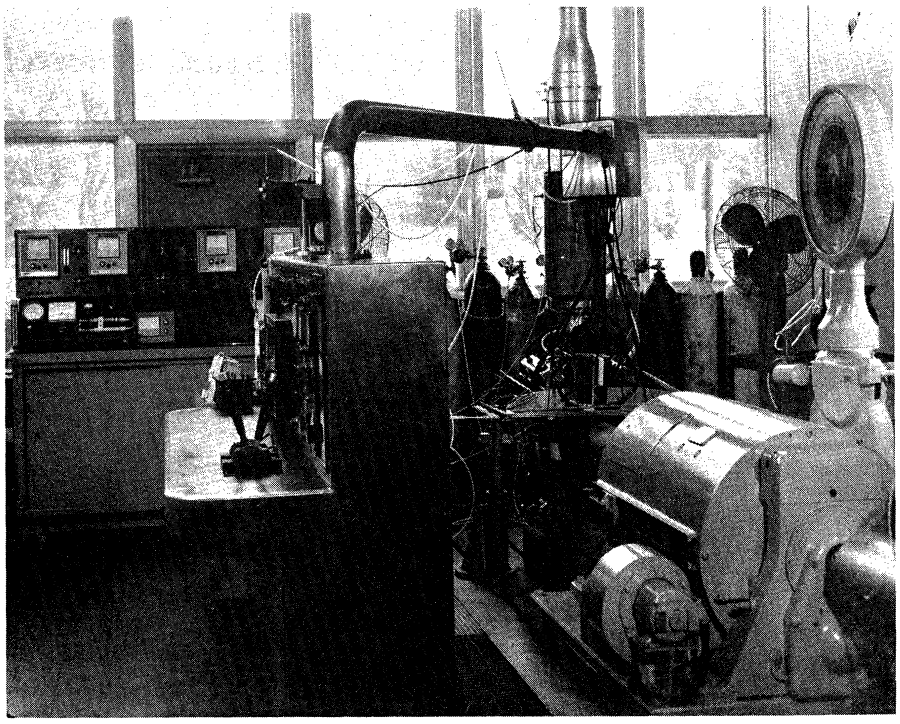

Figure 1. Chevrolet 350 in.^{3} engine set-up for emission test in Room 243 of The University of Michigan Automotive Laboratory.

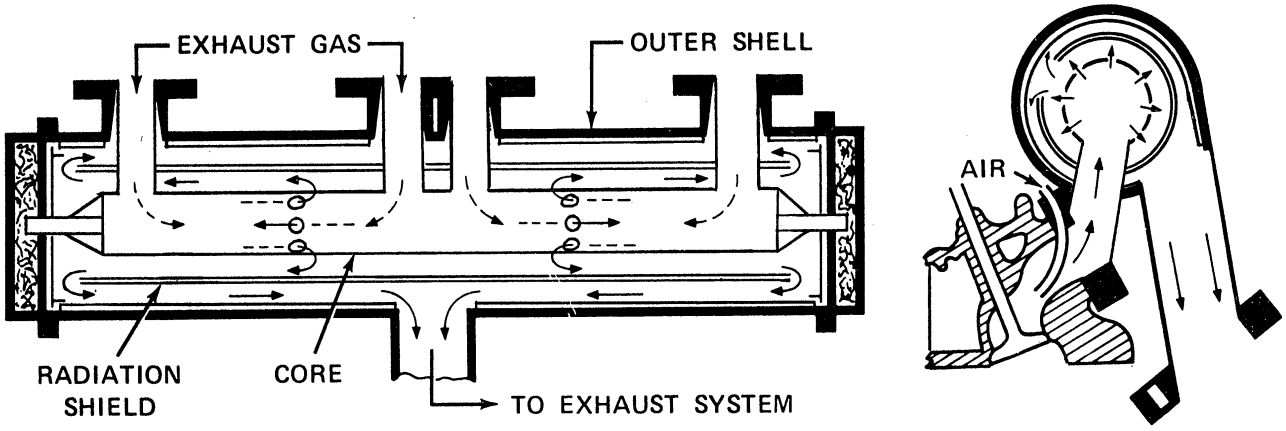

Figure 2. Type V DuPont exhaust manifold reactor. Figure courtesy DuPont Corporation.

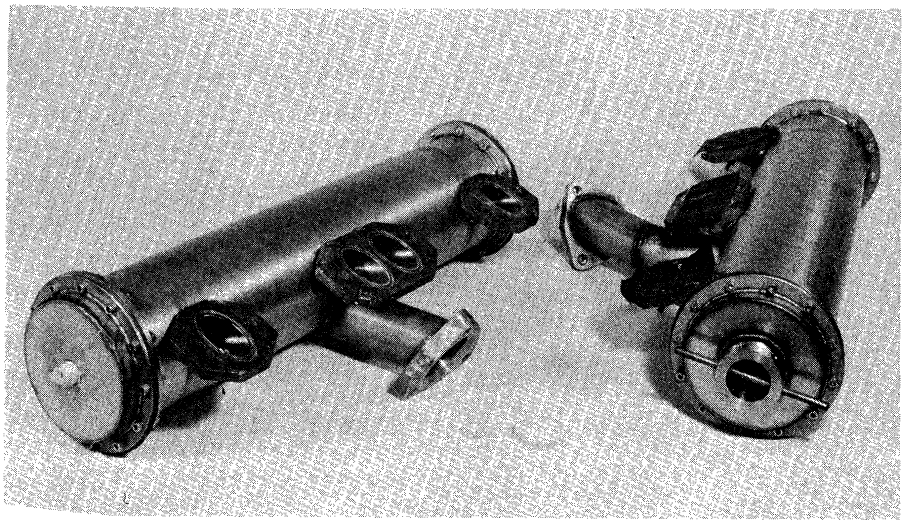

Figure 3. DuPont type V reactor at The University of Michigan. Quartz windows in the right-hand reactor provide a see-through optical path.

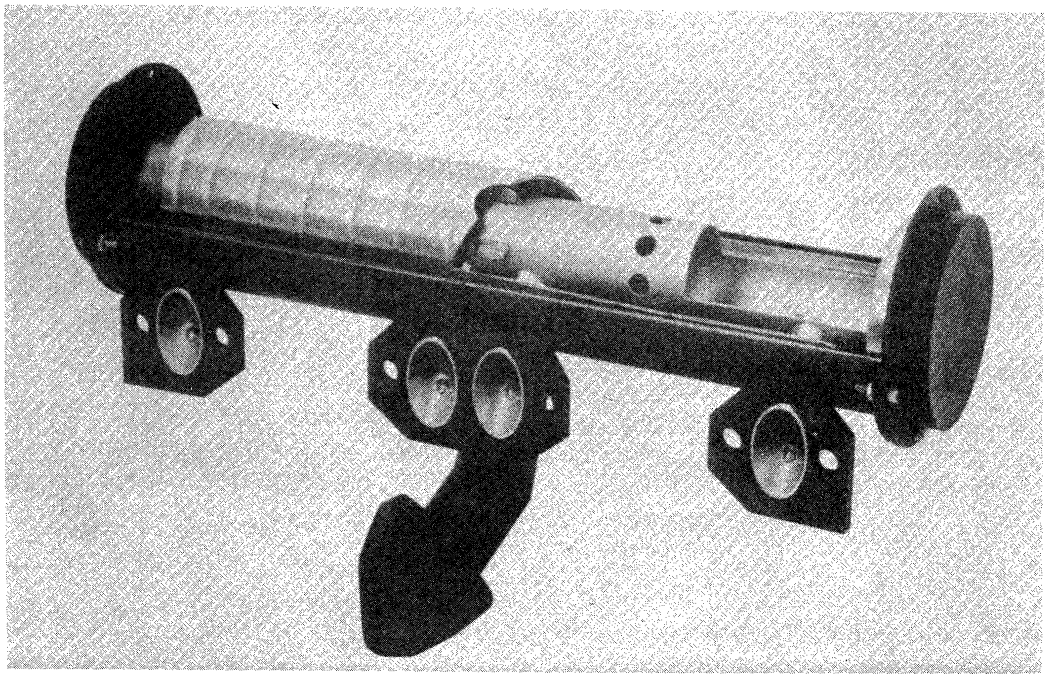

Figure 4. Cutaway view of type V reactor. Courtesy DuPont Corporation.

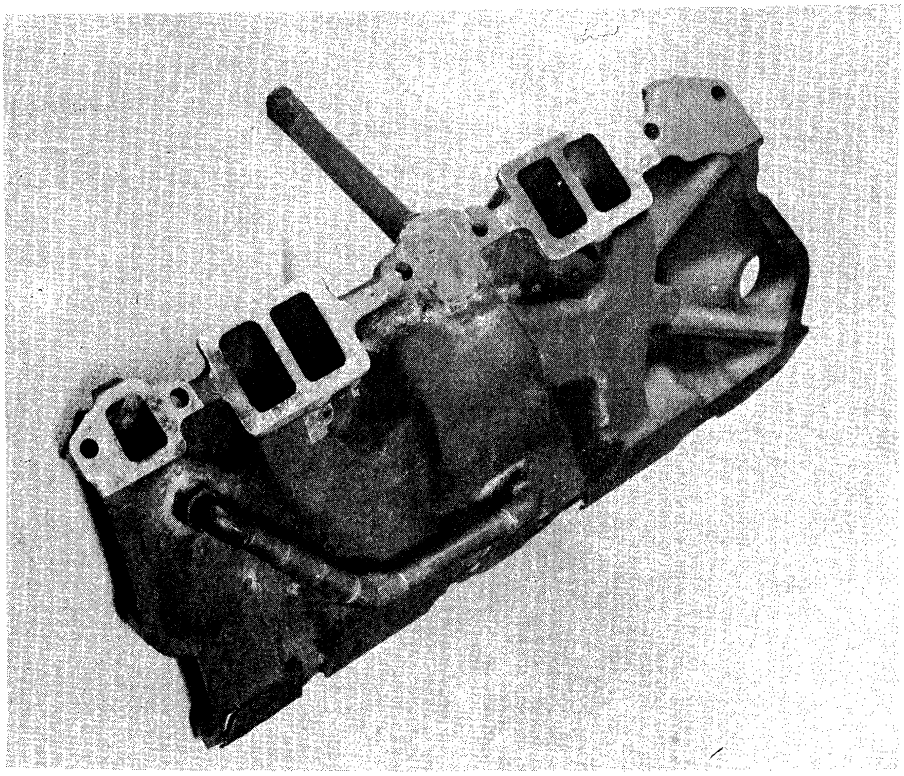

Figure 5. Modified intake manifold. Hot water replaces exhaust as the source for intake charge heat.

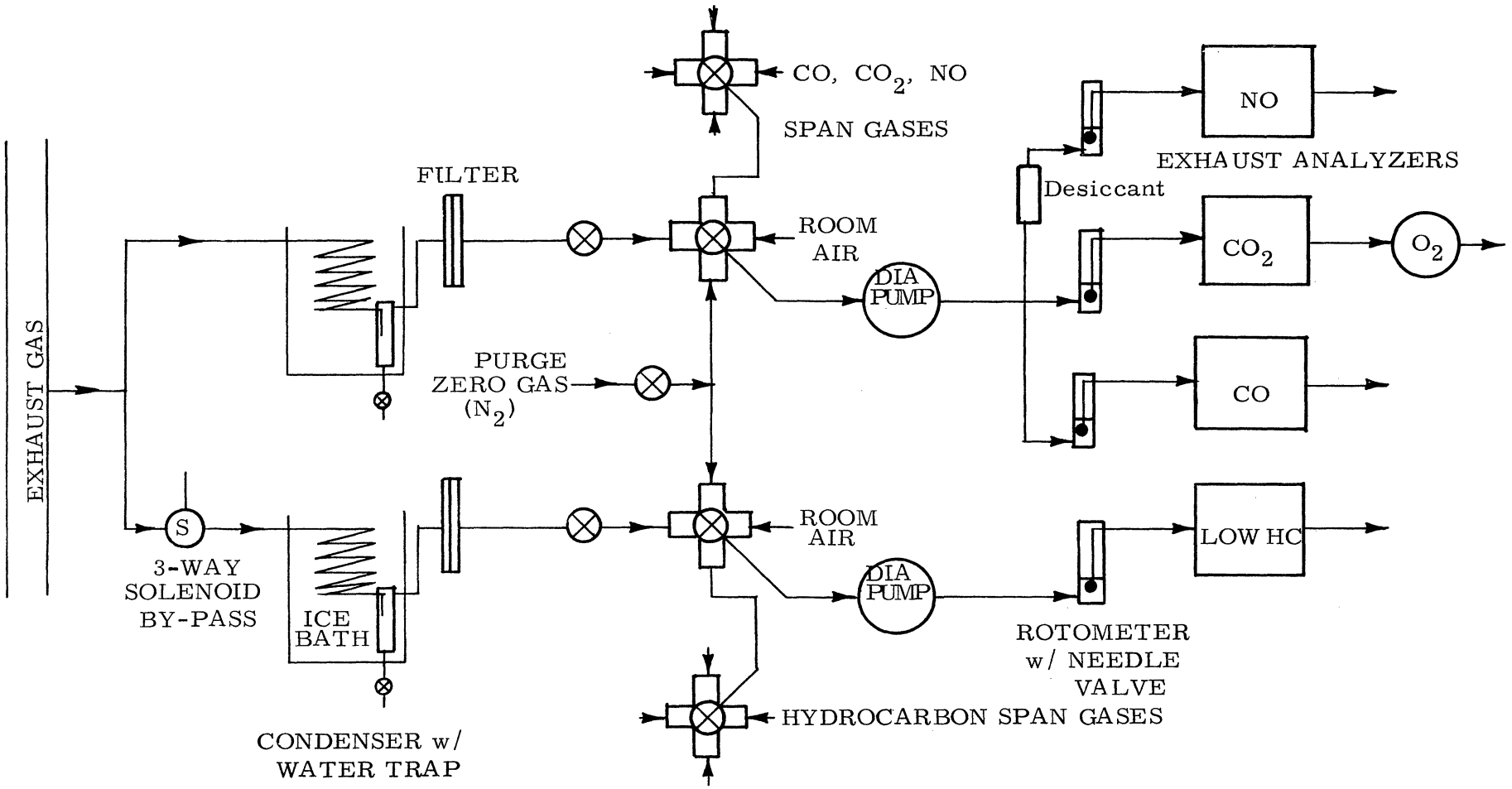

Figure 6. Flow schematic of University of Michigan hydrocarbon, CO, NO, O_2, and CO_2 exhaust gas analysis system.

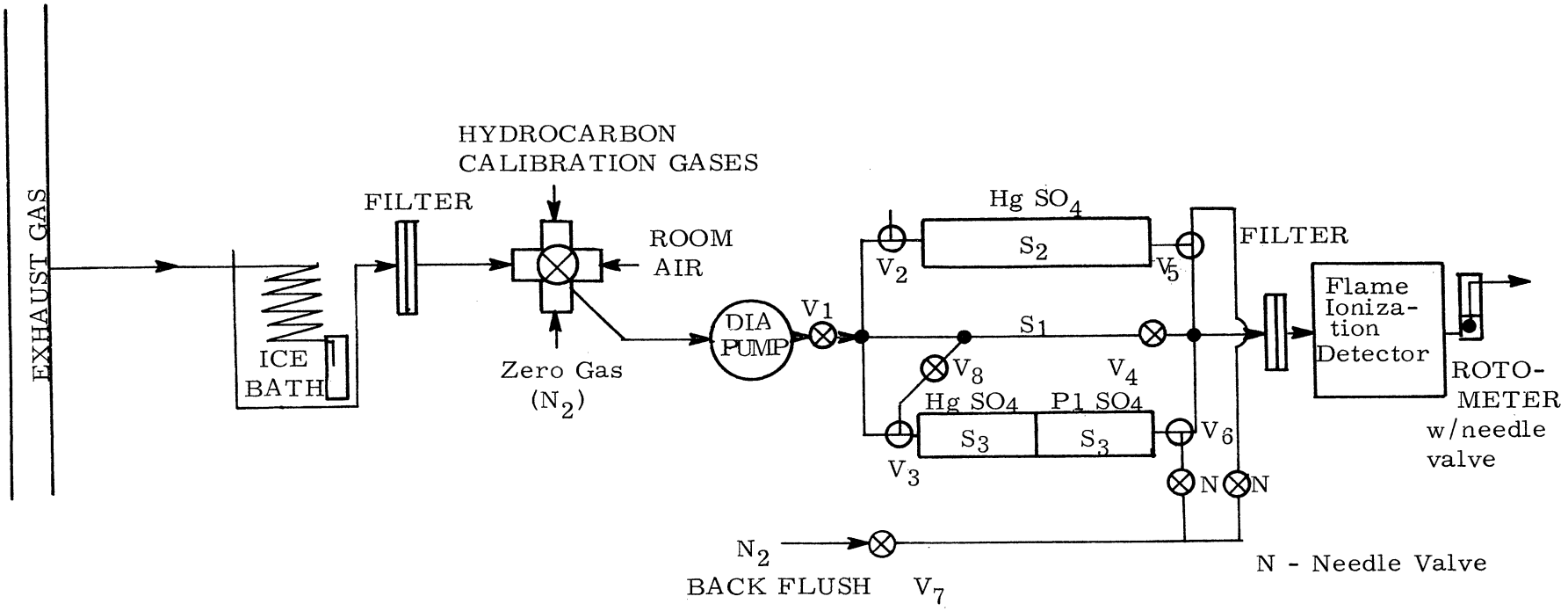

Position	Sample Seen by FID	Flow Path	Scrubber	Operation of Valves $V_{7,8}$	V_1	$V_{2,5}$	$V_{3,6}$	V_4
1	Back flush	S_2S_3	All	On	Off	Off	Off	On
2	Paraffins and benzene	S_3	$HgSO_4$ and Pd	Off	On	Off	On	Off
3	Total olefins	S_2	$HgSO_4$	Off	On	On	Off	Off
4	Total or zero	S_1	None	Off	On	Off	Off	On

Figure 7. Flow schematic of University of Michigan subtractive column-flame ionization hydrocarbon analysis system. The subtractive analyzer is patterned after that of Sigsby, Ref. 8 of Phase I progress.

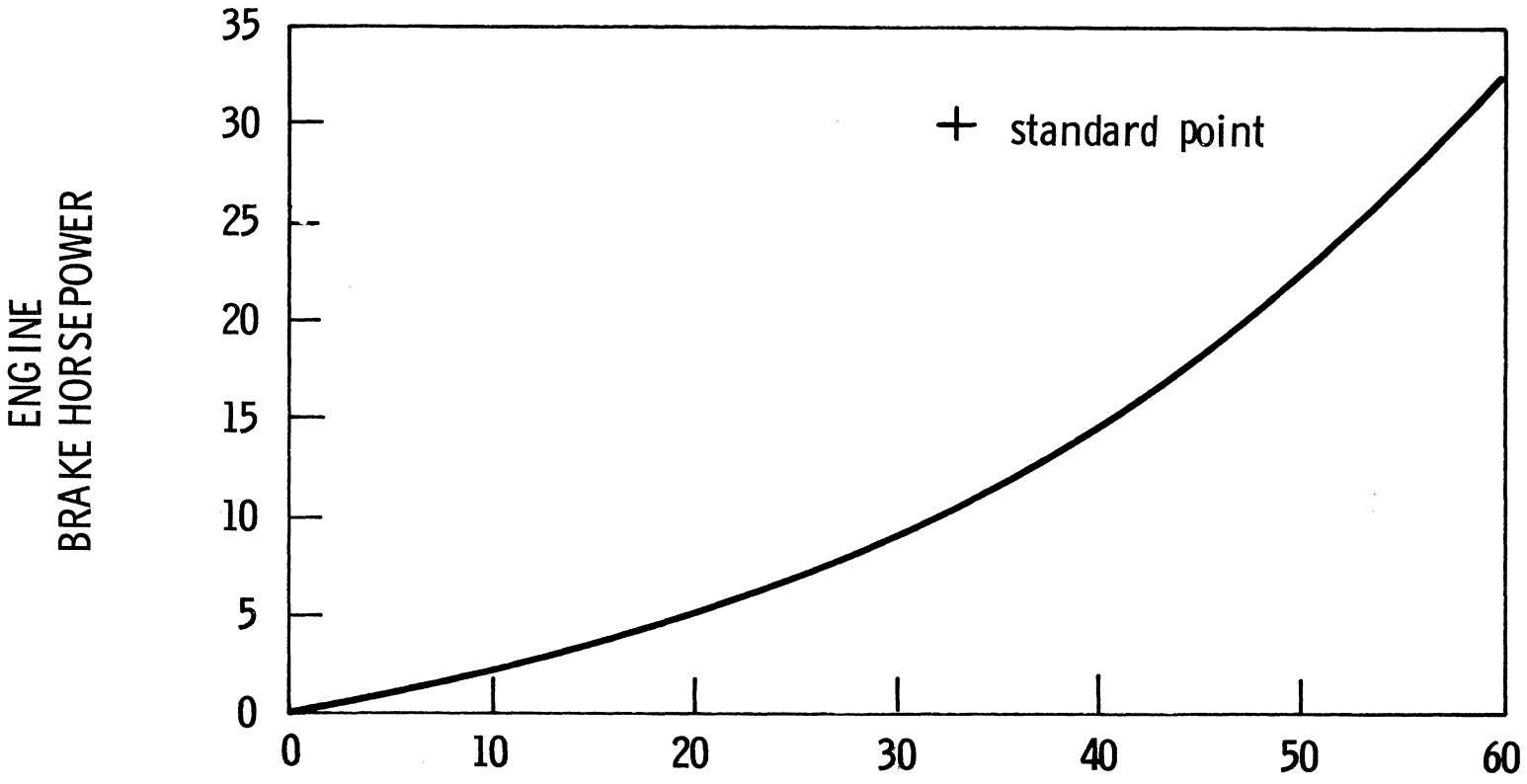

Figure 8. Calculated road load engine horsepower requirement as a function of car speed. Graph based upon assumptions and formulas of Table IV.

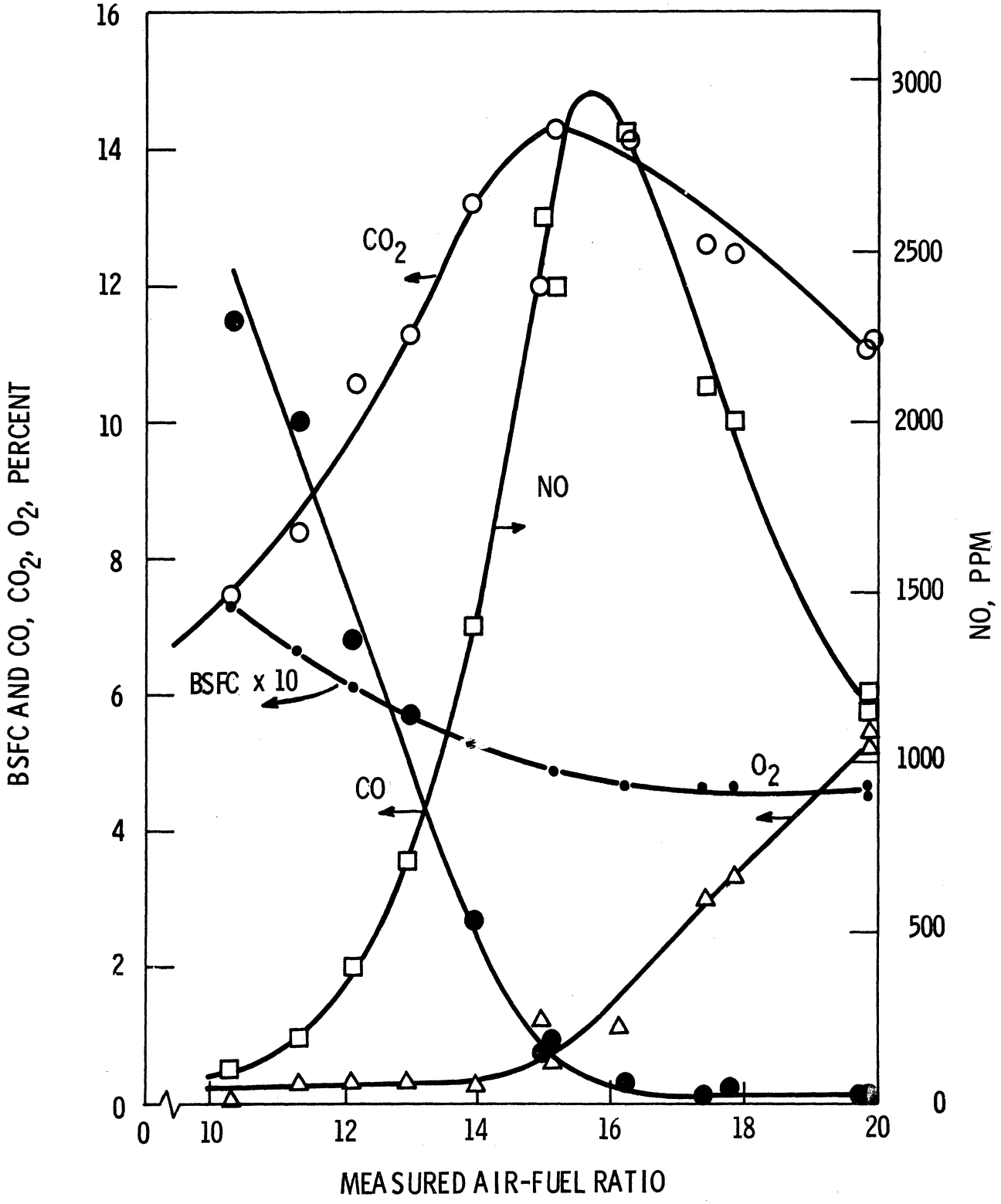

Figure 9. CO_2, CO, O_2, and NO emission vs. air/fuel ratio. 1200 rpm, 50% load, MBT spark, Indolene clear fuel.

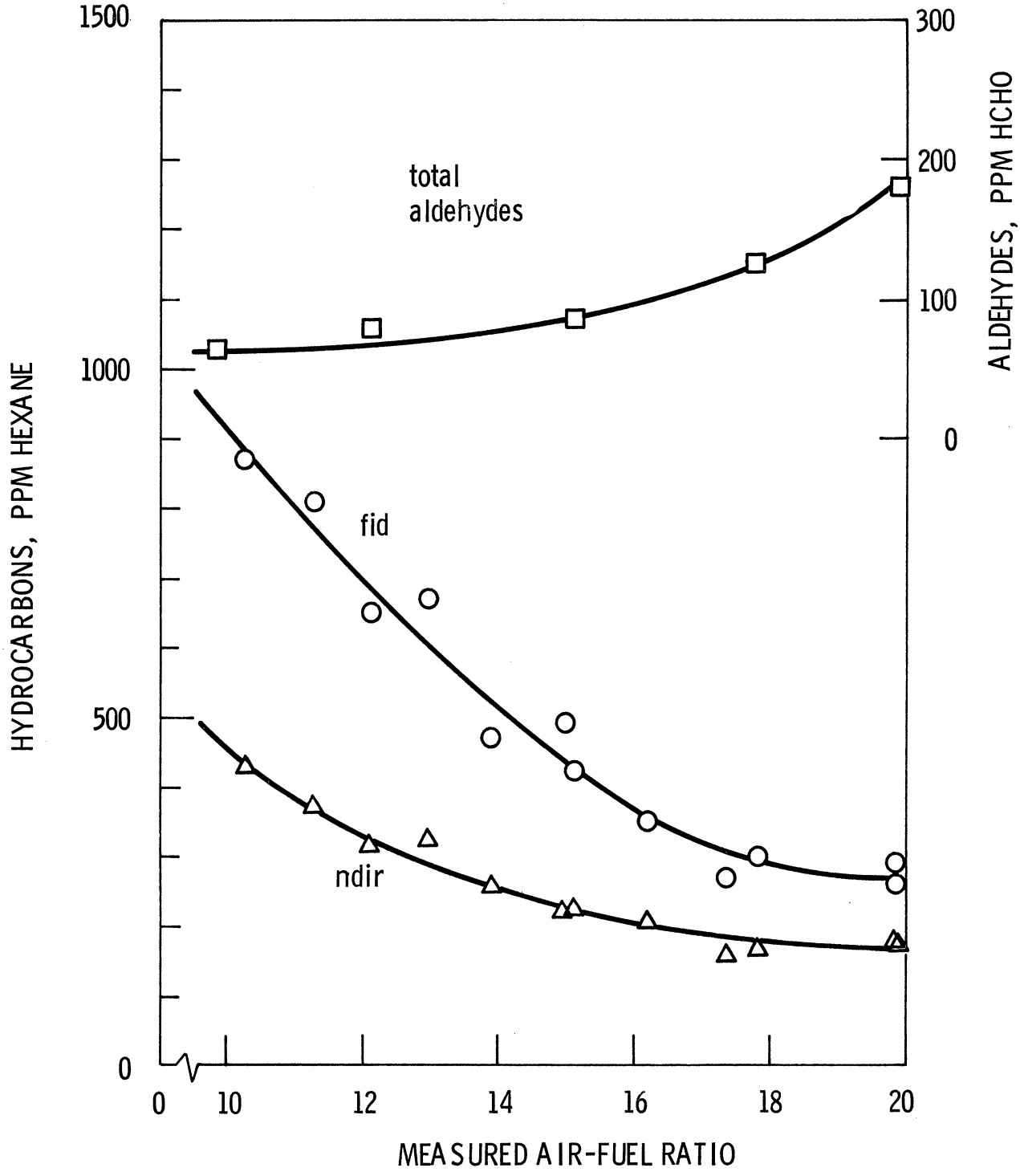

Figure 10. Hydrocarbon and aldehyde emission vs. air/fuel ratio. 1200 rpm, 50% load, MBT spark, Indolene clear fuel.

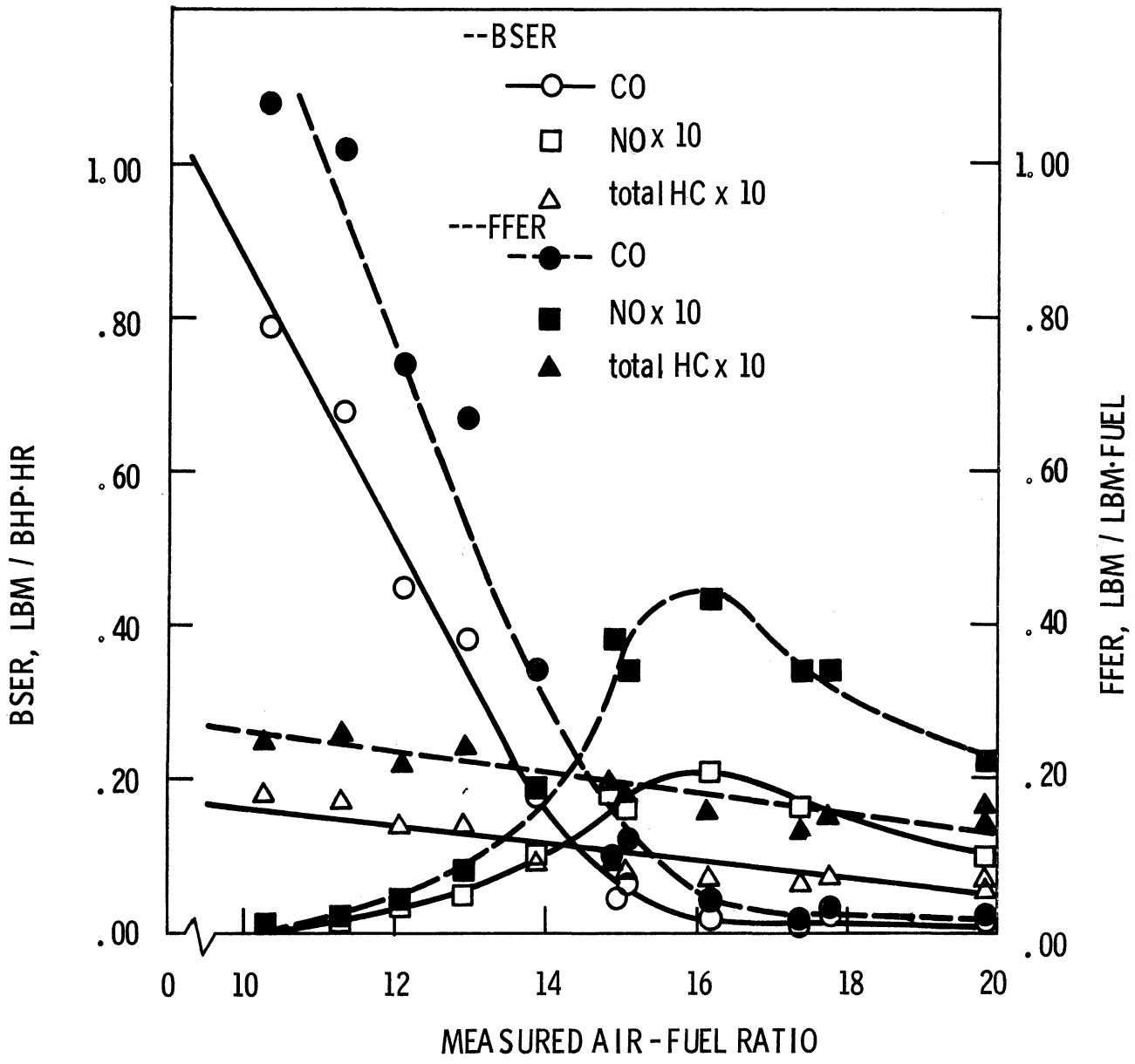

Figure 11. Mass emission vs. air/fuel ratio. 1200 rpm, 50% load, MBT spark, Indolene clear fuel.

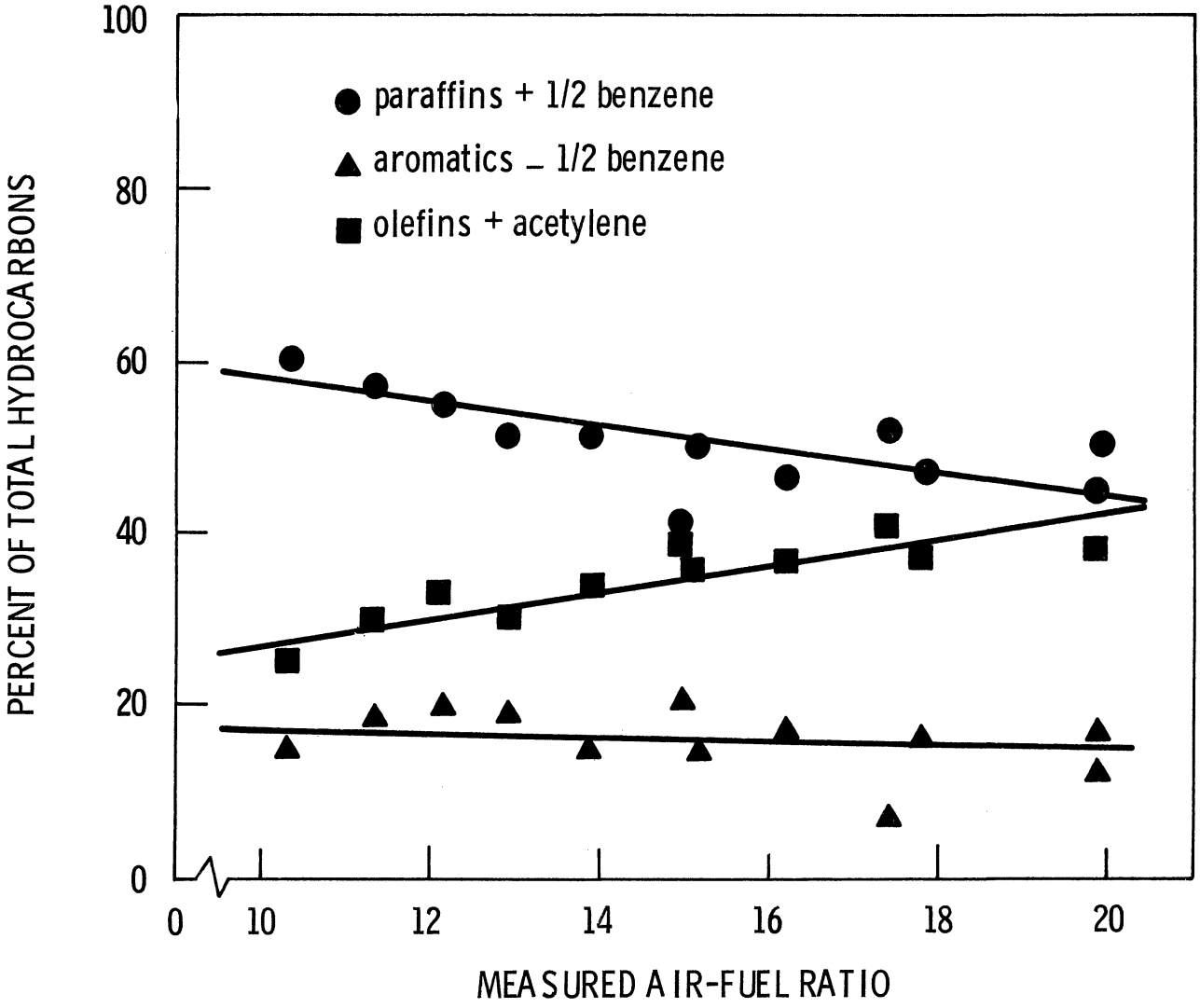

Figure 12. Hydrocarbon class analysis vs. air/fuel ratio.

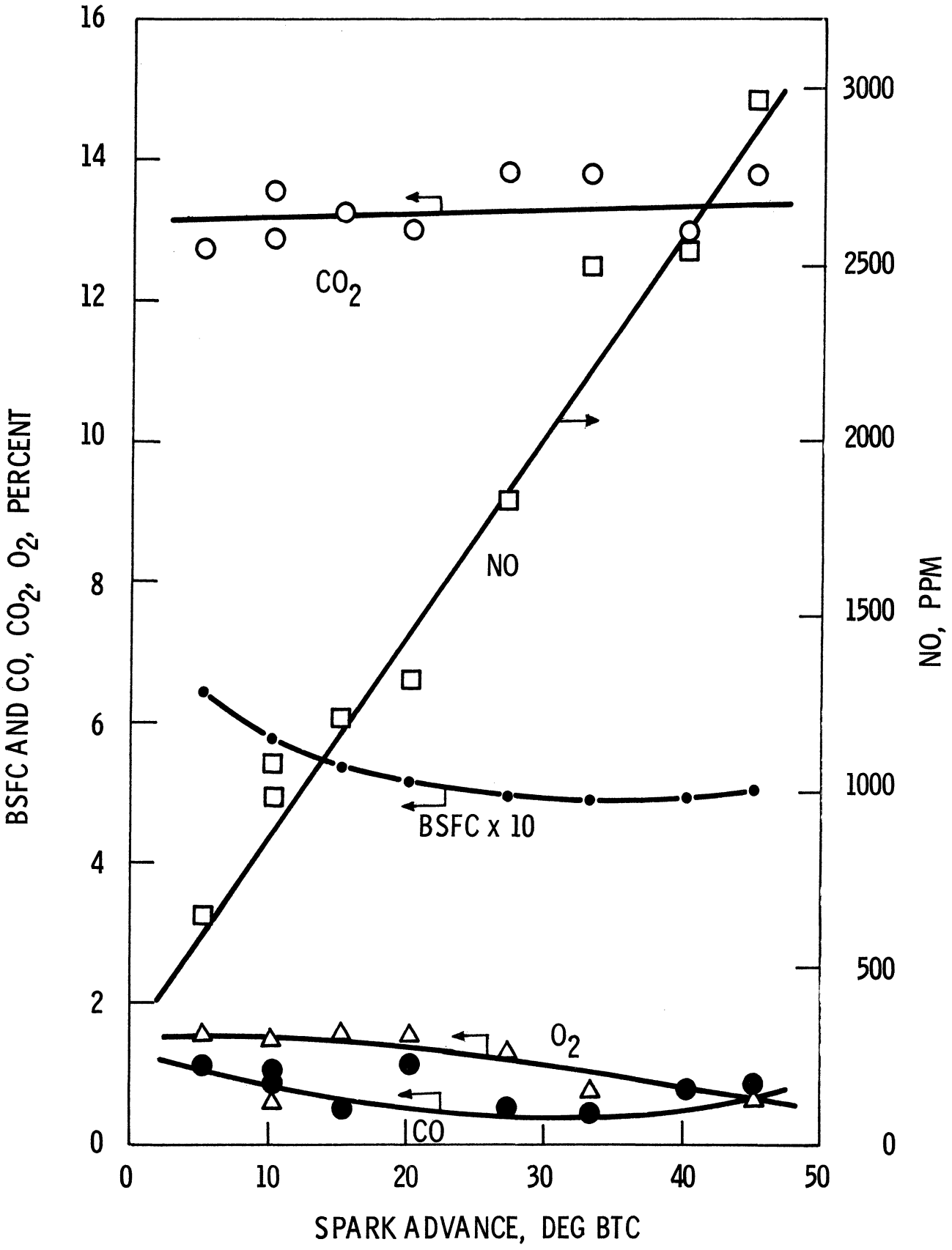

Figure 13. CO_2, CO, O_2, and NO concentration emission vs. spark timing. 1200 rpm, 50% load, 15.4:1 A/F ratio, Indolene 30 fuel.

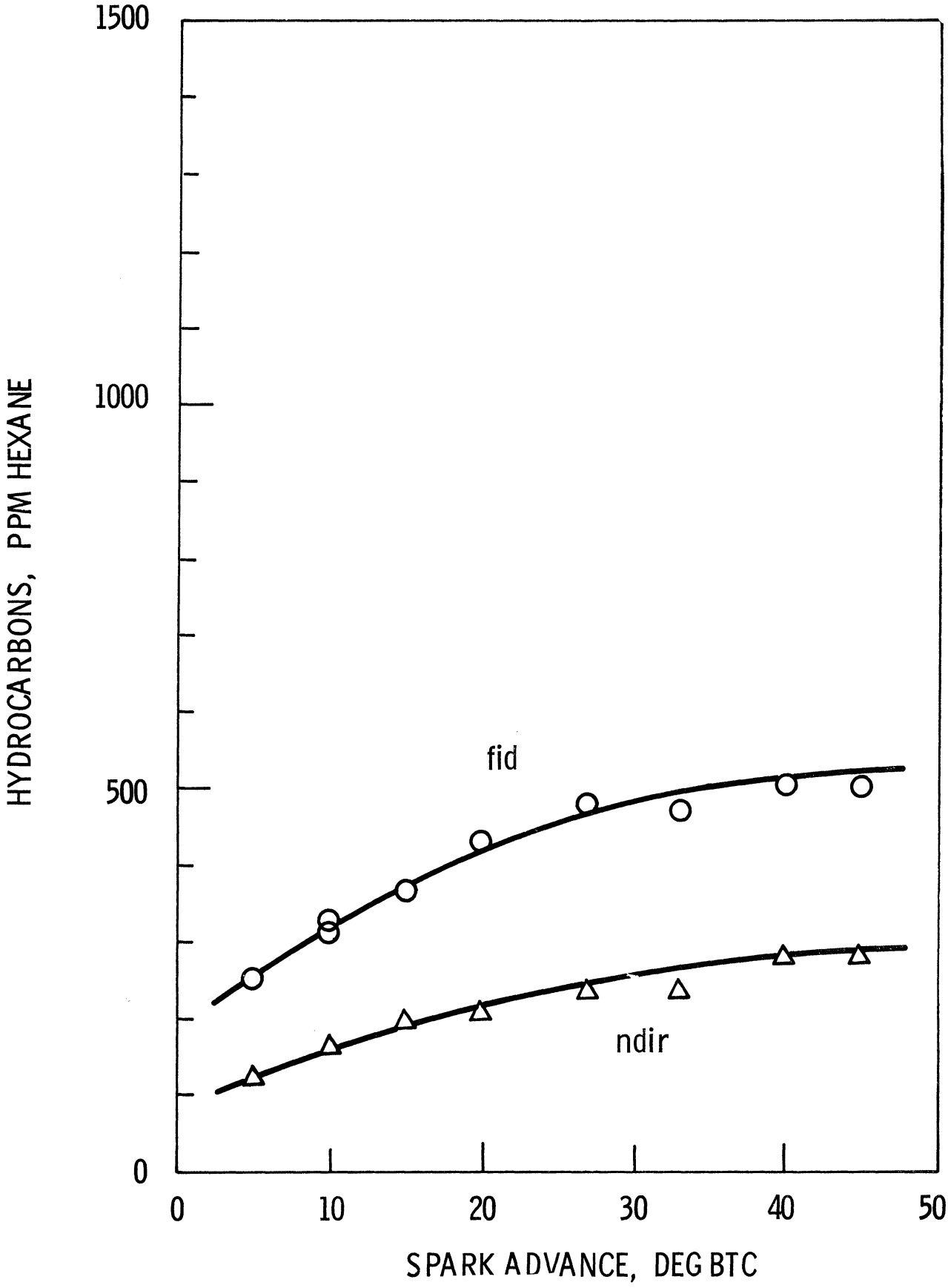

Figure 14. Hydrocarbon emissions vs. spark advance. 1200 rpm, 50% load, 15.4:1 A/F ratio, Indolene 30 fuel.

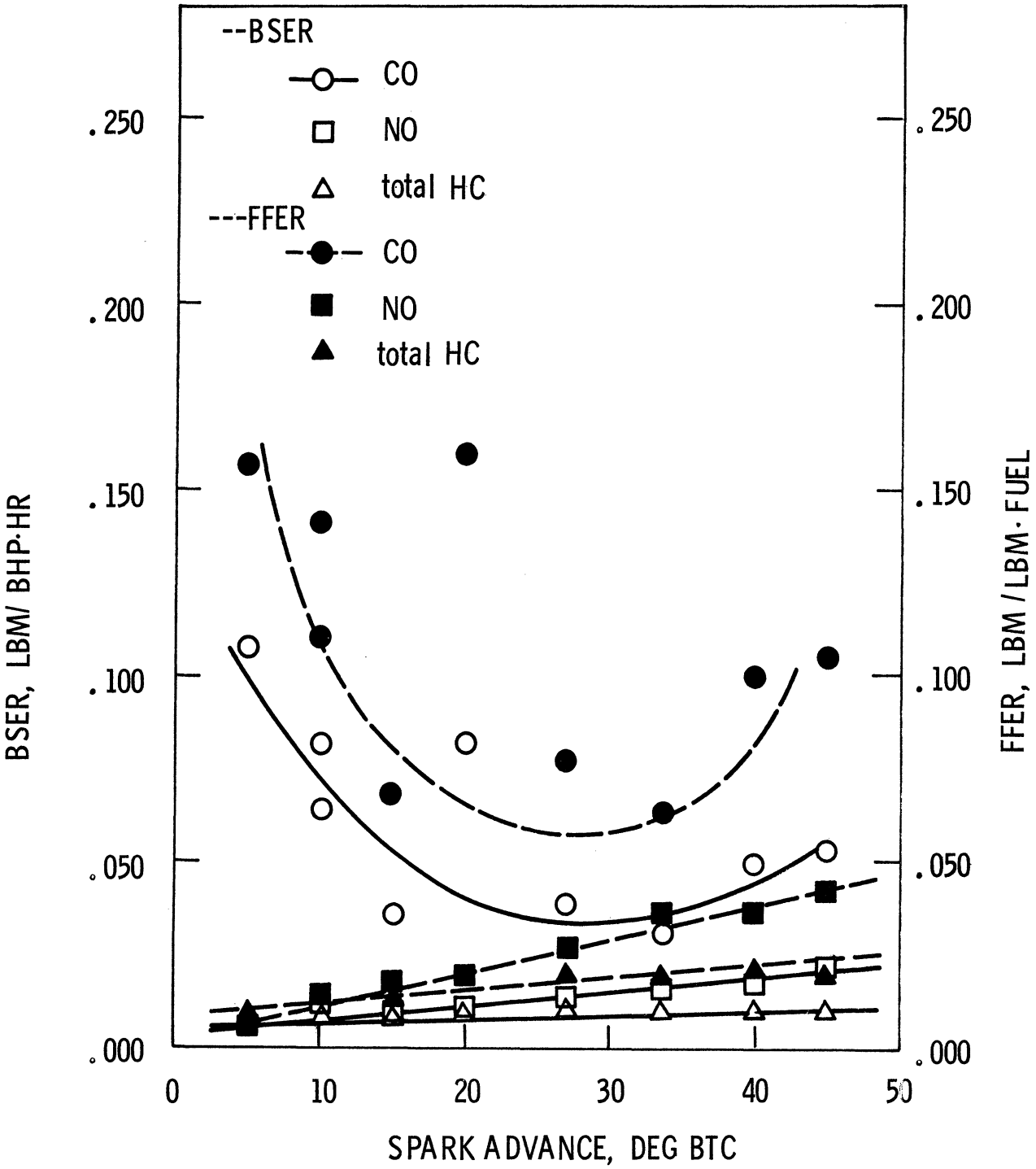

Figure 15. Mass emission vs. spark advance. 1200 rpm, 50% load, 15.4:1 A/F ratio, Indolene 30 fuel.

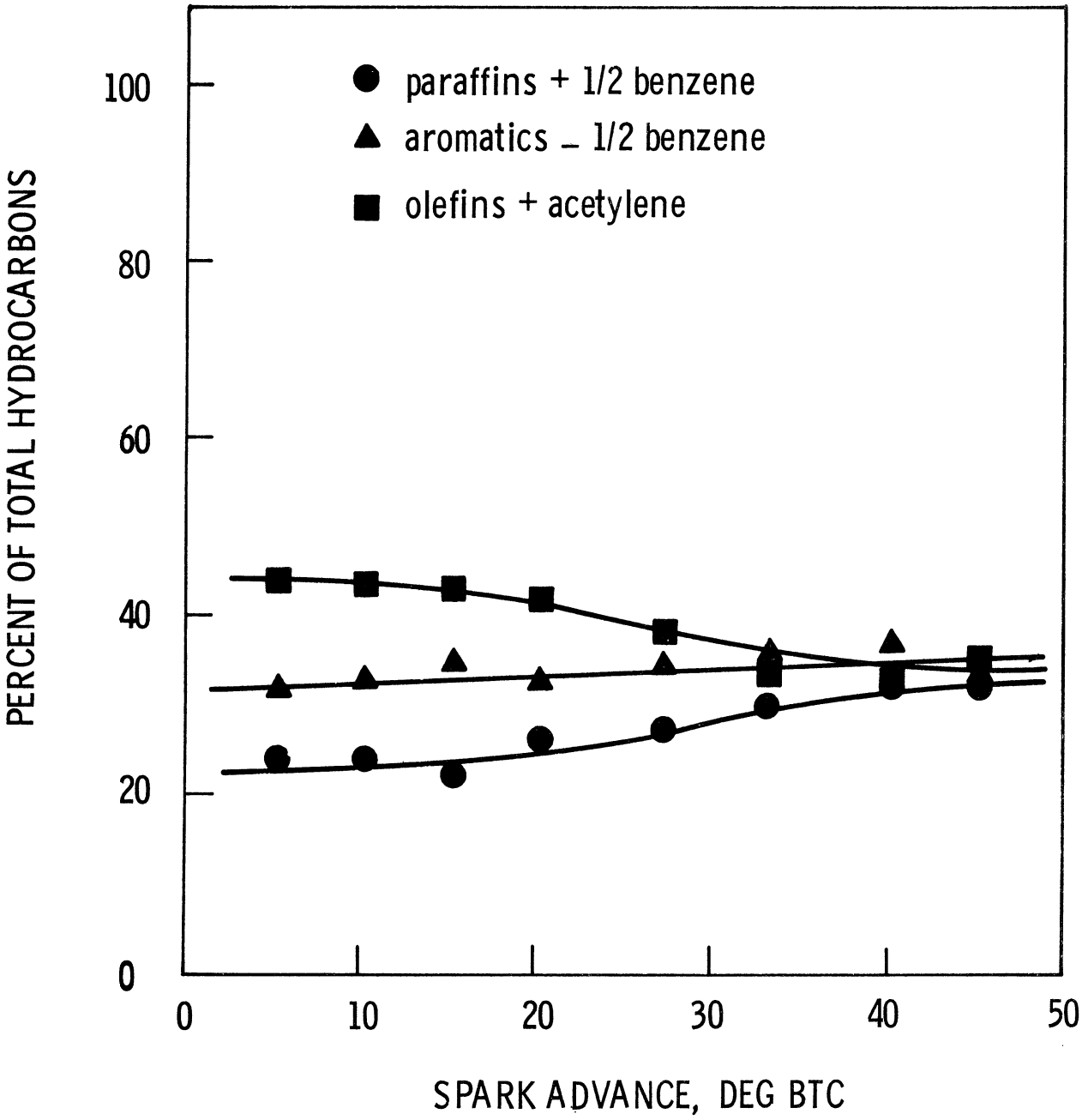

Figure 16. Hydrocarbon class analysis vs. spark advance.

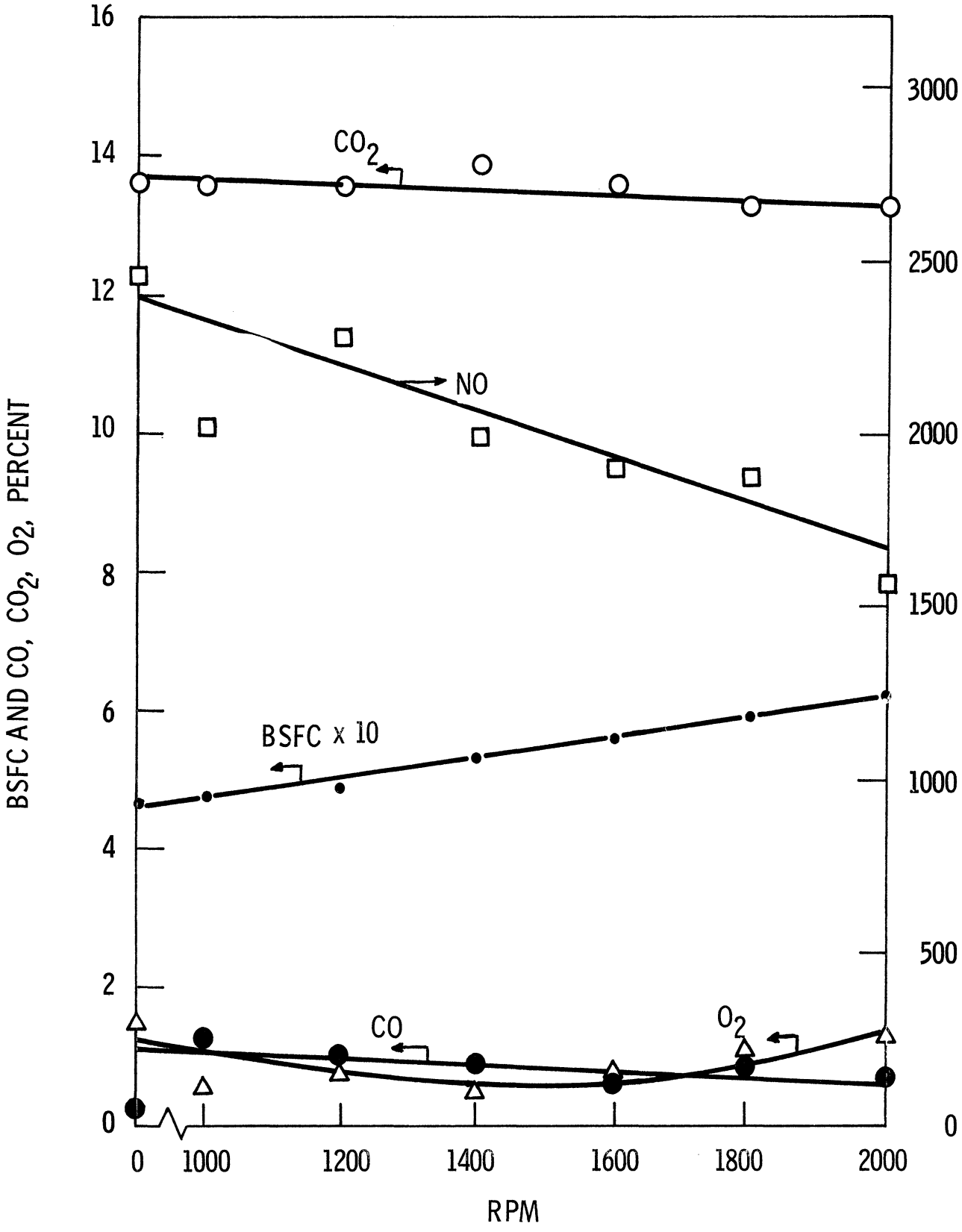

Figure 17. CO_2, CO, O_2, and NO emission vs. engine speed. 50% load, MBT spark, 14.8:1 A/F ratio, Indolene 30 fuel.

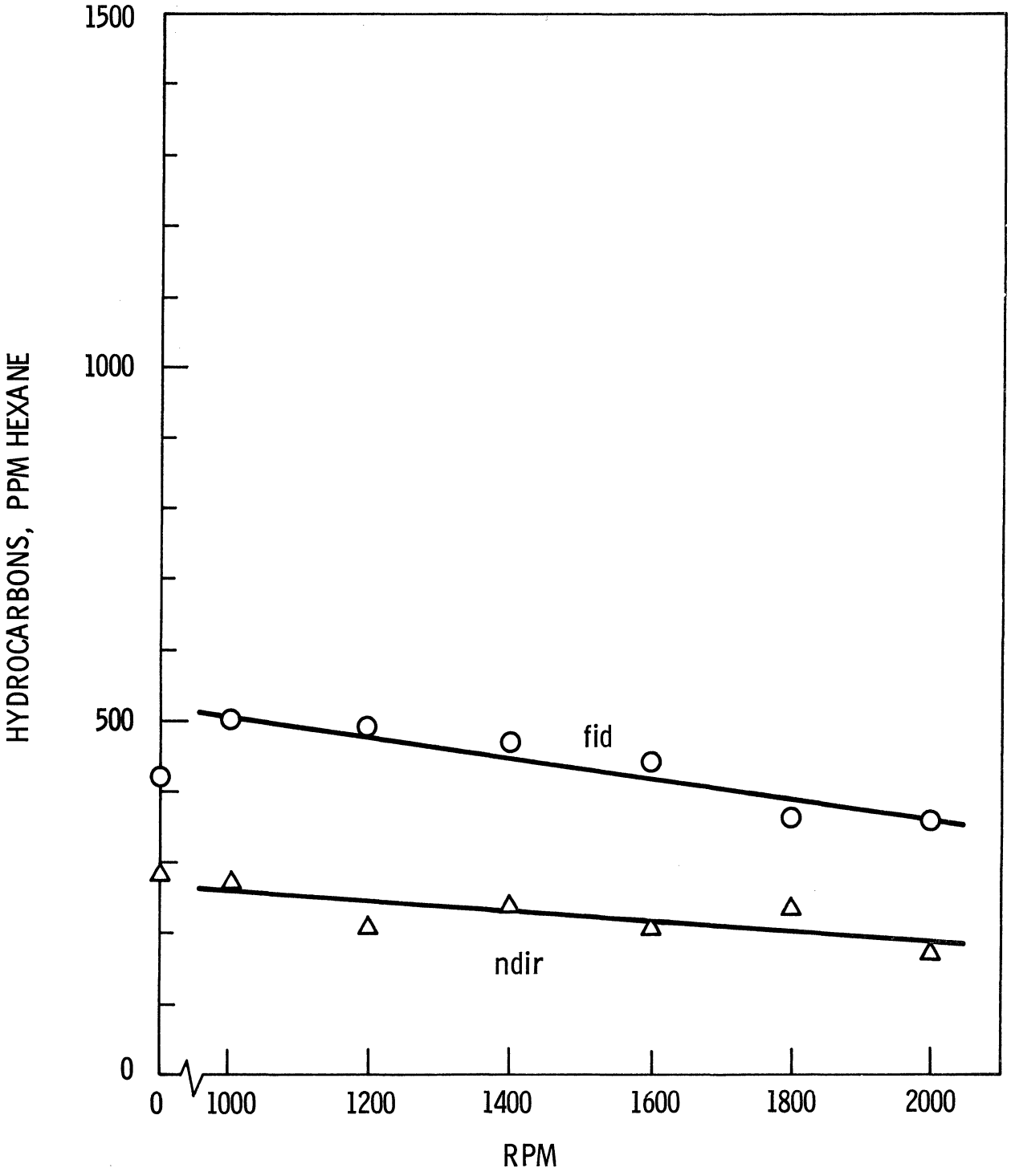

Figure 18. Hydrocarbon emission vs. engine speed. 50% full load, MBT spark, 14.8:1 A/F ratio, Indolene 30 fuel.

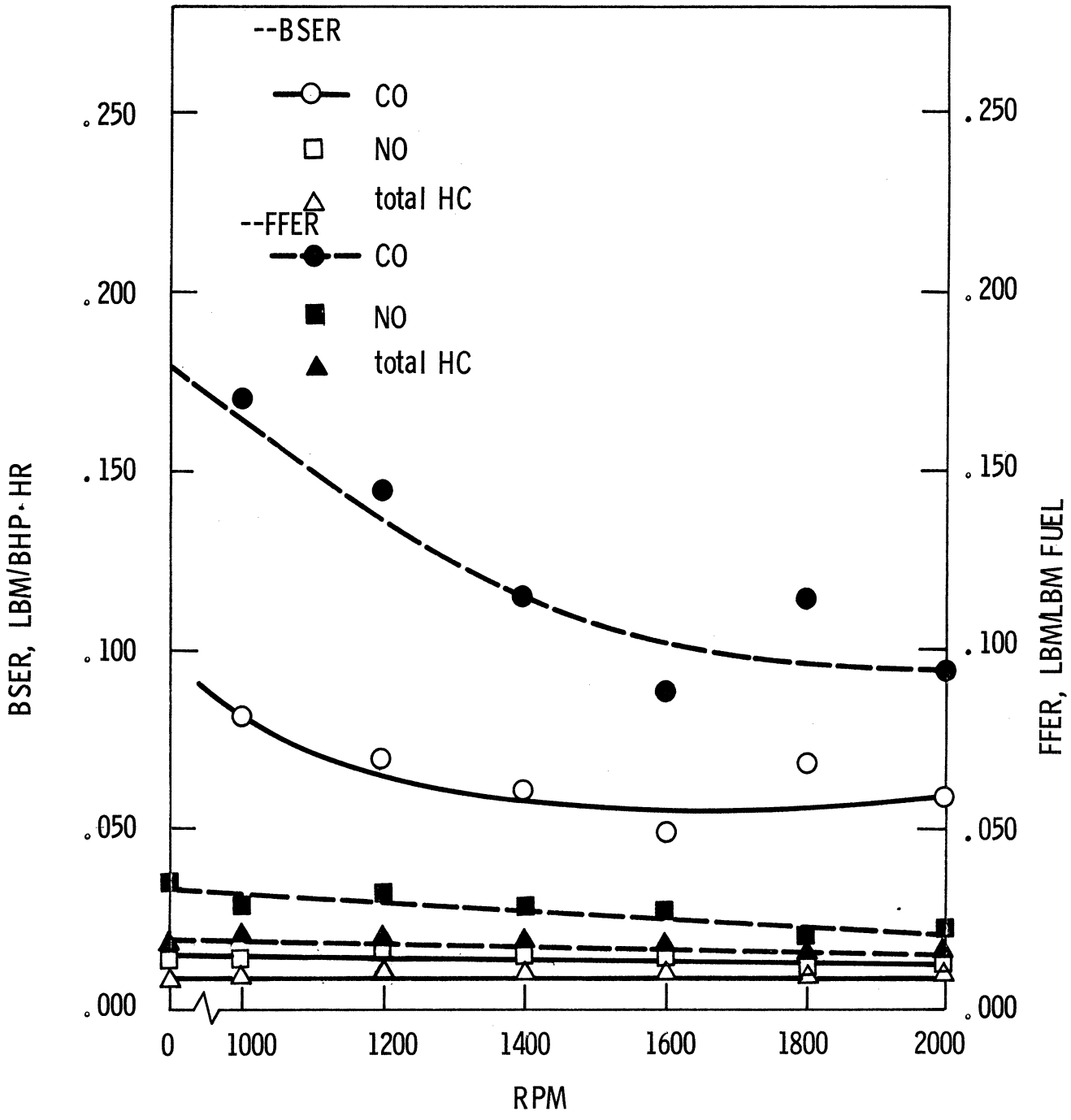

Figure 19. Mass emission vs. engine rpm. 50% load, MBT spark, 14.8:1 A/F ratio, Indolene 30 fuel.

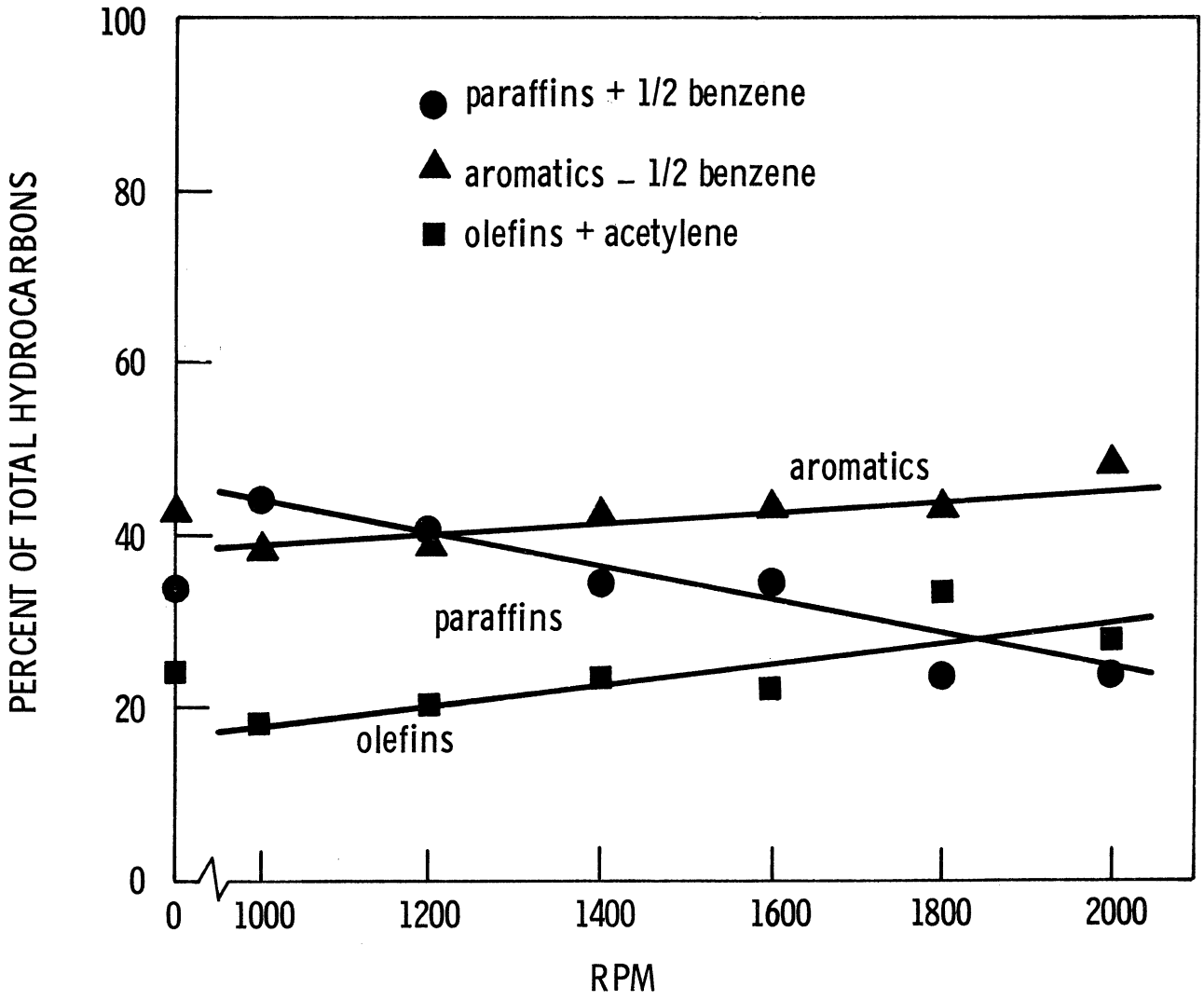

Figure 20. Hydrocarbon class analysis vs. engine speed.

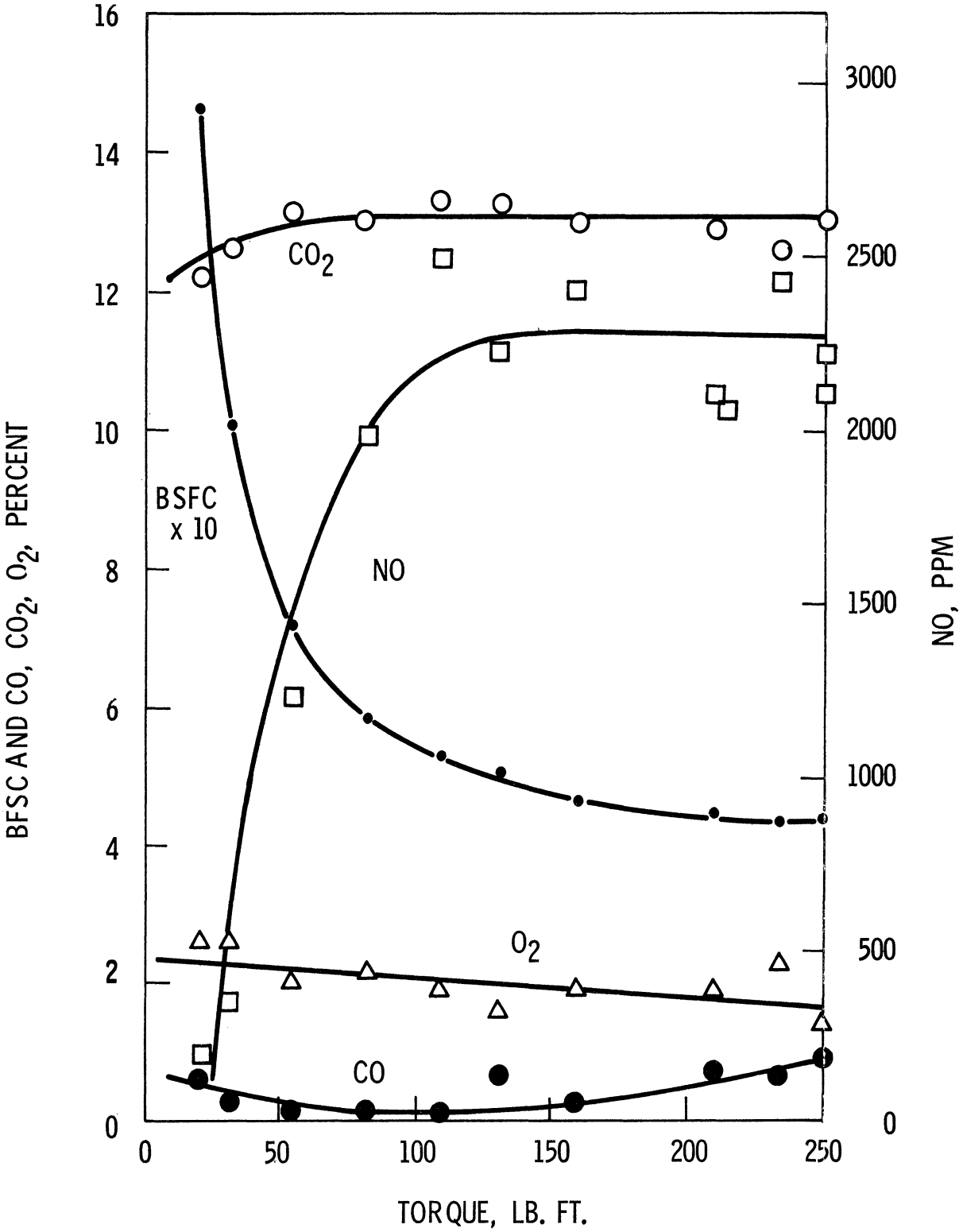

Figure 21. CO_2, CO, O_2, and NO emission vs. torque. 1200 rpm, MBT spark, 15.8:1 A/F ratio, Indolene 30 fuel.

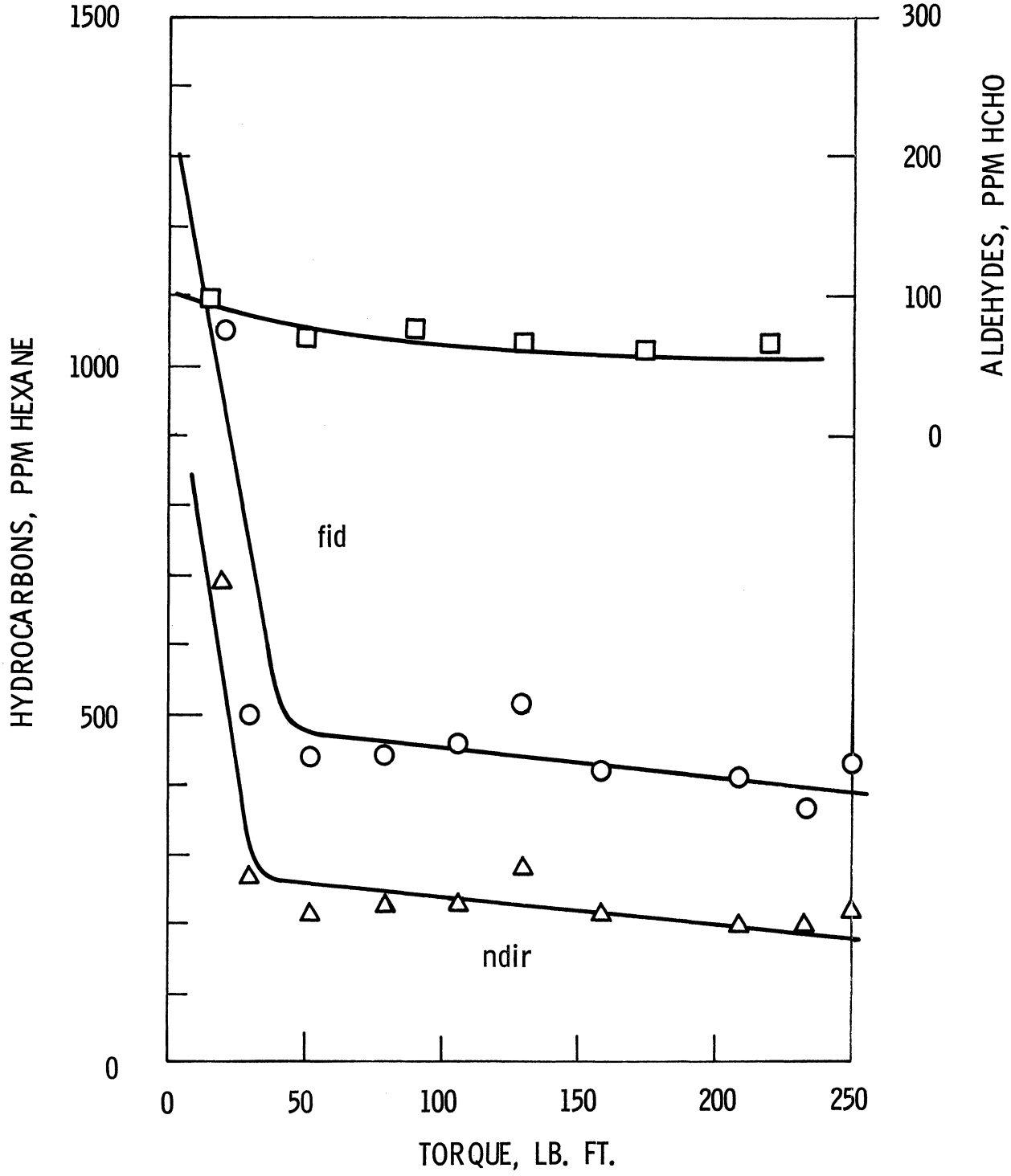

Figure 22. Hydrocarbon and aldehyde emission vs. load. 1200 rpm, MBT spark, 15.8:1 A/F ratio, Indolene 30 fuel.

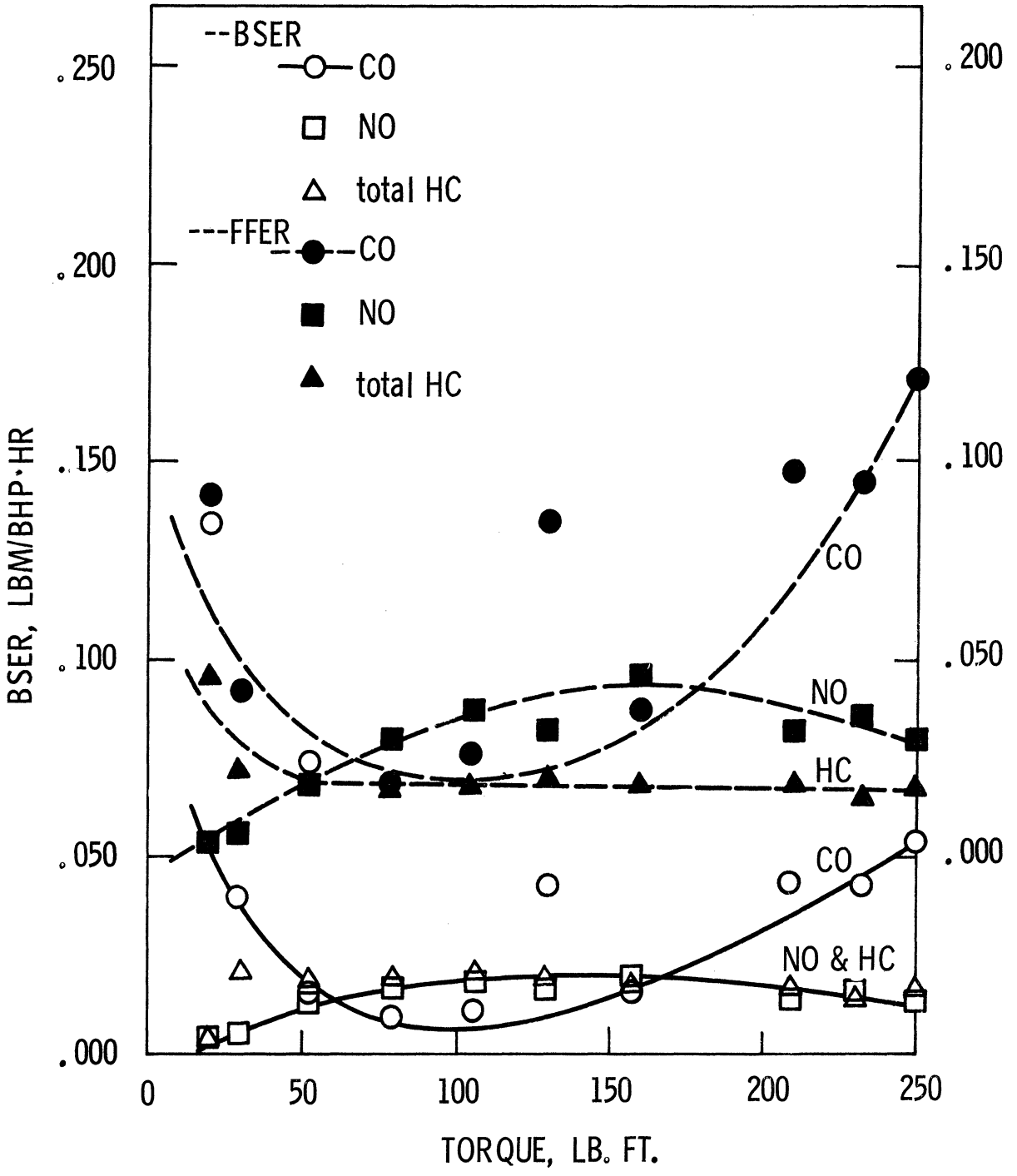

Figure 23. Mass emission vs. load. 1200 rpm, MBT spark, 15.8:1 A/F ratio, Indolene 30 fuel.

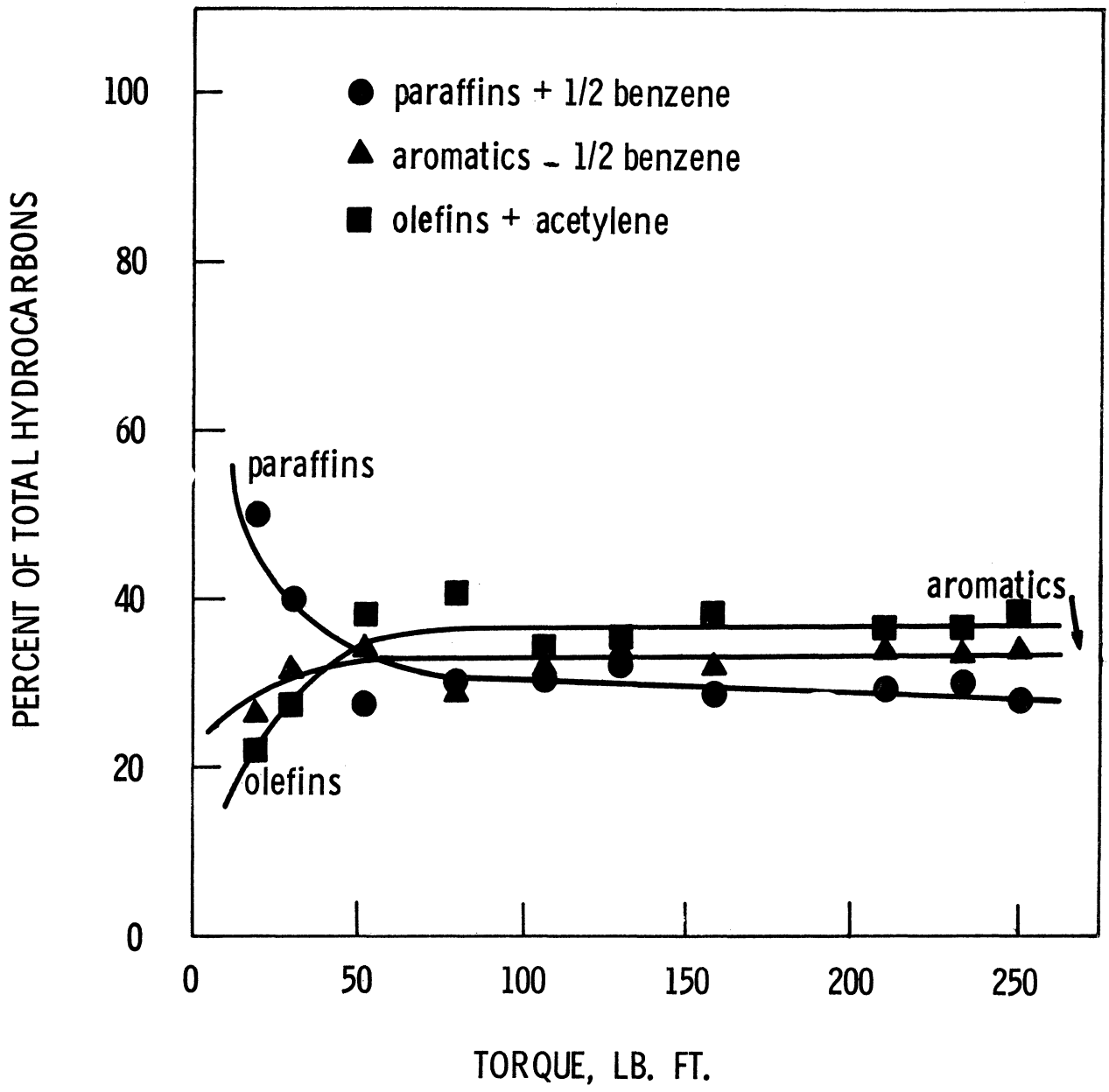

Figure 24. Hydrocarbon class analysis vs. load.

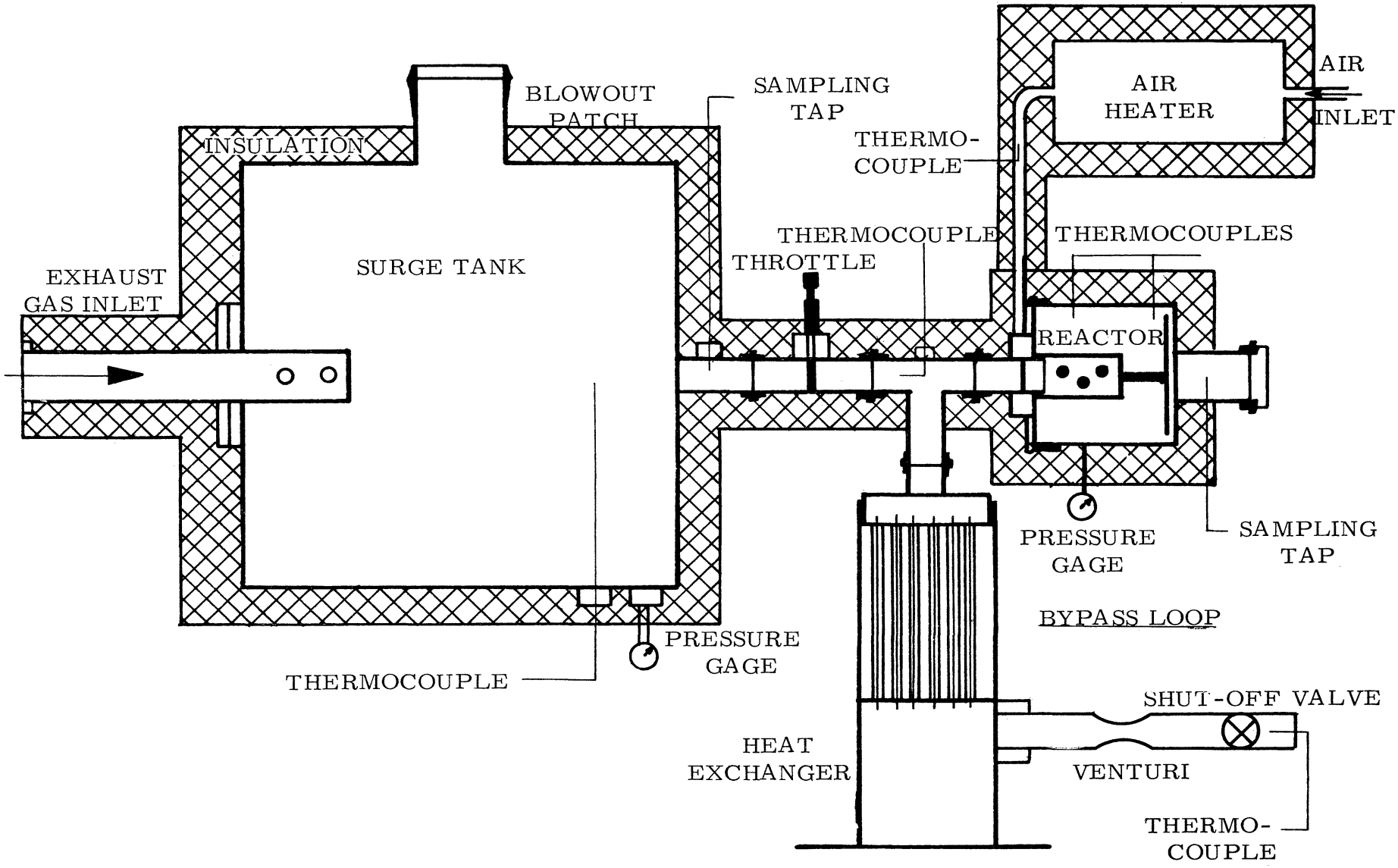

Figure 25. Two-tank experimental reactor system schematic.

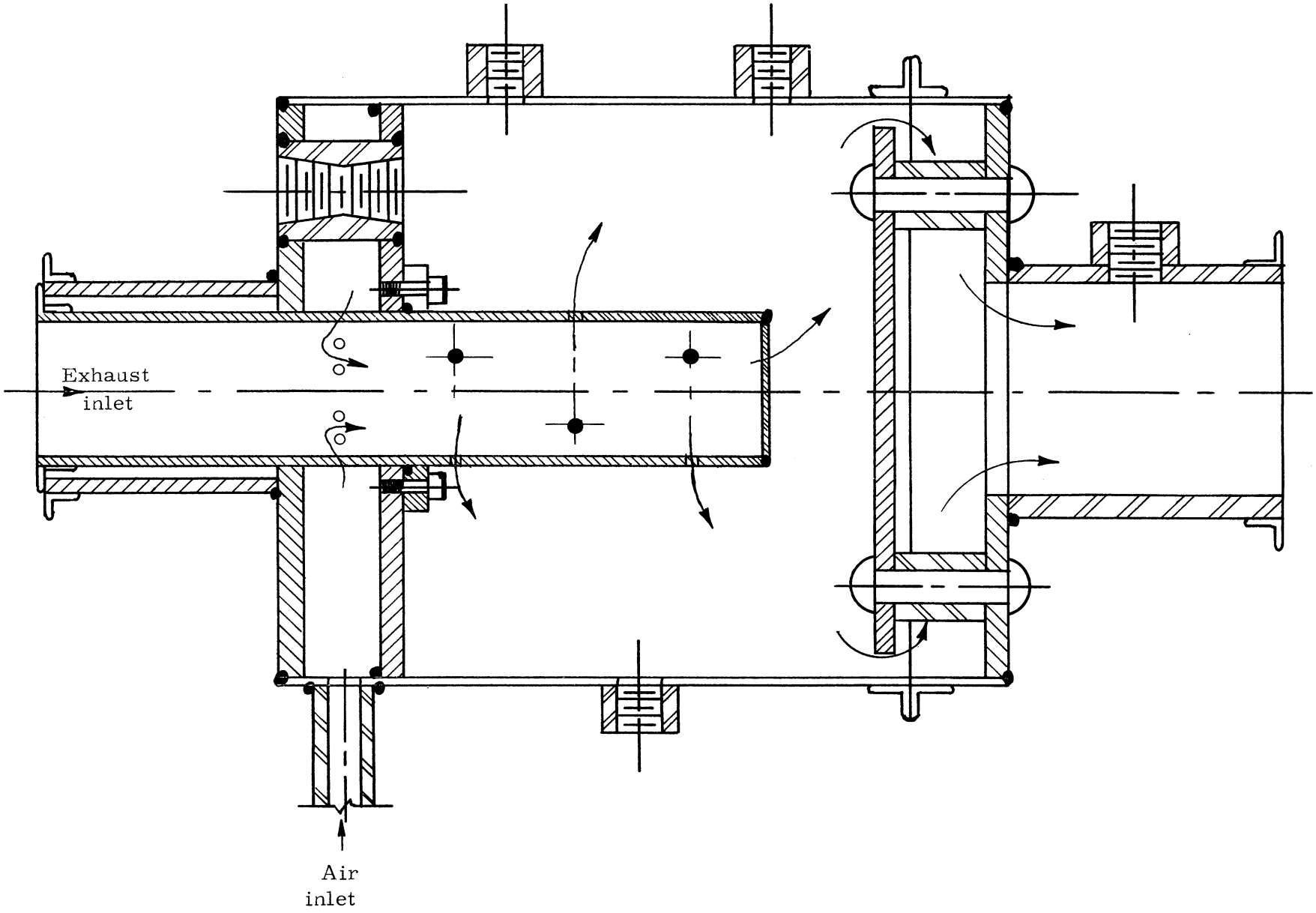

Figure 26. Experimental reactor cross section. Arrows suggest flow.

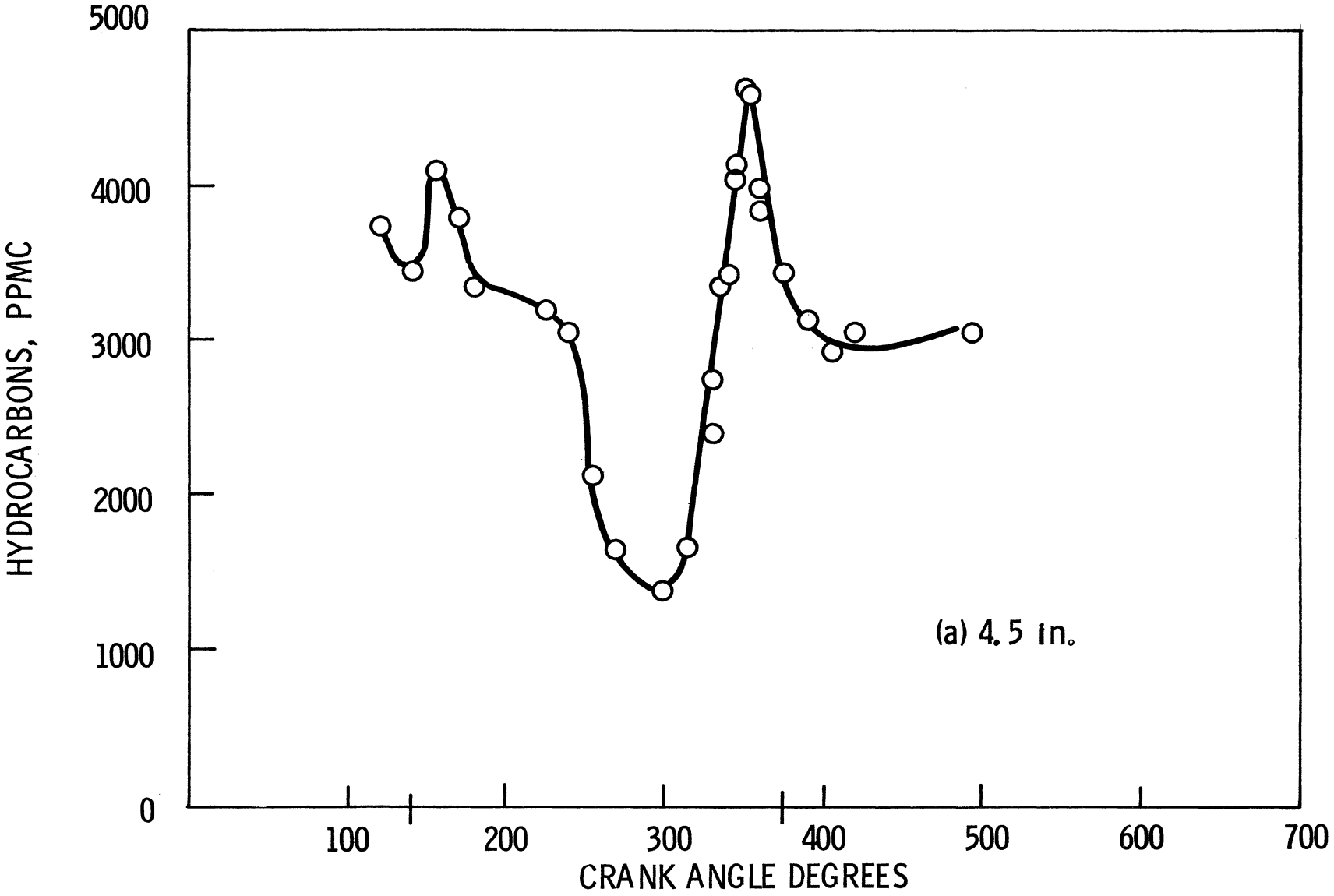

Figure 27. Variation in hydrocarbon concentration downstream of exhaust valve.

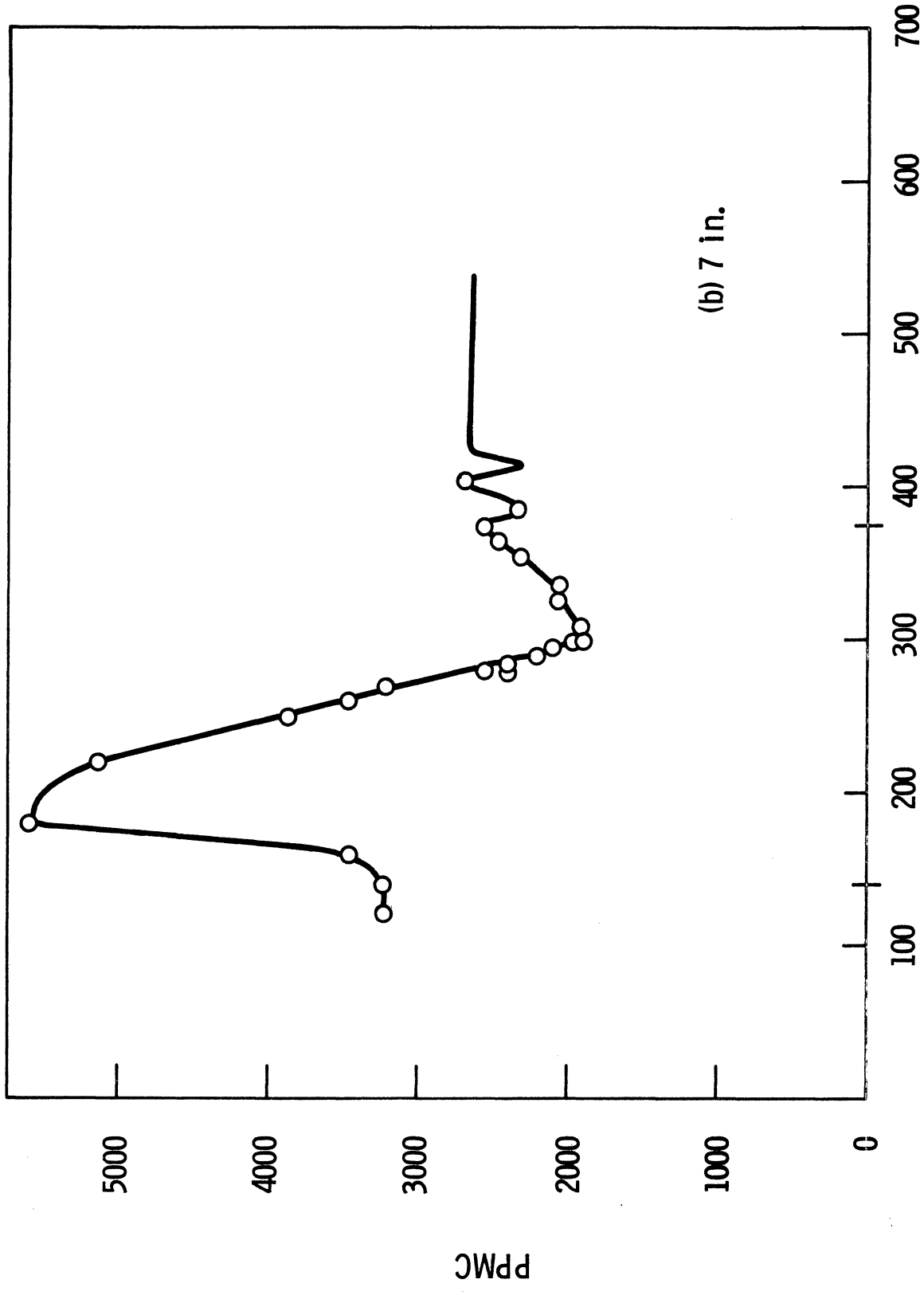

Figure 27. (Continued)

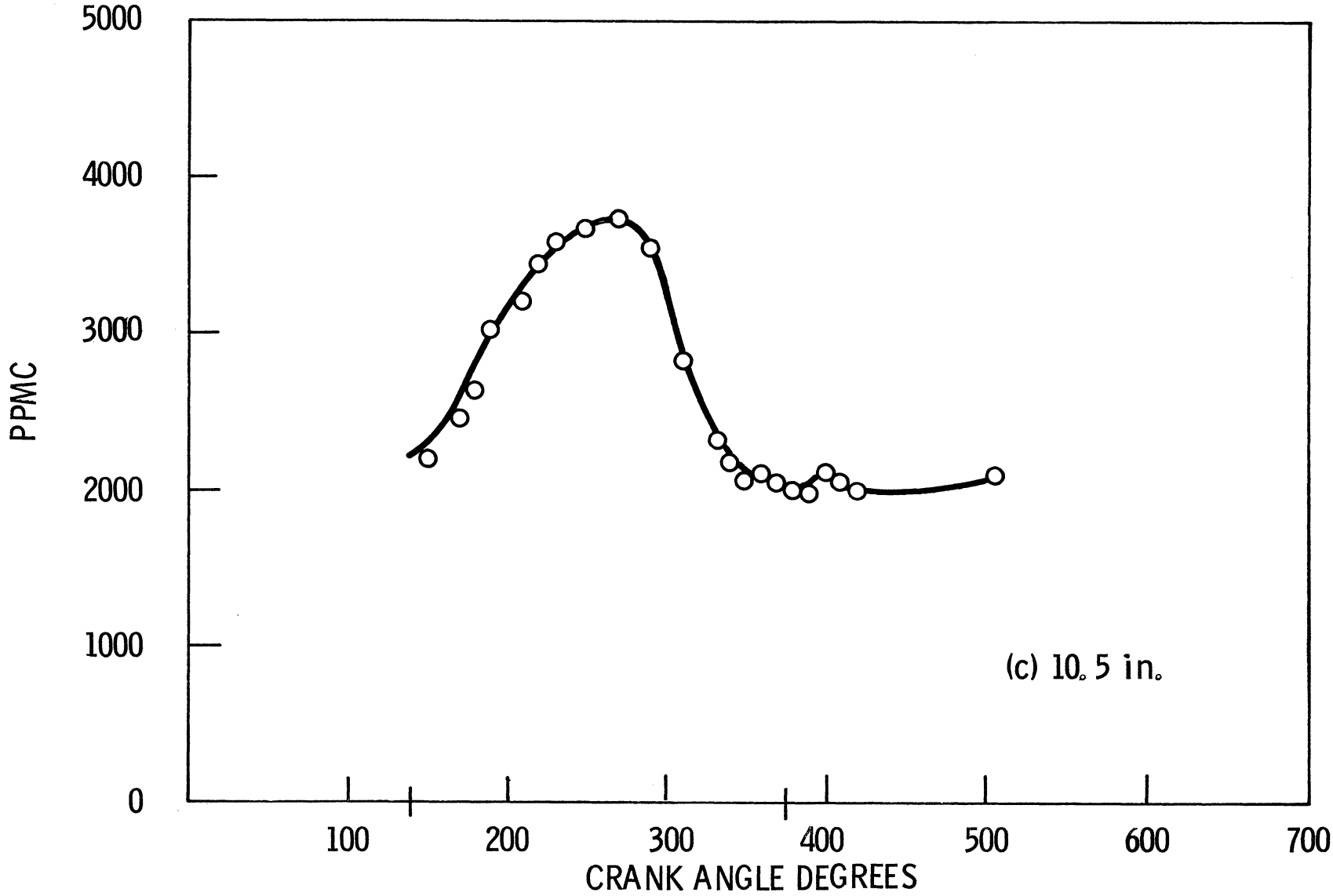

Figure 27. (Continued)

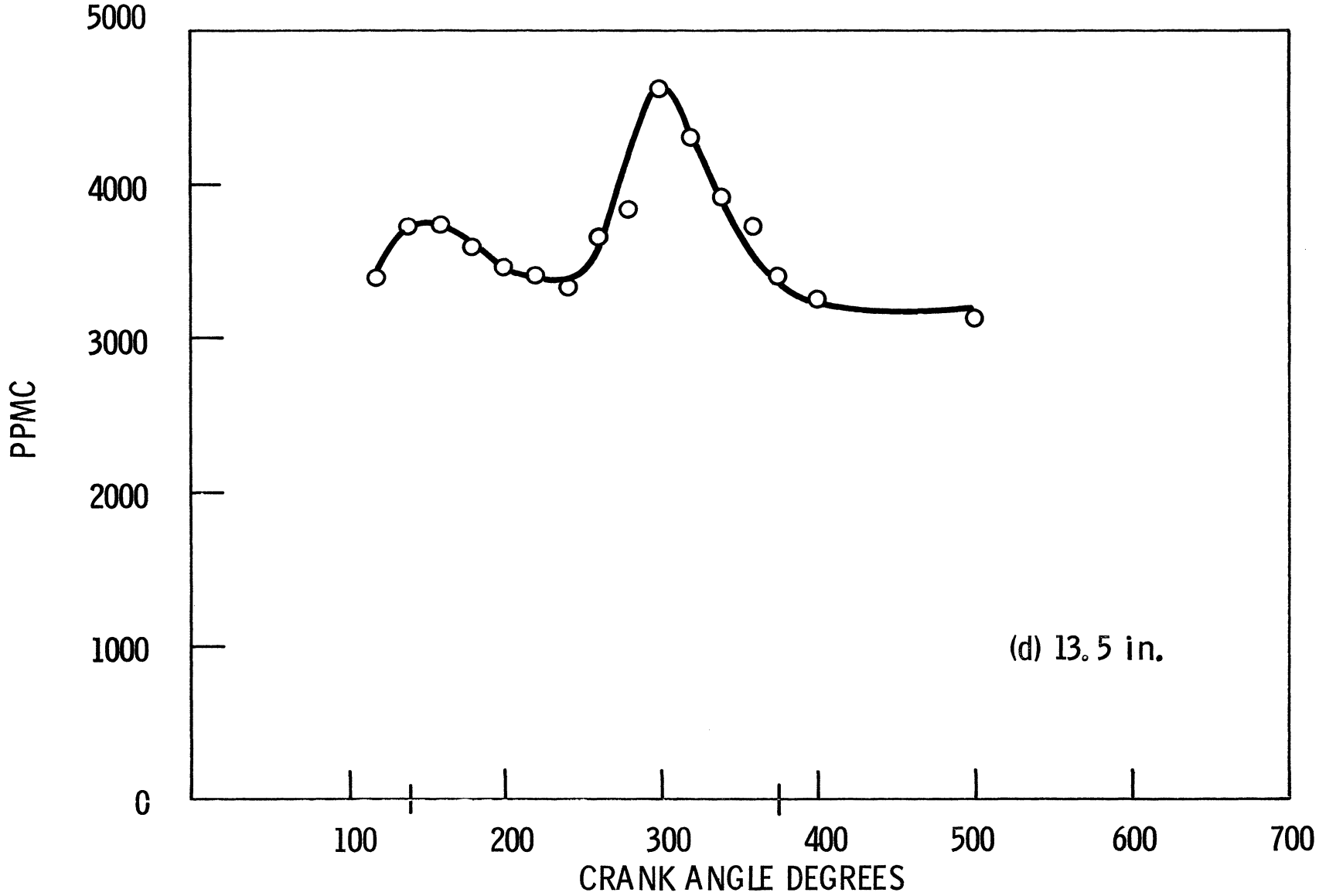

Figure 27. (Continued)

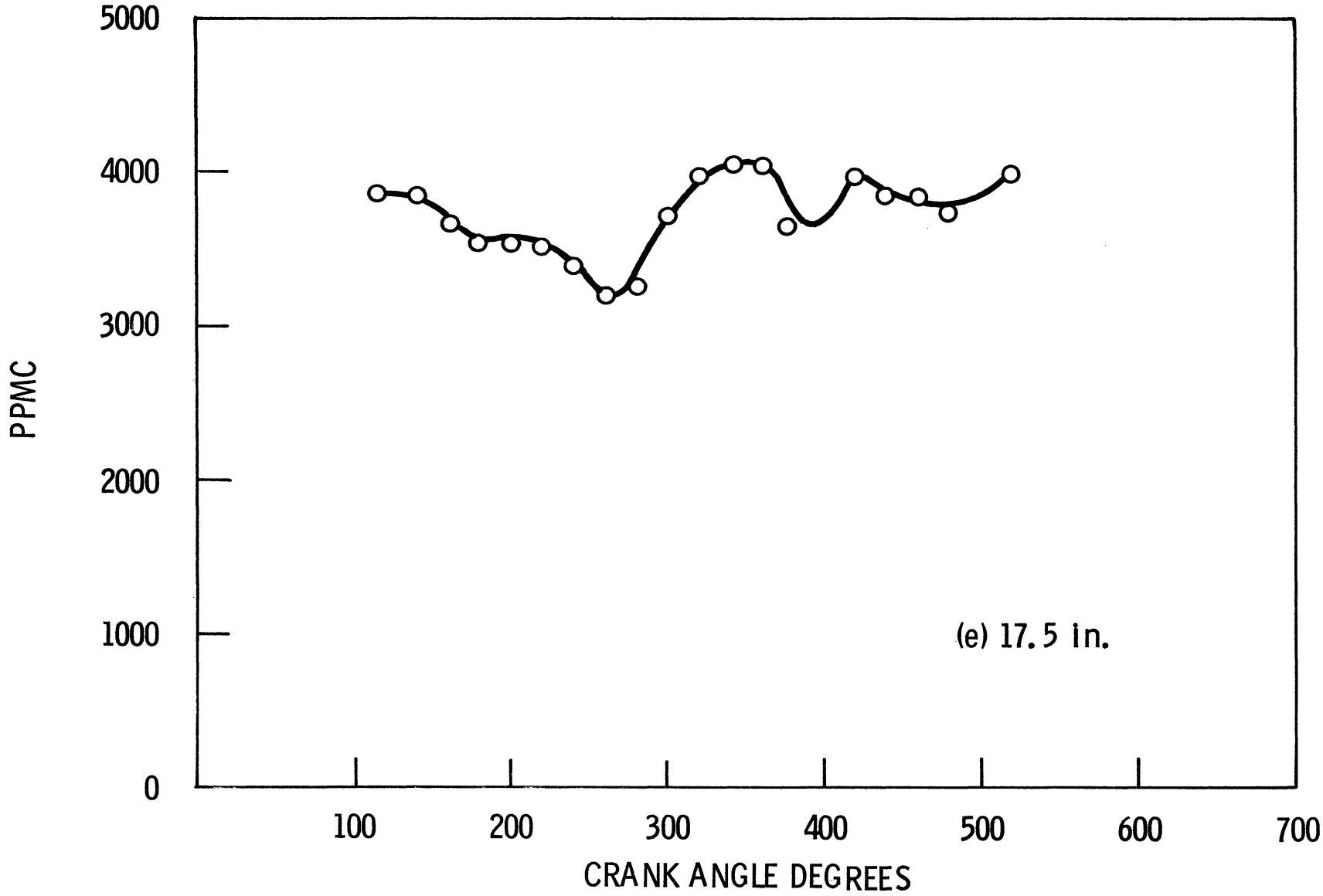

Figure 27. (Concluded)

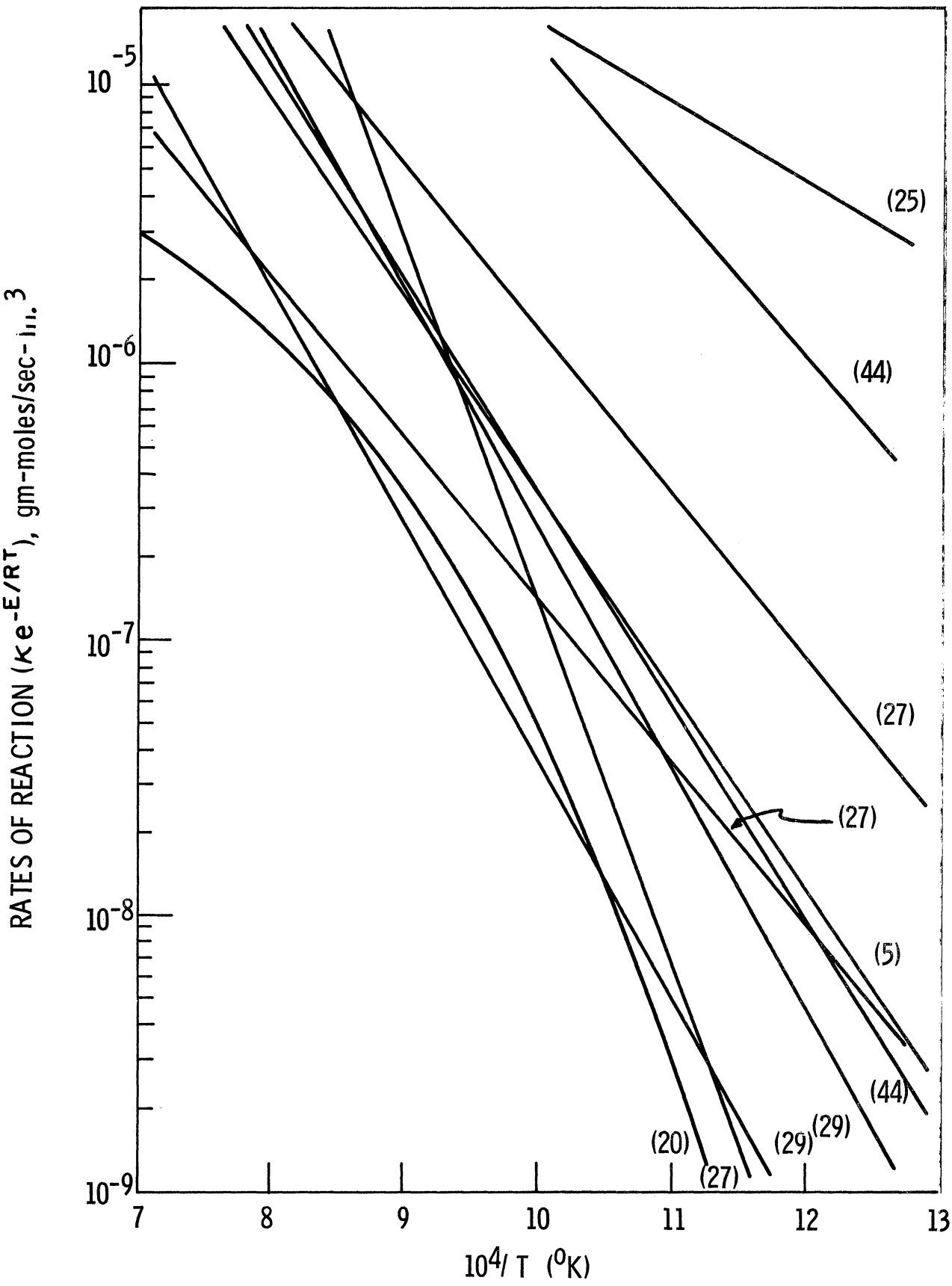

Figure 28. Comparison of reaction rate equations for oxidation of carbon monoxide.

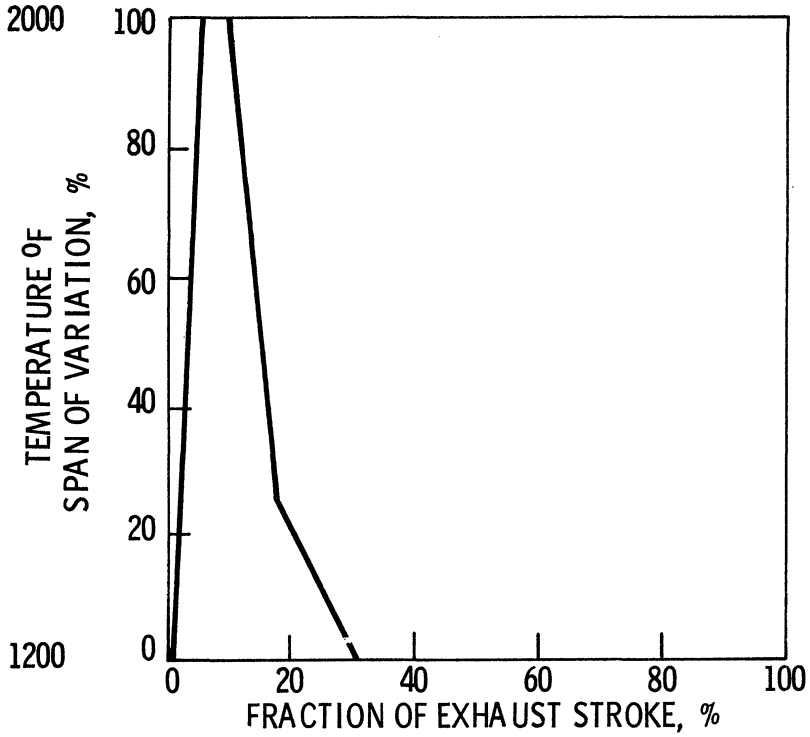

Figure 29. Variation in exhaust temperature.

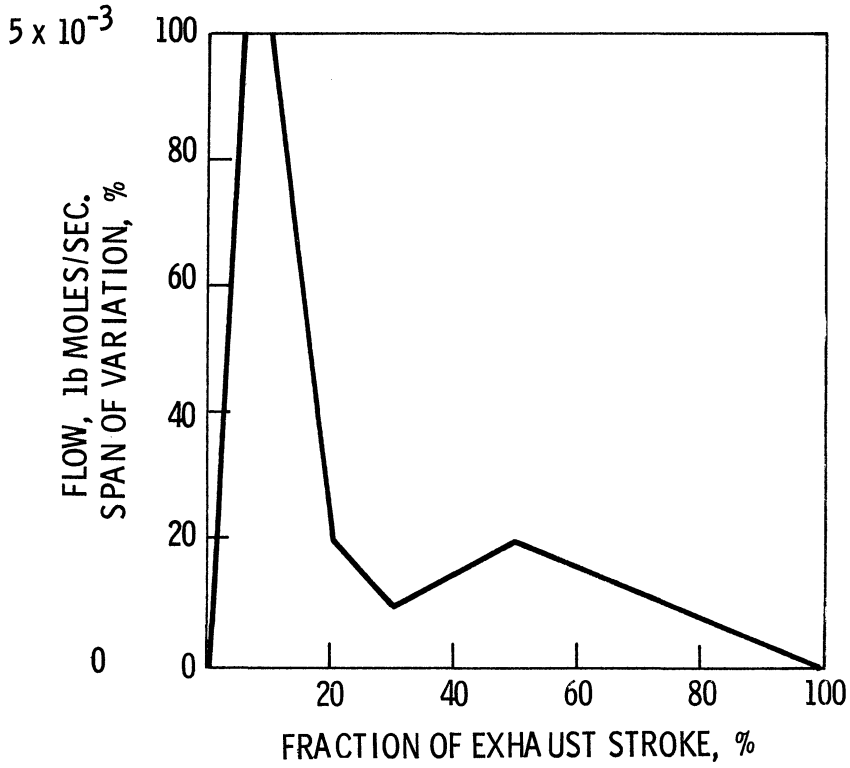

Figure 30. Variation in exhaust flow.

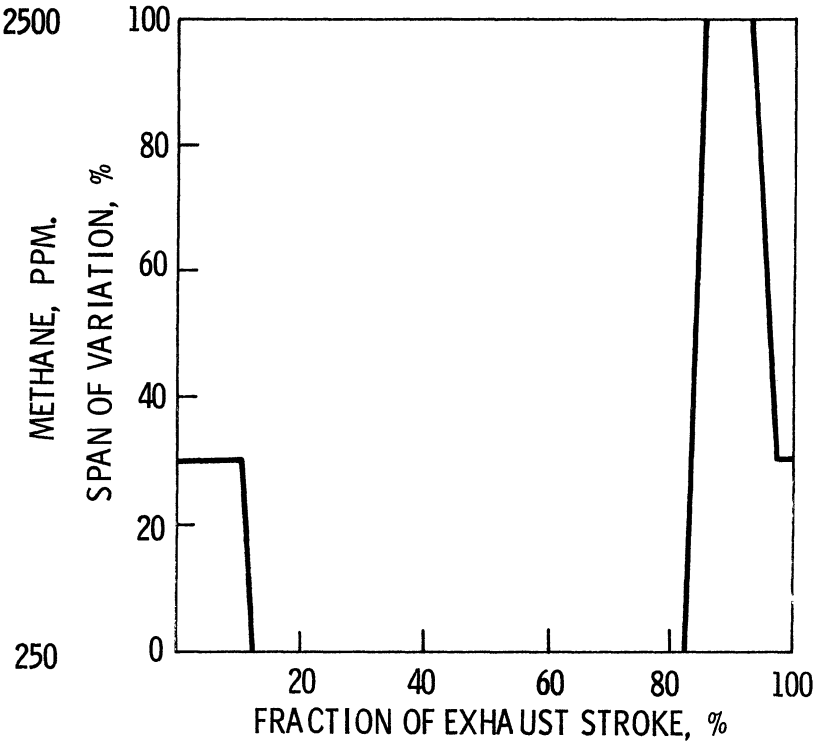

Figure 31. Hydrocarbon concentration (methane).

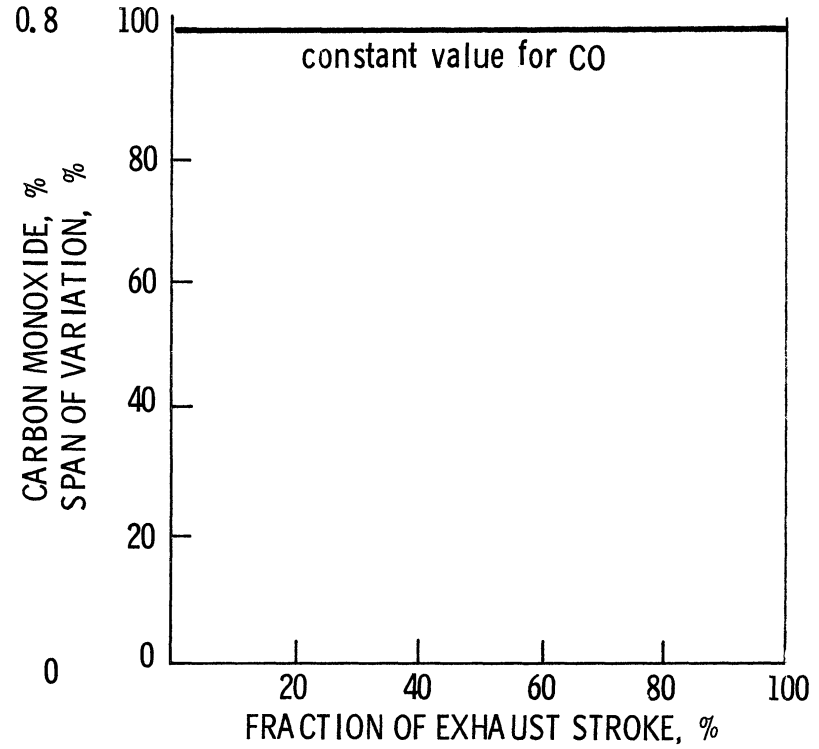

Figure 32. Carbon monoxide concentration.

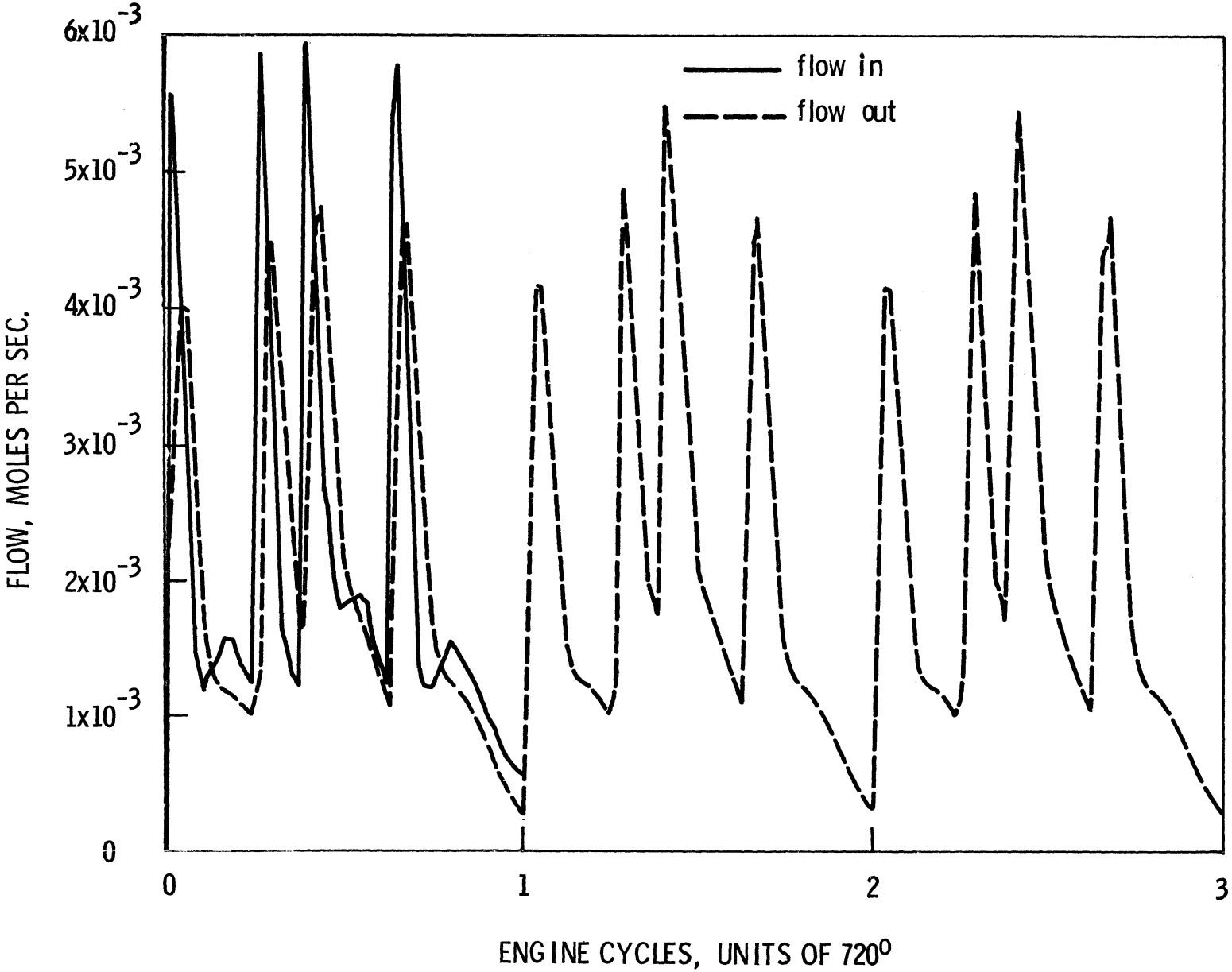

Figure 33. Flow out of reactor.

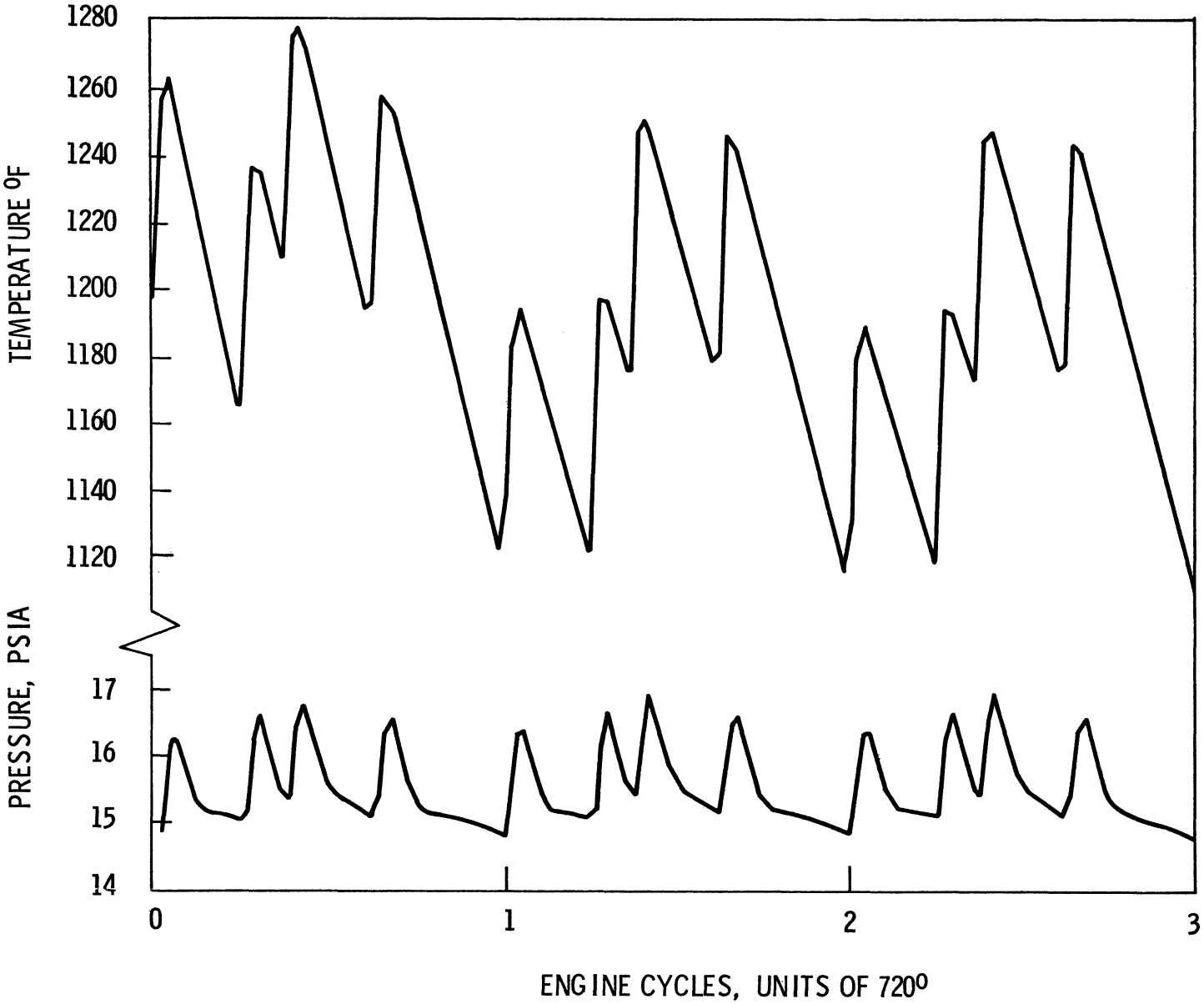

Figure 34. Temperature and pressure in reactor.

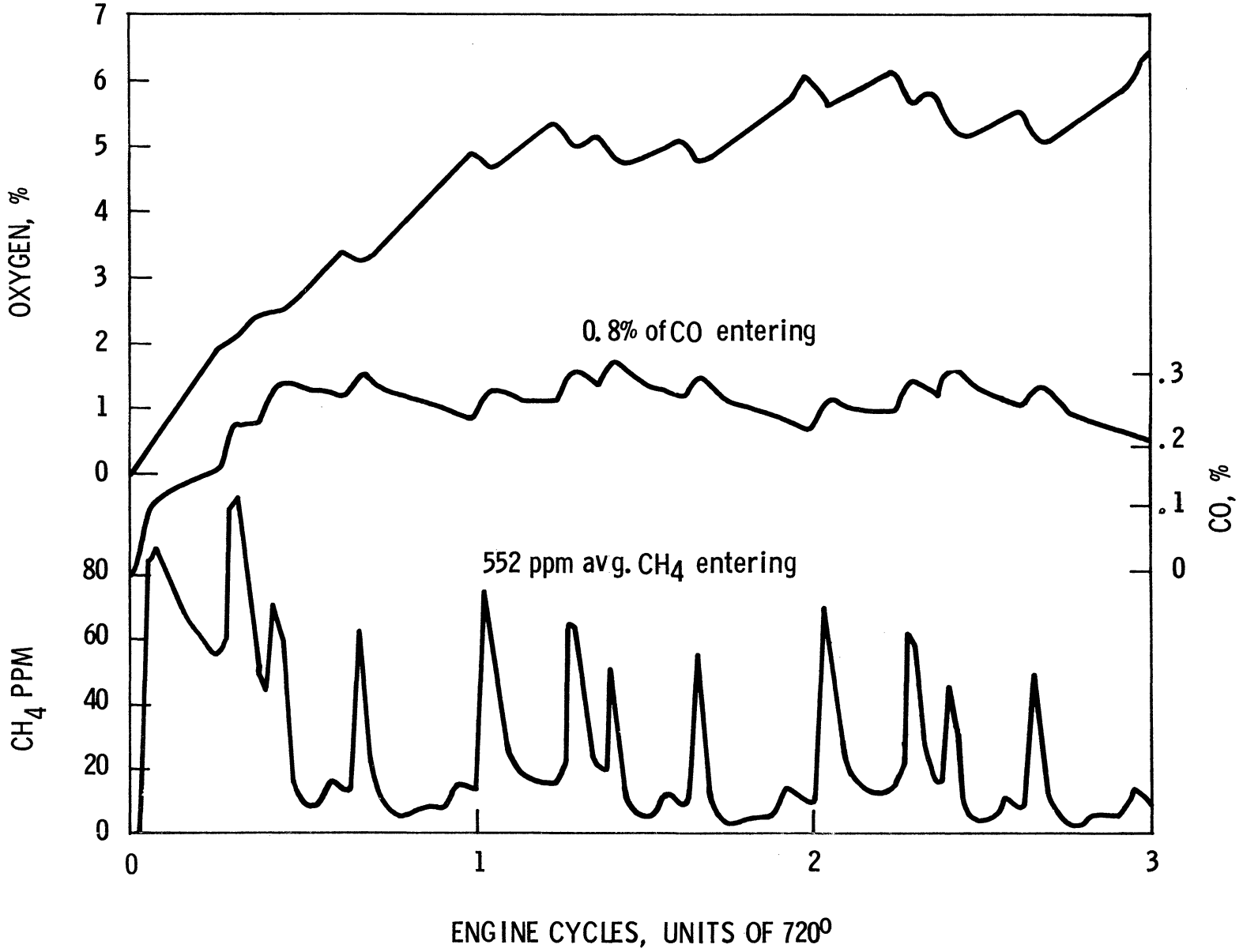

Figure 35. Emission concentrations in reactor.

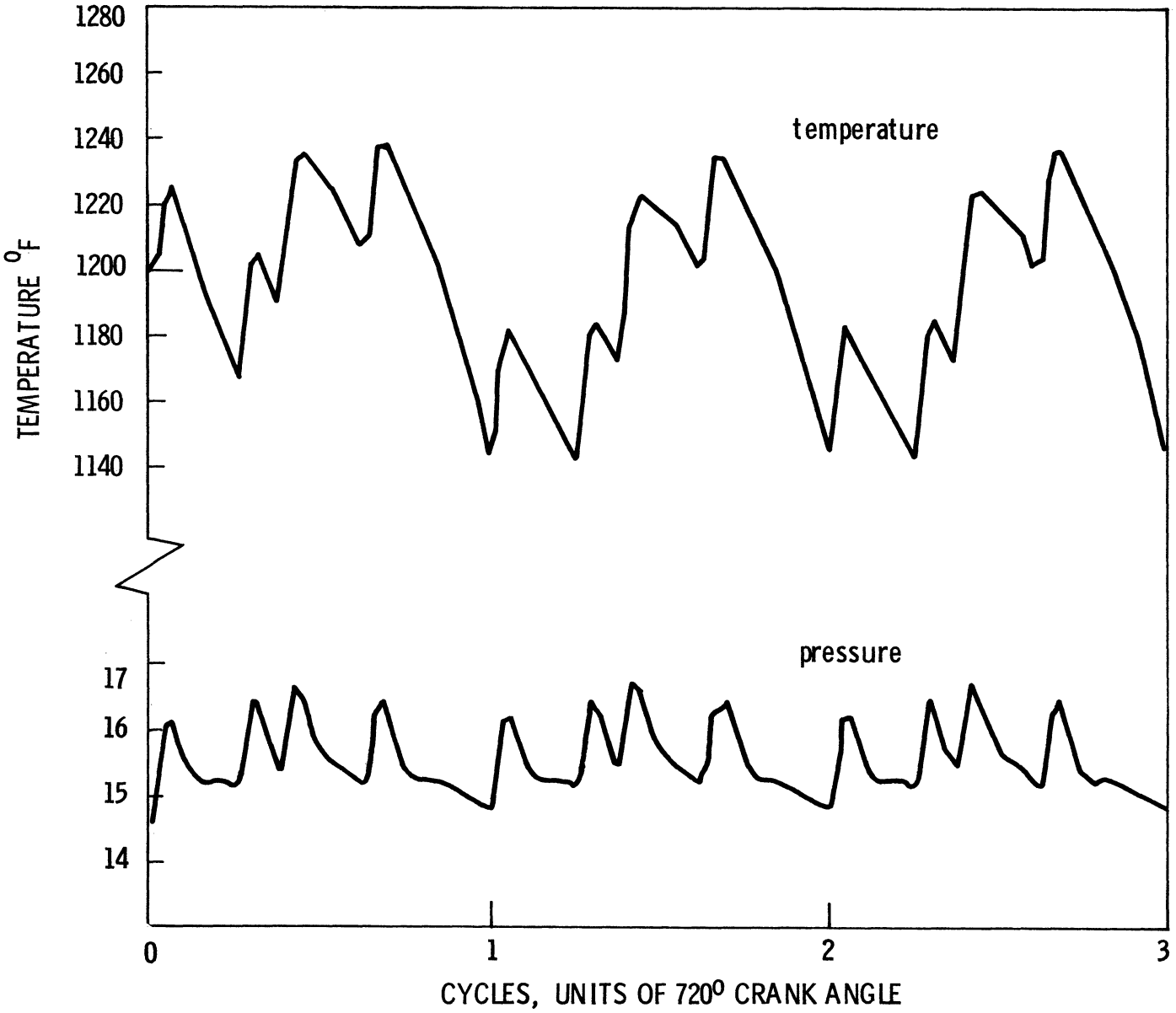

Figure 36. Reactor temperature and pressure based on an enthalpy-averaged temperature and a modulated input—step size 1/50 cycle.

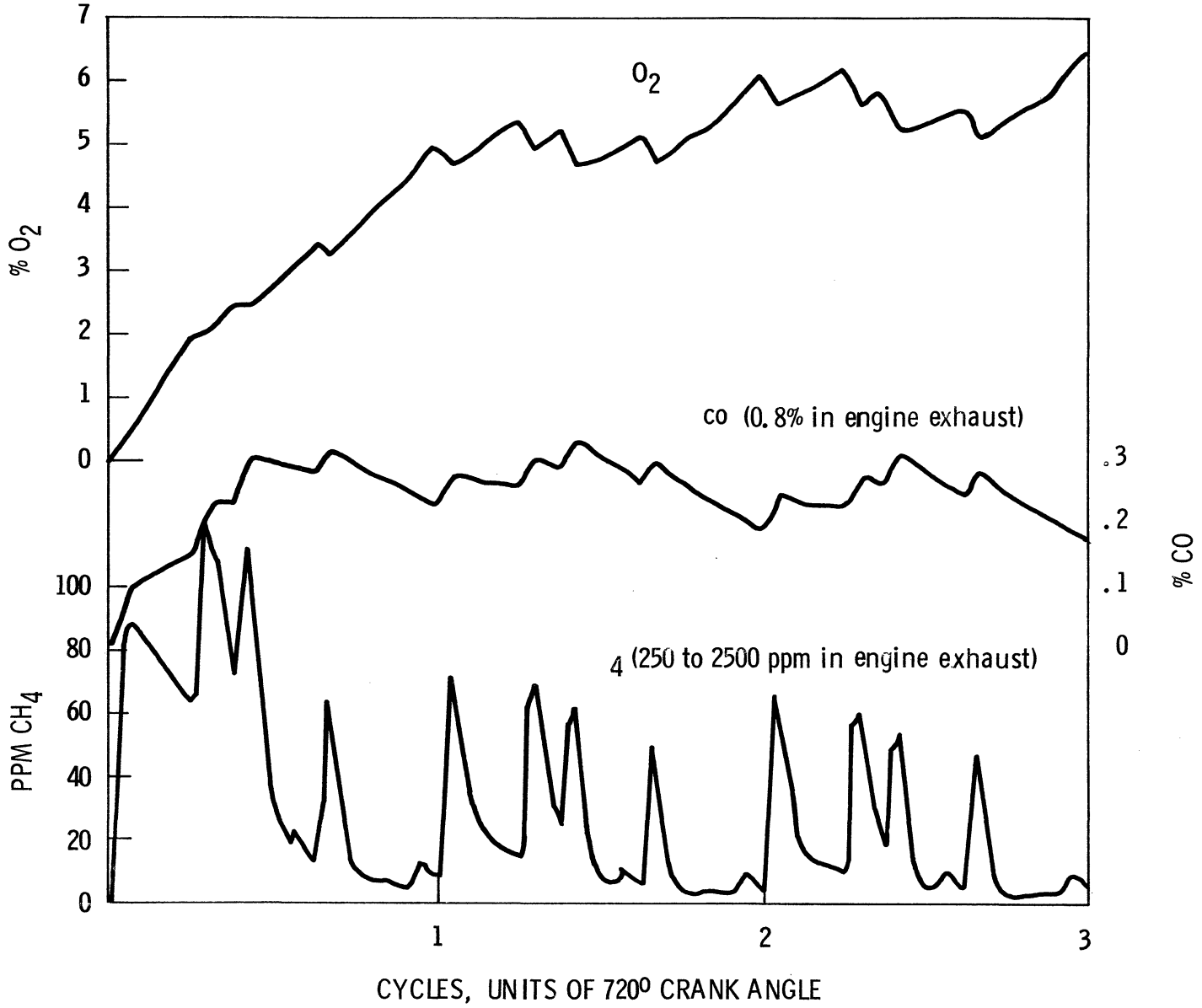

Figure 37. Reactor gas composition based upon an enthalpy-averaged feed temperature and a modulated input—step size 1/50 cycle.

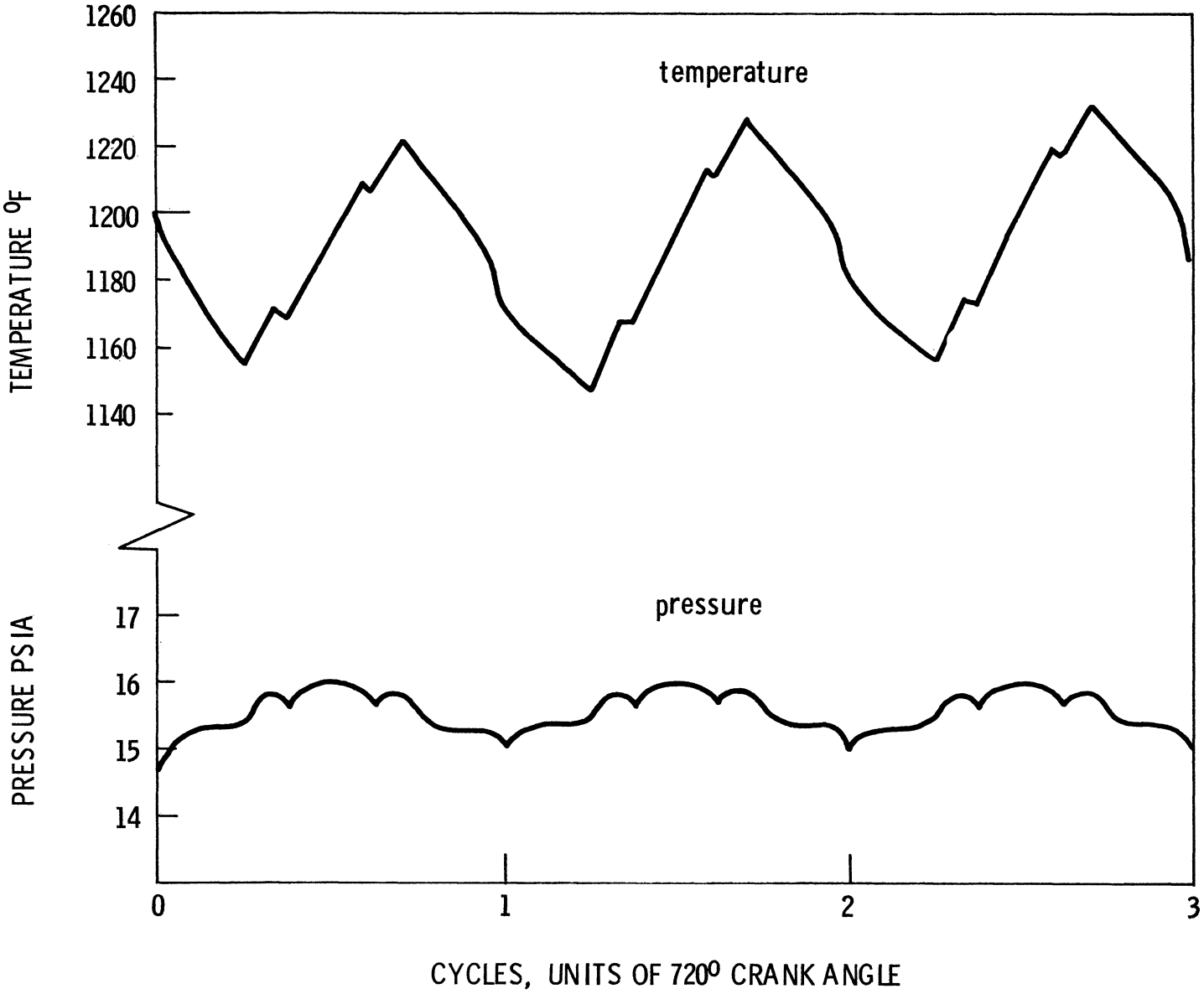

Figure 38. Reactor temperature and pressure based on an enthalpy-averaged feed temperature and time-averaged input for each cylinder—step size 1/50 cycle.

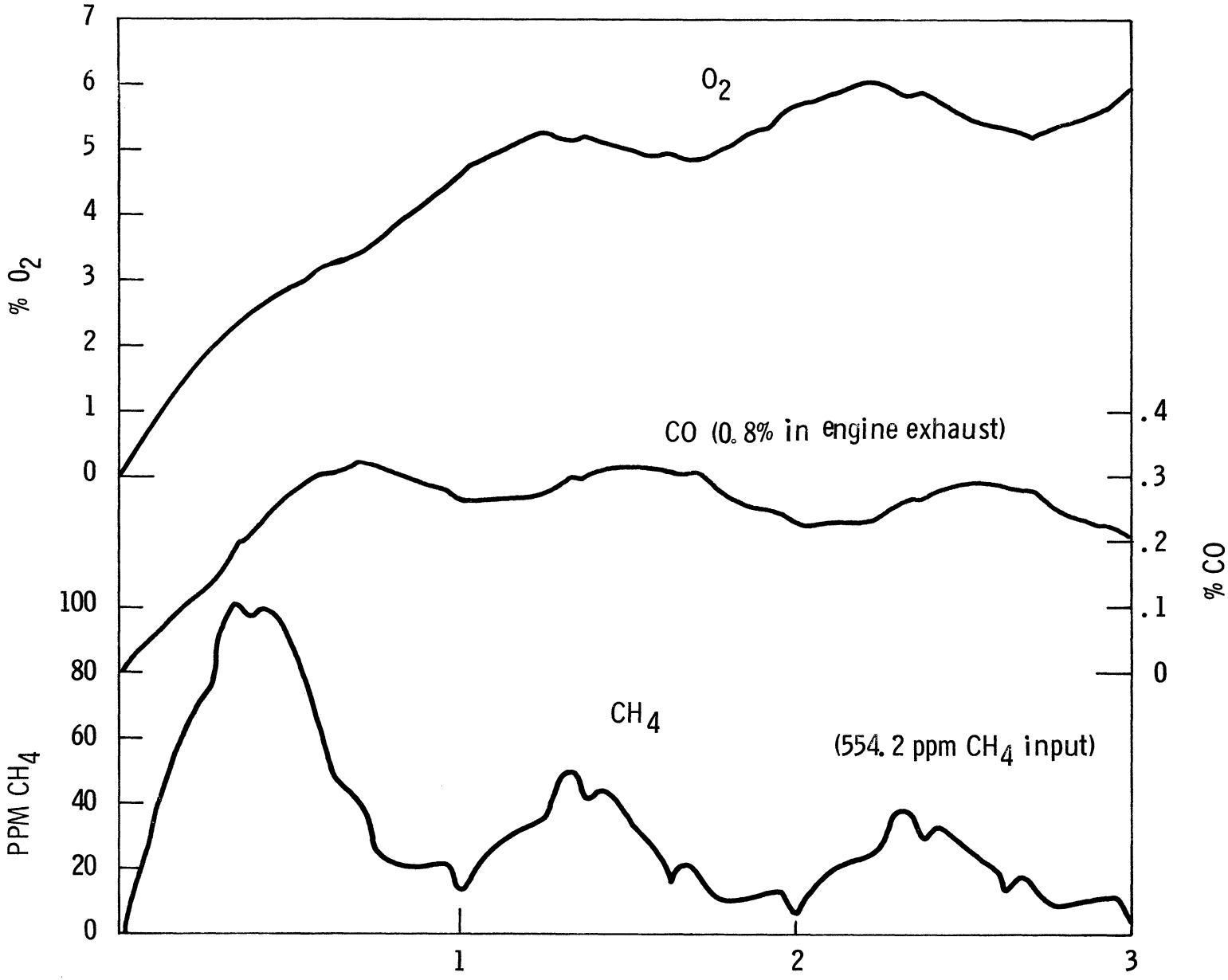

Figure 39. Reactor gas composition based upon an enthalpy-averaged feed temperature and time-averaged inputs for each cylinder.

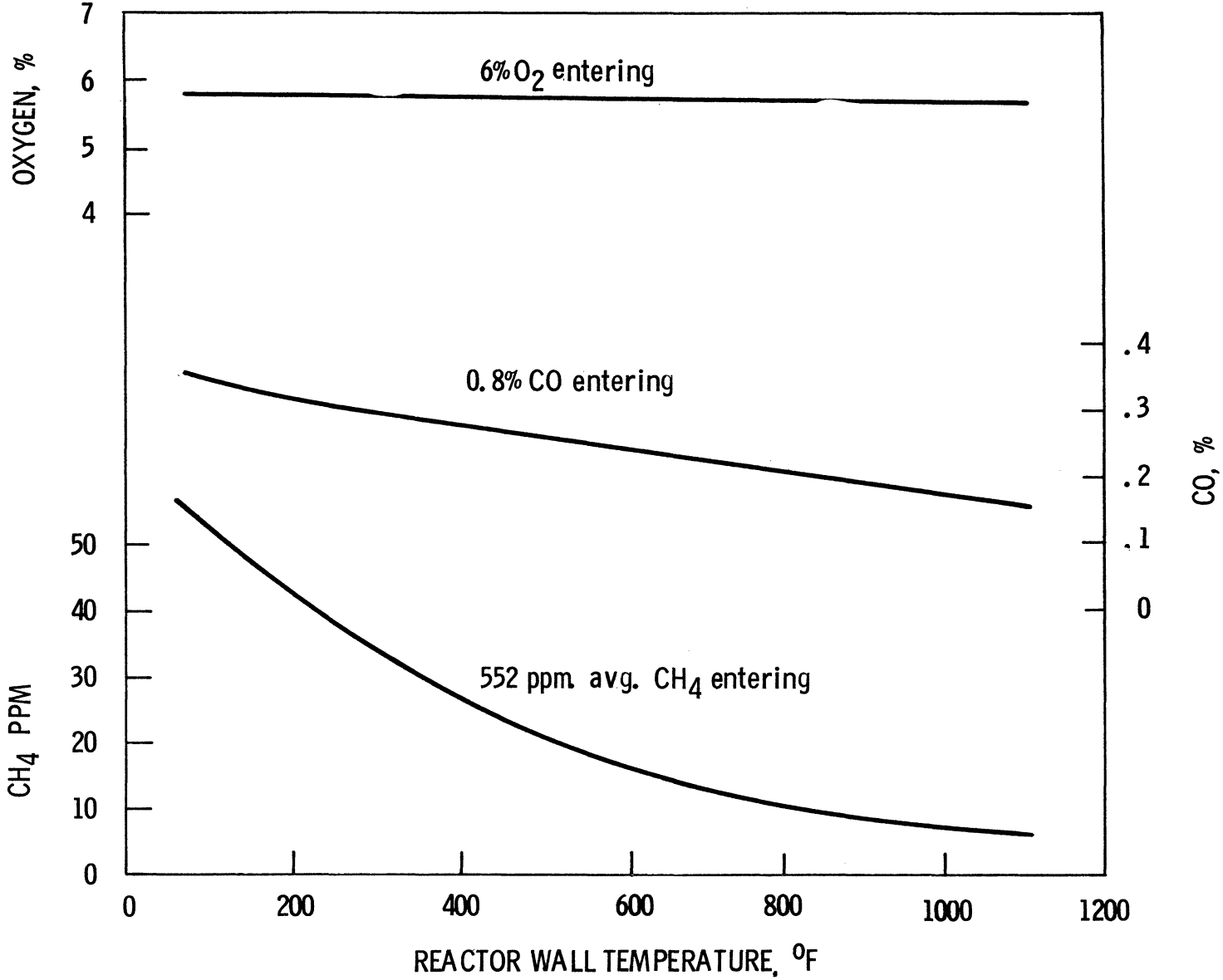

Figure 40. Emission concentrations during reactor warm-up.

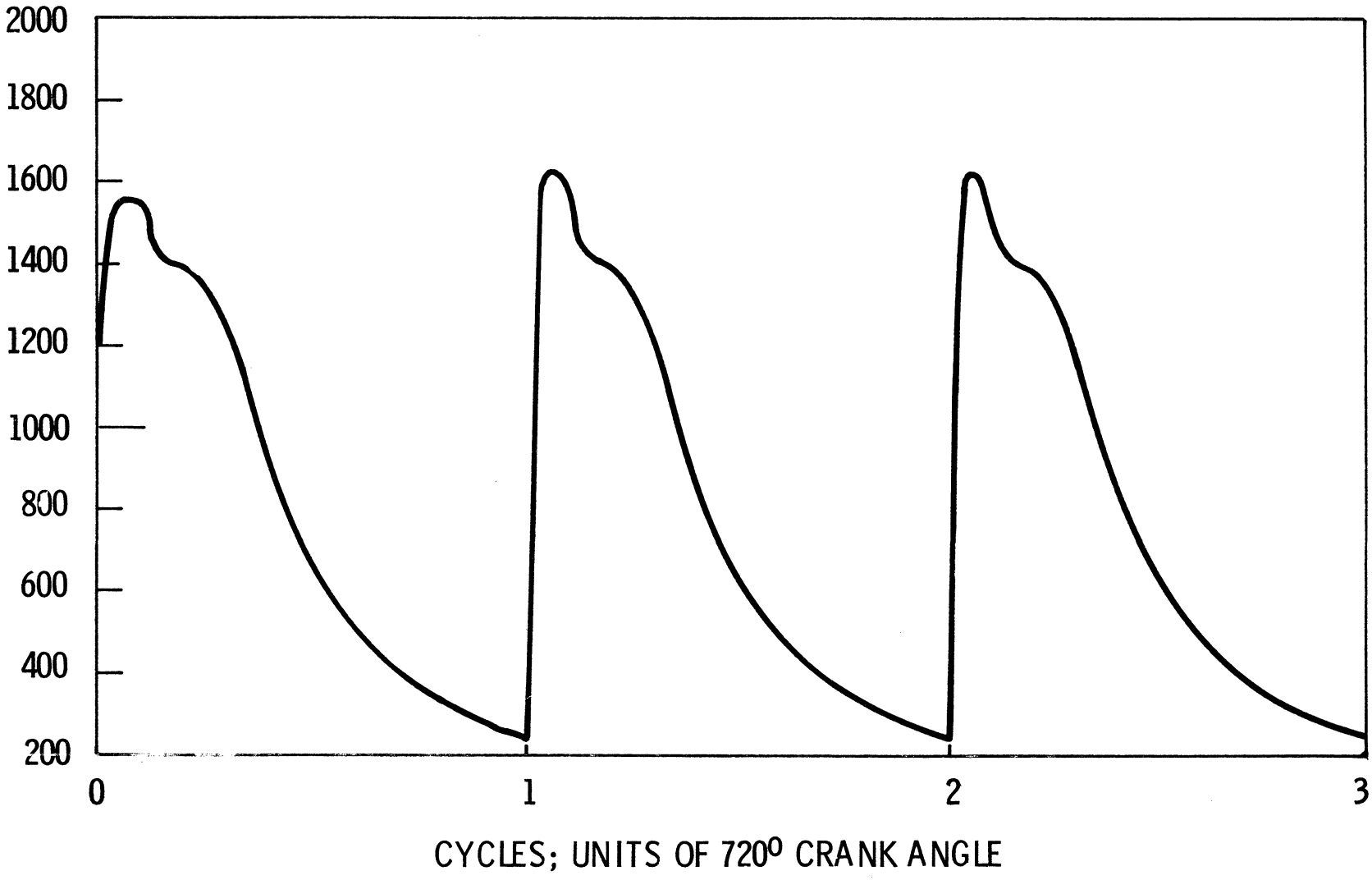

(a) Reactor Temperature Variation with Cycle Time (Tank Volume 7.5 in.^{3})

Figure 41. Exhaust manifold simulation.

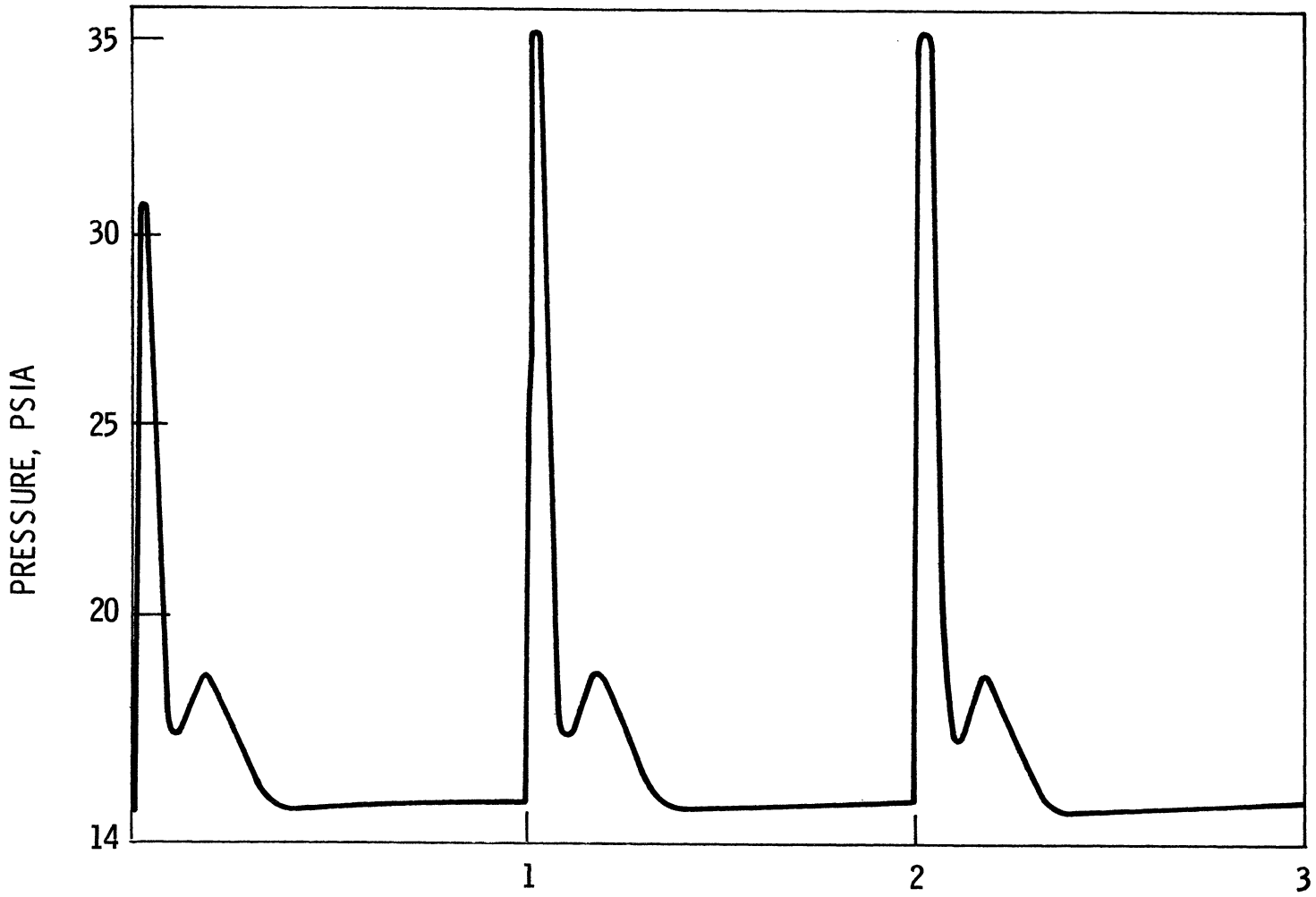

(b) Reactor Pressure Variation with Cycle Time (Tank Volume 7.5 in.^{3})

Figure 41. (Continued)

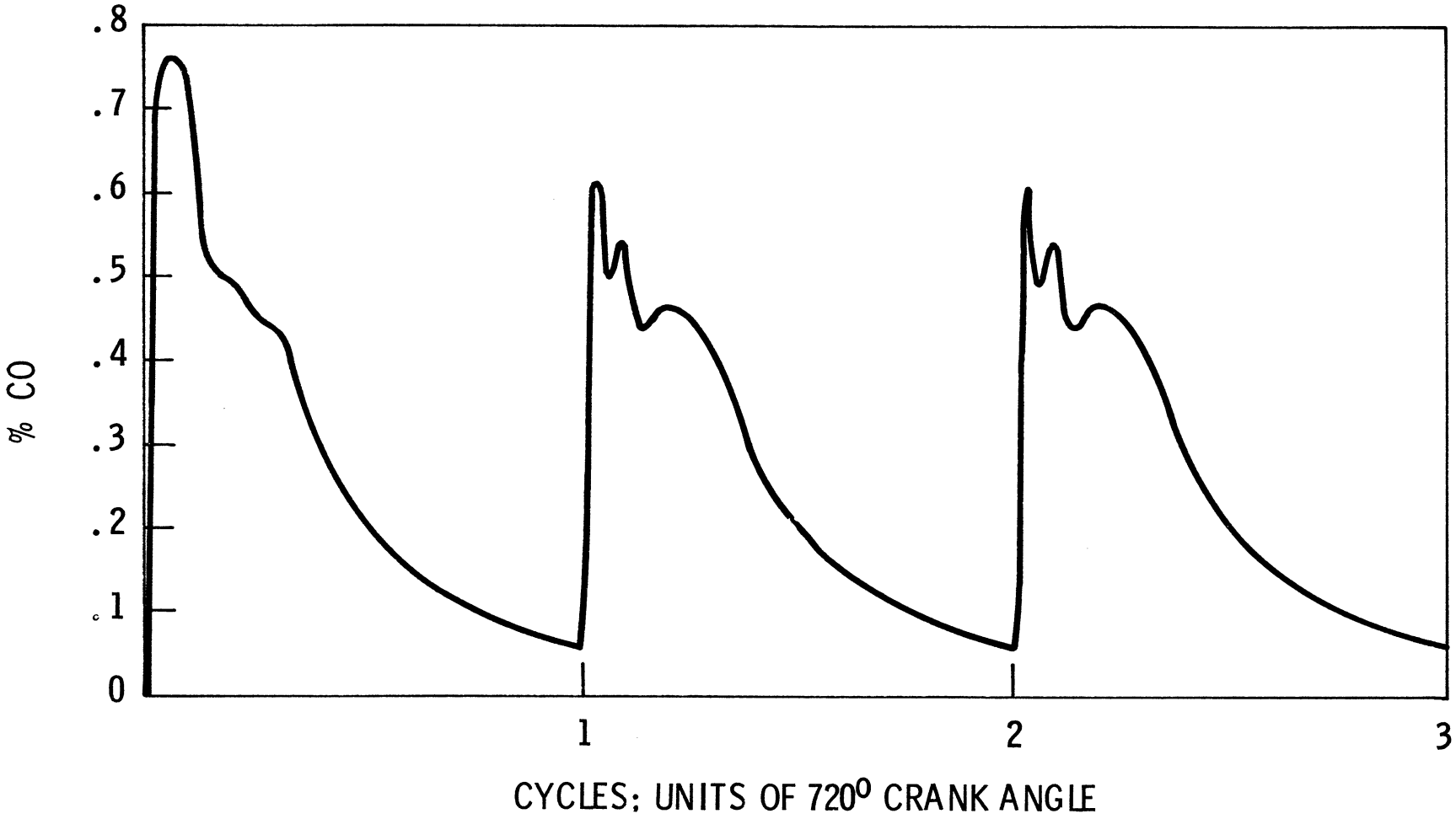

(c) CO Concentration vs. Cycle Time (Tank Volume 7.5 in.^{3})

Figure 41. (Continued)

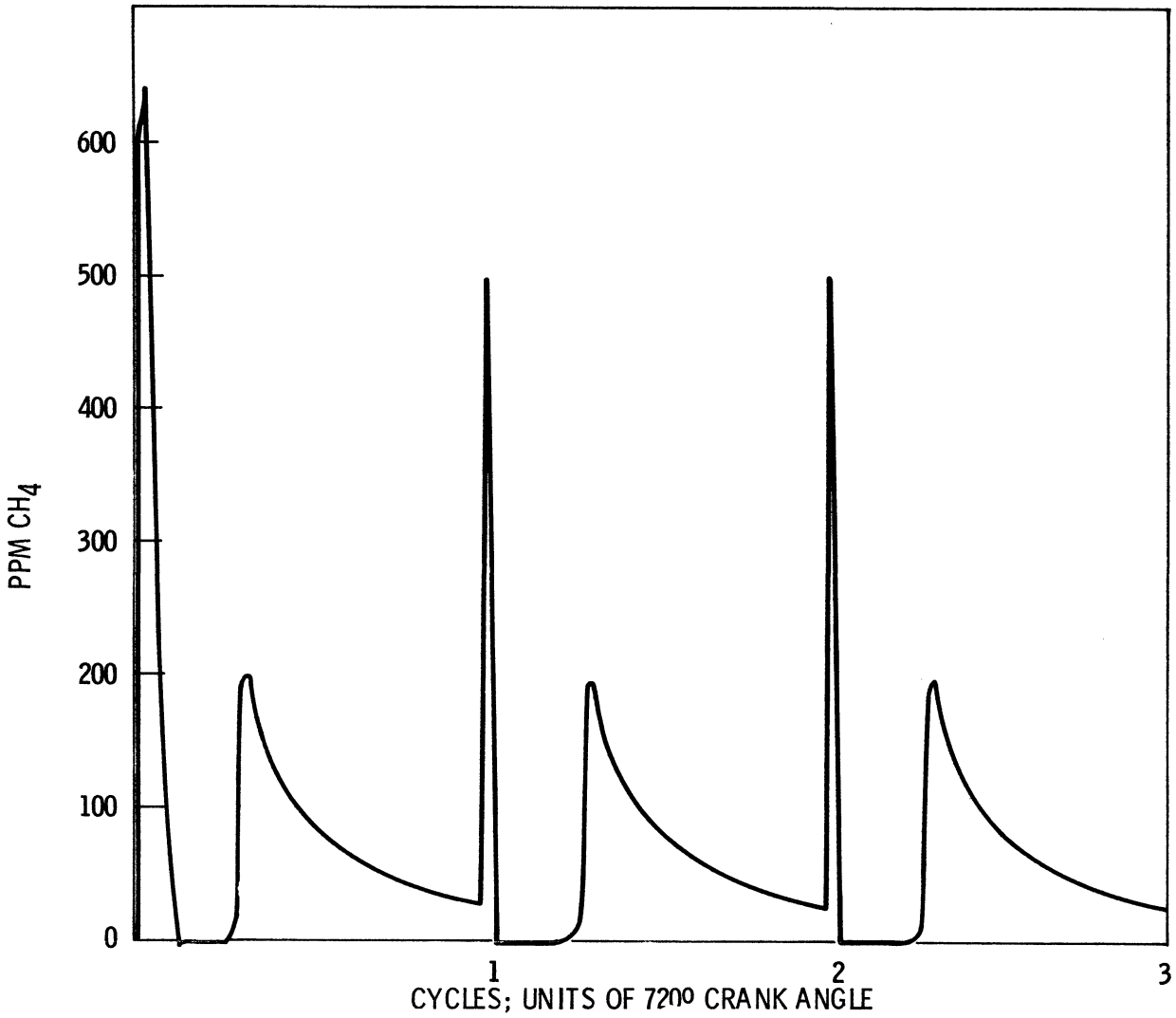

(d) CH_4 Concentration vs. Cycle Time (Tank Volume 7.5 $in.^3$)

Figure 41. (Continued)

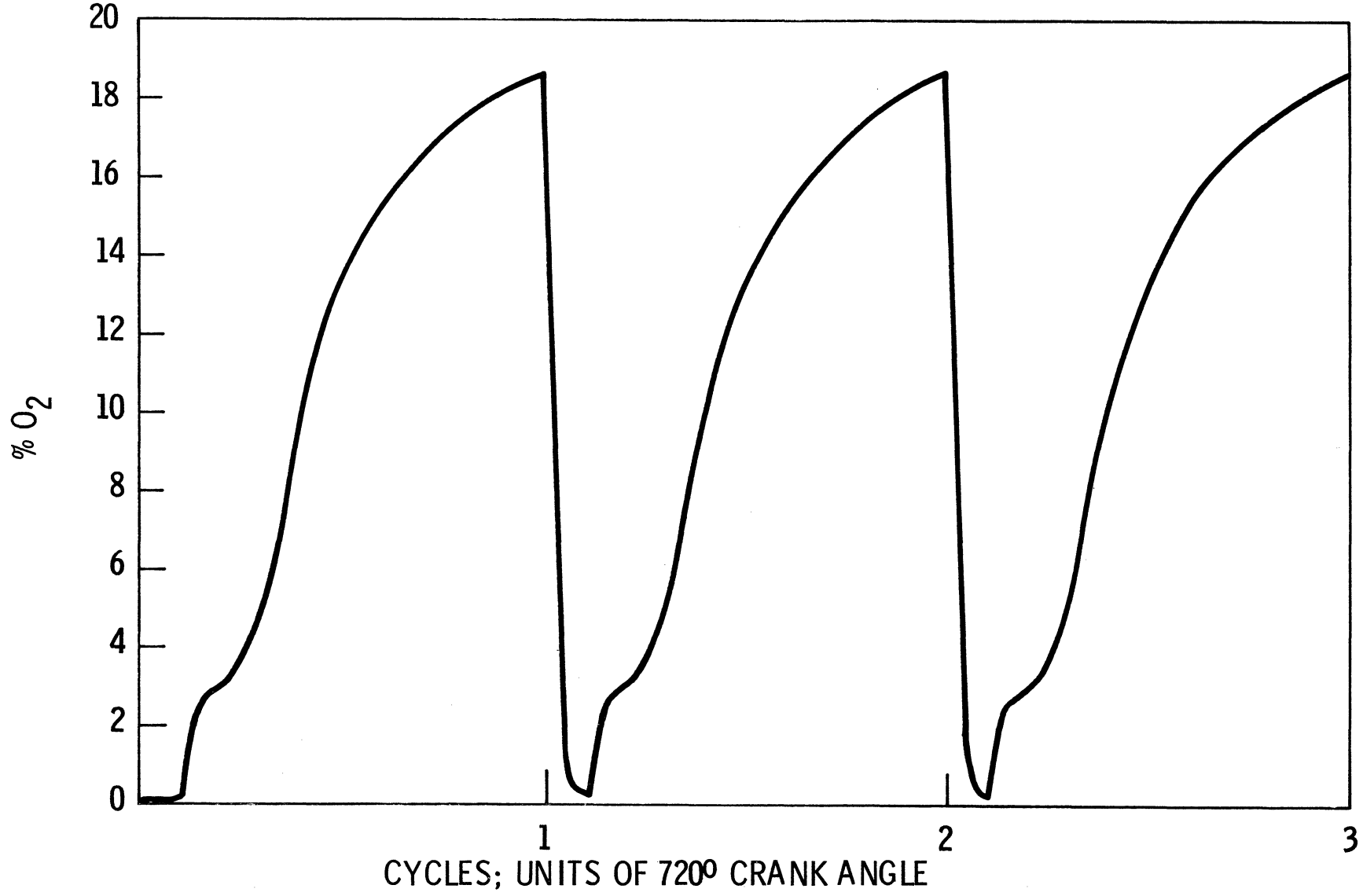

(e) O_2 Concentration vs. Cycle Time (Tank Volume 7.5 $in.^3$)

Figure 41. (Concluded)

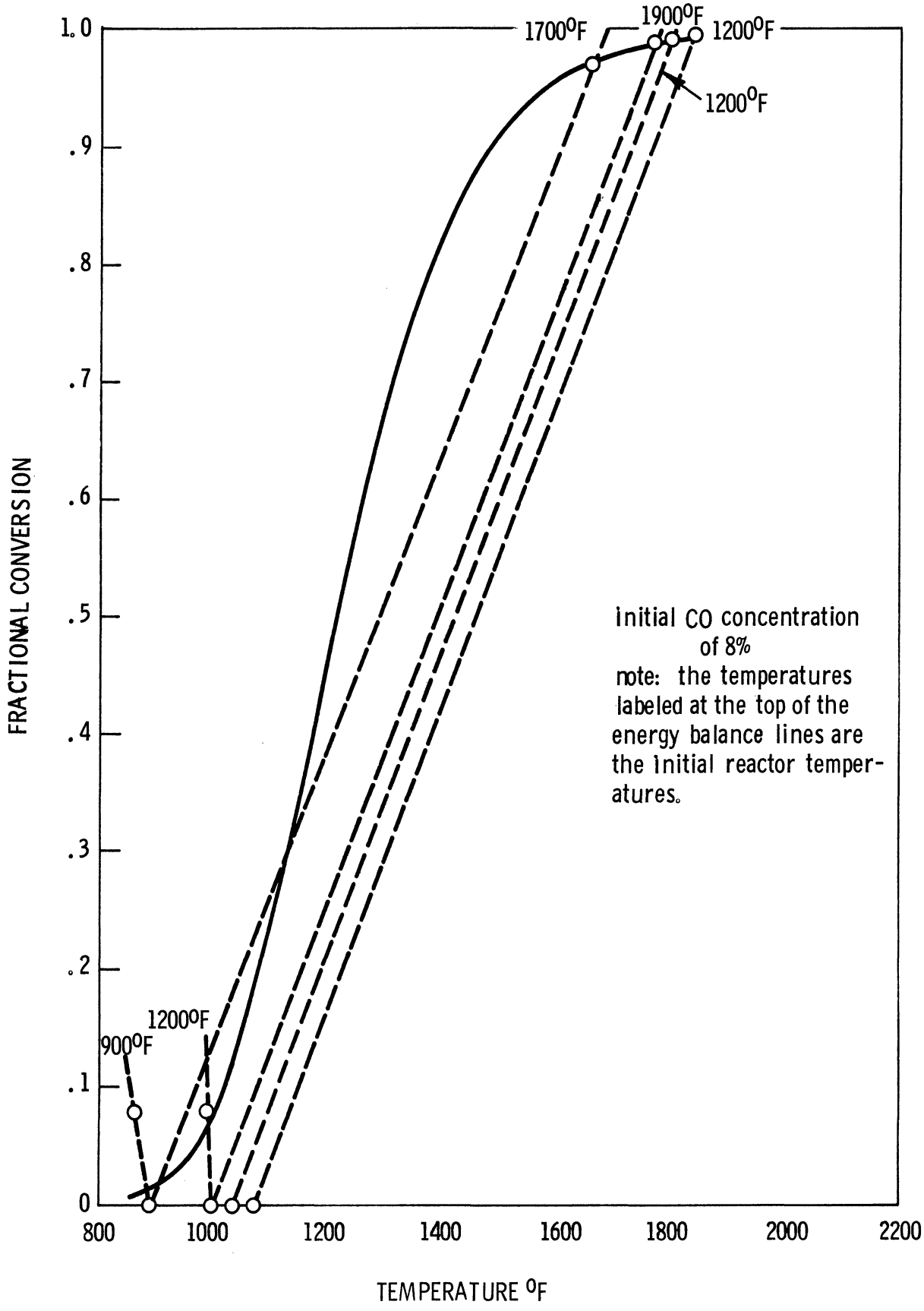

Figure 42. A combined mass and energy balance on CO.

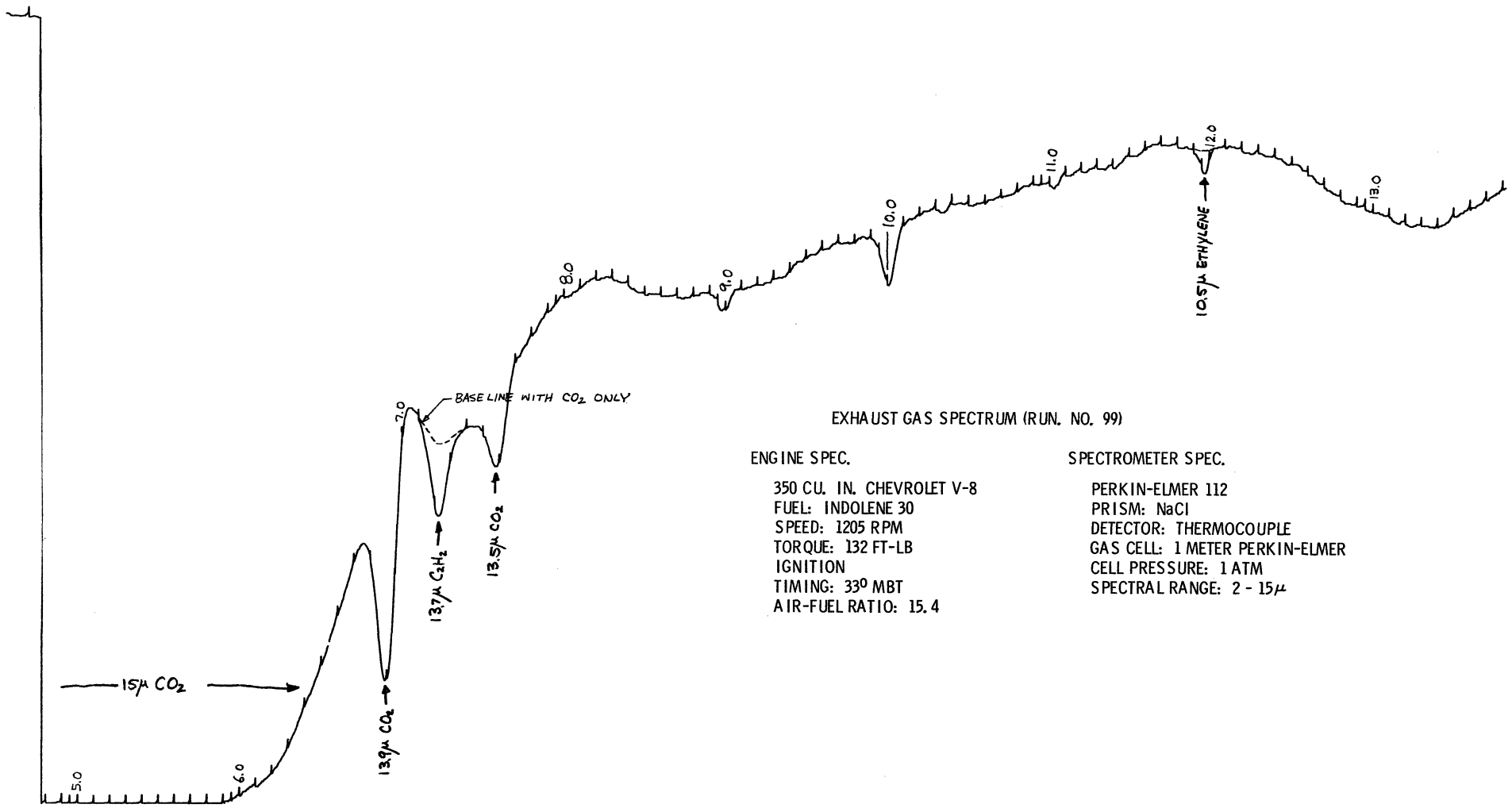

Figure 43. Spectrographic analysis of exhaust gas (typical).

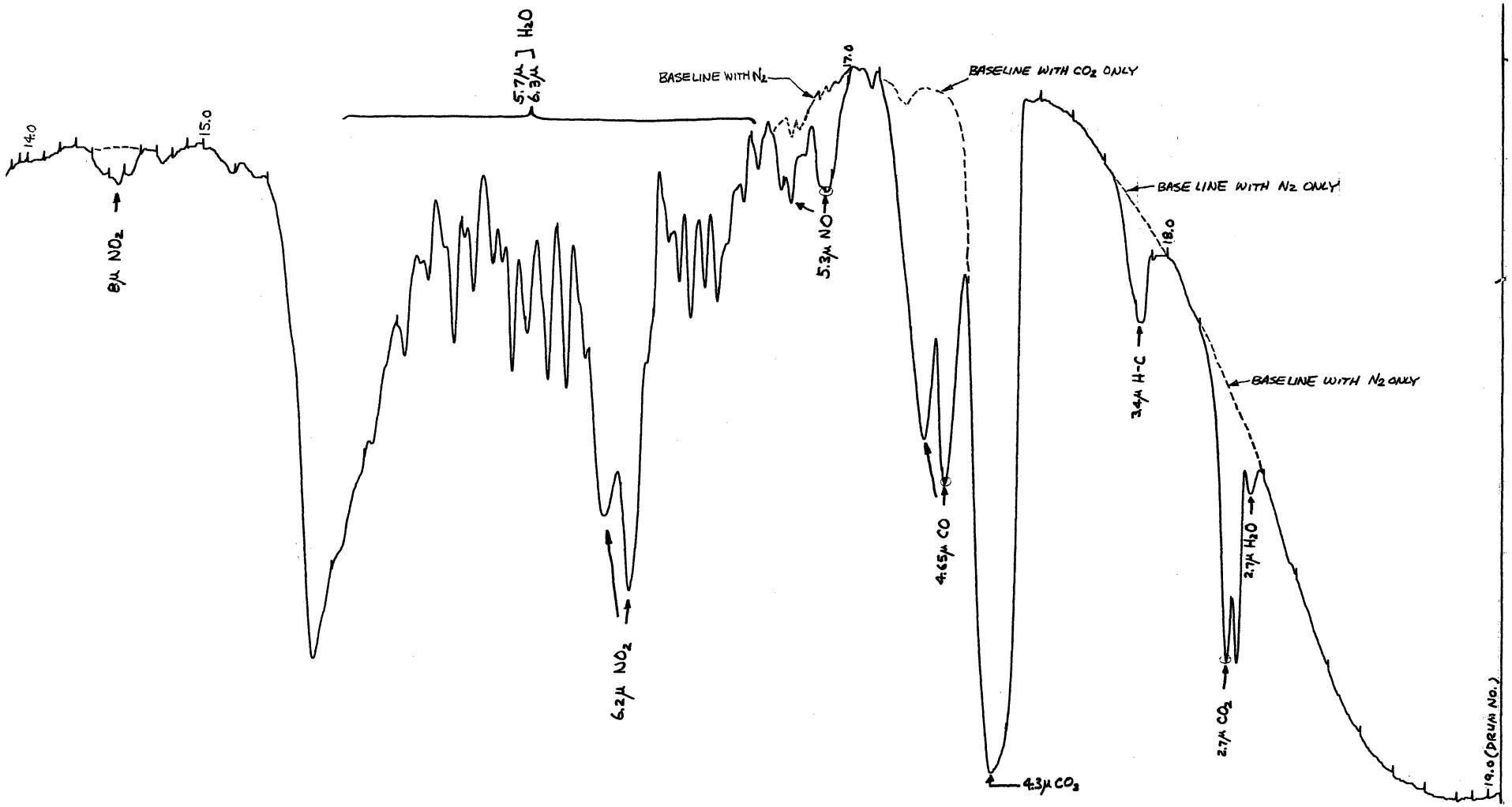

Figure 43. (Concluded)

APPENDIX

ENGINE TEST DATA SUMMARY FOR CURVES OF FIGURES 9-24

CRC TEST RESULTS

Series: 3A5 Variable: Spark Location: Tailpipe
Fuel: IND 30 Spark: Submitted by: MWG
RPM: 1200 BHP: ~30 Date: 6/23/70

Run	Torque	BSFC	A/F calc.	A/F SPINDT	Spark	Low HC ppm	HCHO ppn	FID ppm			TOTAL HC		CO_2	CO			NO			O_2	H_2	PBTE η_{th}
								Para	Para & Arom	Total	BSER	FFER	%	%	BSER	FFER	ppm	BSER	FFER	%		%
124	132.8	.642	15.45	14.98	5	126	--	60	140	250	.00661	.0103	12.74	1.17	.1007	.1570	649.	.00599	.00933	1.55	--	21.8
120	134.4	.580	15.37	14.32	10	166	--	80	190	330	.00775	.0134	13.57	1.07	.0819	.141	1088.	.00892	.0154	.60	--	24.1
127	131.8	.575	15.20	15.06	10	162	--	75	180	320	.00748	.0130	12.9	.84	.0639	.1111	992.	.00809	.0141	1.50	--	24.3
126	133.4	.534	15.26	15.24	15	198	--	80	210	370	.00805	.0151	13.29	.51	.0361	.0676	1219.	.00925	.0173	1.60	--	26.2
122	132.8	.515	15.60	14.84	20	207	--	110	250	430	.00921	.0179	13.01	1.17	.0816	.159	1319.	.00985	.0192	1.52	--	27.2
125	131.3	.499	15.38	14.91	27	234	--	130	300	480	.00983	.0197	13.85	.58	.0387	.0775	1837.	.0131	.0263	1.30	--	28.0
119	135.5	.489	15.64	14.59	33	234	--	140	310	470	.00946	.0193	13.85	.47	.0308	.0629	2500.	.0176	.0359	.75	--	28.6
123	133.4	.493	15.48	--	40	279	--	160	345	505	.0103	.0209	13.01	.75	.0497	.101	2554.	.0174	.0354	--	--	28.4
121	132.3	.503	15.50	14.39	45	279	--	160	330	500	.0103	.0204	13.85	.79	.0529	.105	2981.	.0214	.0424	.68	--	27.8

BSER: brake specific emission rate lbm/bhp hr
FFER: fuel fraction emission rate lbm/lbm fuel

CRC TEST RESULTS

Series: IA5 Variable: A/F Location: Tailpipe
Fuel: Indolene Clear Spark: MBT Submitted by: MWG
RPM: 1200 BHP: ≈30 Date: 2/12/70

Run	Spark	Torque	BSFC	A/F	A/F	Low HC	HCHO	FID ppm			TOTAL HC		CO_2	CO			NO			O_2	H_2
				SPINDT	calc	ppm	ppm	Para	Para & Arom	total	BSER	FFER	%	%	BSER	FFER	ppm	BSER	FFER	%	
87	42	130	.450	18.97	19.87	177	180	130	160	260	.00625	.0139	11.2	0.1	.0078	.0174	1200	.01006	.02237	5.4	--
77	33	134	.463	18.80	19.85	177	--	130	180	290	.00717	.0155	11.1	0.1	.0081	.0174	1150	.00992	.02144	5.2	--
78	33	131	.461	16.78	17.82	168	127	140	190	300	.00667	.01448	12.5	0.2	.0145	.0314	2000	.01552	.03366	3.3	--
86	34	130	.461	16.62	17.37	159	--	140	160	270	.00586	.0127	12.6	0.1	.0071	.0153	2100	.01590	.03446	3.0	--
79	33	131	.469	14.94	16.19	204	--	160	220	350	.00723	.01542	14.1	0.3	.0202	.0430	2850	.02053	.04381	1.1	--
82	34	132	.488	14.30	15.11	222	86	210	270	420	.00846	.01735	14.3	0.9	.0590	.1210	2400	.01686	.03485	0.6	--
76	34	131	.495	14.77	14.97	222	--	200	300	490	.00993	.02007	--	0.7	.0462	.0934	2600	.01839	.03716	1.2	--
83	34	132	.523	13.35	13.90	259	--	240	310	470	.00938	.01795	13.2	2.7	.1755	.3357	1400	.00975	.01865	0.25	--
80	34	131	.570	12.17	12.96	325	--	340	470	670	.01367	.02398	11.3	5.7	.3787	.6642	710	.00505	.00886	0.30	--
84	35	131	.605	11.78	12.11	315	80	360	490	650	.01319	.02182	10.6	6.8	.4494	.7433	400	.00083	.00468	0.30	--
81	34	131	.664	10.52	11.28	373	--	460	610	810	.01692	.02549	8.4	10.0	.6799	1.0245	190	.00138	.00209	0.25	--
85	34	132	.734	9.86	10.28	431	64	520	650	870	.01845	.02514	7.5	11.5	.7941	1.0818	100	.00074	.00101	0.02	--

BSER: brake specific emission rate lbm/bhp hr
FFER: fuel fraction emission rate lbm/lbm fuel

CRC TEST RESULTS

Series: 4A4
Fuel: Indolene 30

Variable: RPM
BHP: ~30 (50% load--1200 rpm)

Location: Tailpipe
Submitted by: JHD
Date: 4/27/70

Run	Spark	Torque	BSFC	A/F calc.	A/F SPINDT	RPM	LOW HC ppm	HCHO ppm	FID ppm Para	FID ppm Para & Arom	FID ppm total	TOTAL HC BSER	TOTAL HC FFER	CO_2 %	CO %	CO BSER	CO FFER	NO ppm	NO BSER	NO FFER	O_2 %	H_2
112	22	176	.464	15.07	15.27	900	279	--	140	320	420	.008	.018	13.6	.23	.015	.031	2454	.017	.036	1.5	--
107	27	158	.477	14.79	14.10	1001	270	--	220	410	500	.010	.021	13.6	1.28	.082	.171	2027	.014	.029	.55	--
106	33	137	.487	14.92	14.33	1195	207	--	200	390	490	.010	.020	13.6	1.07	.070	.145	2275	.016	.033	.75	--
108	32	113	.530	14.81	14.26	1401	243	--	160	360	470	.010	.019	13.9	.86	.061	.115	1989	.015	.029	0.5	--
109	34	100	.559	14.88	14.57	1599	207	--	150	340	440	.010	.018	13.6	.65	.049	.088	1913	.015	.028	0.8	--
110	33	87	.591	14.75	14.73	1796	234	--	85	240	360	.009	.015	13.3	.86	.068	.115	1387	.012	.020	1.1	--
111	39	79	.620	14.62	14.94	2001	171	--	85	260	360	.009	.015	13.3	.72	.059	.095	1571	.014	.022	1.3	--

BSER: brake specific emission rate lbm/bhp hr
FFER: fuel fraction emission rate lbm/lbm fuel

CRC TEST RESULTS

Series: 2A4 Variable: LOAD Location: Tailpipe
Fuel: Indolene 30 Spark: MBT Submitted by: JHD
RPM: 1200 Date: 6/18/70

Run	Spark	BSFC	A/F calc.	A/F SPINDT	Torque	LOW HC ppm	HCHO ppm	FID ppm Para	FID ppm Para & Arom	FID ppm total	TOTAL HC BSER	TOTAL HC FFER	CO_2 %	CO %	CO BSER	CO FFER	NO ppm	NO BSER	NO FFER	O_2 %	H_2	PBTE %
130	36	1.467	15.25	15.44	19.95	670.	--	550.	850.	1100.	.06549	.04463	12.22	.69	.1338	.0912	198.	.00411	.00280	2.6	--	9.53
131	36	1.031	16.19	16.05	30.45	270.	--	200.	360.	500.	.02192	.02125	12.6	.30	.0428	.0415	353.	.00540	.00523	2.6	--	13.56
135	36	.719	16.13	15.71	52.50	216.	--	120.	270.	440.	.01338	.01860	13.15	.16	.0158	.0220	1235.	.0131	.0182	2.05	--	19.44
133	36	.583	16.27	15.82	80.59	225.	--	130.	260.	440.	.01093	.01876	13.01	.13	.0105	.0180	1989.	.0172	.0295	2.15	--	23.99
137	35	.524	15.93	15.58	107.62	225.	--	140.	300.	460.	.01009	.01925	13.29	.16	.0114	.0218	2500.	.0191	.0365	1.9	--	26.68
128	33	.507	15.18	15.08	130.20	279.	--	170.	340.	515.	.01055	.02079	13.29	.65	.0434	.0854	2232.	.0139	.0314	1.6	--	27.56
134	31	.464	16.05	15.57	158.81	211.	--	120.	255.	420.	.00820	.01767	13.01	.27	.0172	.0370	3143.	.0214	.0461	1.9	--	30.13
136	27	.447	15.84	15.34	210.79	198.	--	120.	260.	410.	.00767	.01716	12.9	.72	.0439	.0981	2106.	.0137	.0307	1.9	--	31.26
132	25	.433	16.21	15.70	233.10	193.	--	110.	230.	365.	.00672	.01550	12.6	.69	.0414	.0954	2431.	.0156	.0360	2.3	--	32.27
129	23	.440	15.13	14.87	250.42	216.	--	120.	265.	430.	.00761	.01731	13.01	.93	.0536	.1219	2106.	.0130	.0295	1.4	--	31.81

BSER: brake specific emission rate lbm/bhp hr
FFER: fuel fraction emission rate lbm/lbm fuel

DISTRIBUTION LIST

Contract Distribution	No. of copies
Mr. Alan E. Zengel Assistant Project Manager Coordinating Research Council, Inc. 30 Rockefeller Plaza New York, New York 10020	300
Dr. P.R. Ryason Chevron Research Company 576 Standard Avenue Richmond, California 94802	2
Mr. R.J. Corbeels Research and Technical Department Texaco, Inc. P.O. Box 509 Beacon, New York	1
Dr. E.N. Cantwell Automotive Emissions Division Petroleum Laboratory E.I. DuPont de Nemours and Company, Inc. Wilmington, Deleware 19898	1
Dr. J.B. Edwards Research Section Chrysler Corporation 12800 Oakland Avenue Detroit, Michigan 48203	1
Mr. G.D. Kittredge Department of Health, Education, and Welfare Motor Vehicle Research and Development 5 Research Drive Ann Arbor, Michigan	15
Dr. H. Niki Scientific Laboratory Ford Motor Company P.O. Box 2053 Dearborn, Michigan 48121	2

DISTRIBUTION LIST (Concluded)

Contract Distribution	No. of Copies
Mr. R.C. Schwing Research Center Laboratories Fuels and Lubricants Department General Motors Corporation General Motors Technical Center 12 Mile and Mound Roads Warren, Michigan 48090	12
Mrs. Mary Englehart Department of Health, Education, and Welfare National Air Pollution Control Administration 411 W.Chapel Hill Street Durham, North Carolina 27701	1

Internal Distribution	
Professor J.A. Bolt, Dept. of Mech. Eng., Auto. Lab., N.C.	1
Professor B. Carnahan, Dept. of Chem. Eng., East Eng. Bldg.	1
Professor J.A. Clark, Dept. of Mech. Eng., West Eng. Bldg.	1
Professor D.E. Cole, Dept. of Mech. Eng., Auto Lab., N.C.	1
Professor N.A. Henein, Dept. of Mech. Eng., Auto. Lab., N.C.	1
Professor R. Kadlec, Dept. of Chem. Eng., East Eng. Bldg.	1
Professor H. Lord, Dept. of Mech. Eng., Auto. Lab., N.C.	1
Professor J.J. Martin, Dept. of Chem. Eng., East Eng. Bldg.	1
Professor W. Mirsky, Dept. of Mech. Eng., Auto. Lab., N.C.	1
Mr. E. Sondreal, Dept. of Chem. Eng., East Eng. Bldg.	1
Professor D.J. Patterson, Dept. of Mech. Eng., Auto. Lab., N.C.	2
Project File	33
	370